2022

Role of impaired lipid metabolism and immune dysregulation in the pathogenesis of cardiovascular disease

BOSTON UNIVERSITY

SARGENT COLLEGE OF HEALTH AND REHABILITATION SCIENCES

Dissertation

ROLE OF IMPAIRED LIPID METABOLISM AND IMMUNE DYSREGULATION IN THE PATHOGENESIS OF CARDIOVASCULAR DISEASE

by

SHI SU

B.S., Simmons College, 2012
M.A., Boston University, 2014

Submitted in partial fulfillment of the

requirements for the degree of

Doctor of Philosophy

2022

Approved by

First Reader

Peter Kang, M.D.
Associate Professor of Medicine
Harvard Medical School

Co-first Reader

Vassilis Zannis, Ph.D.
Professor *Emeritus* of Biochemistry and Medicine
Boston University School of Medicine

Third Reader

Konstantinos Drosatos, Ph.D.
Professor of Pharmacology & Systems Physiology
University of Cincinnati

DEDICATION

I would like to dedicate this work to Dr. Vassilis I. Zannis.

ACKNOWLEDGMENTS

I would like to give my deepest gratitude to my mentor and advisor, Dr. Vassilis Zannis. Dr. Zannis is truly a father figure to me. He taught me everything I know in science and introduced me to the wonderful world of lipid metabolism.

Dr. Zannis always puts the needs of students at his highest priority and goes out of his way to fully help every student he teaches. In addition to continuously stimulating my scientific thinking, Dr. Zannis taught me scientific writing by going line by line to guide me write grant proposals and thesis, slide by slide to help me perfect scientific presentations. He is always patient, understanding and encouraging, and helps me grow as a scientist in every way he can.

As a loving Greek father, Dr. Zannis also teaches me life lessons through sports events, art, music and history. Every time you go to him with a question, he not only gives you his sage advice, but also provides you with heart healthy Mediterranean meals rich in extra virgin olive oil, nuts and fruits. Moreover, he makes the best dolmades in the world!

I cannot thank Dr. Zannis enough for all the guidance he has provided me in many aspects of my life. He also teaches me to be resilient no matter how difficult the circumstances are. Dr. Zannis is a true scientist and the most devoted mentor that I admire, and I will continue striving to follow his example.

I would like to thank Dr. Peter Kang for his patience, kindness and understanding, for respecting all the choices I made, and for giving me the opportunity and freedom to explore in cardiovascular research and gain independency and to exercise writing.

I would like to thank Dr. Monty Krieger for his inspiration in the SR-BI project, for being a role model as a true scientist, and for his very enlightening feedback at every meeting and the manuscript reviews.

I would like to thank Dr. Konstantinos Drosatos for all the stimulating questions at every committee meeting to help me ponder deeper into the projects, and for his very careful review and very helpful feedback on my thesis. I really admire his rigorous attitude towards science.

I would like to thank Drs. Kathleen Morgan, Bassilis Zikopoulos, Vaishali Moulton and Iannis Adamopoulos. I'm thankful for what they taught me during my time in the division.

I would like to thank Dr. Qingen Ke for teaching me all the surgical techniques and echocardiography for cardiovascular research, as well as medical backgrounds in cardiovascular disease, and I always enjoy watching his superb Jinghu performances.
I would like to thank Dr. Zhifen Chen, for her wonderful friendship that started with a collaboration, and for guiding me in human genetics research.

I would like to thank Dr. Abel Fueyo, my amigo-sensei, for being my peer mentor and best friend, and a genius scientist, and someone who I can always count on to solve all the questions I have, anytime, anywhere.

I would like to thank Dr. Takayuki Katsuyama for understanding the difficulties that I have encountered and offering all the help during my time doing immunology research. I would like to thank Dr. Eri Katsuyama for always being supportive and for bringing in so much fun.

I would like to thank Dr. Masataka Umeda, for teaching me the EAE experiments and helping me throughout the study, even when the experiments coincided with the weekends and holidays, even the Christmas break. I would like to thank Dr. Catalina Burbano, for patiently teaching me how to perform cell staining for flow cytometry and data analyses, step by step, in a way that is incredibly easy to understand.

I would like to thank Dr. Ping-Min Chen for patiently explaining the immunology concepts behind every experiment and is always ready to help whenever I go to him with questions. “Please, have a seat,” was always the welcoming first response Ping-Min had for me when I asked questions. I would like to thank Dr. Marc Scherlinger for never hesitating to help whenever I ask for it, and for being loving, caring and supportive. “Just one minute please,” was the longest I ever had to wait for Marc to answer any of my questions. I would like to thank Dr. Wenliang Pan for answering all my questions whenever I run into technical difficulties. I would like to thank Christina Ioannidis, for her witty humor that always had me laughing to tears and her encouragement and help along the way. I would also like to thank Dr. Abhigyan Satyam for not only helping me whenever I come across any problems but also constantly reminding me to enjoy life outside of work. I would like to thank Dr. Ryo Hisada for showing me how to perform cell sorting, for helping me with gating strategies, for going over the protocol with me to help me figure out what might have gone wrong for my negative results, for always being patient and understanding when listening to my concerns. I would like to thank Dr. Ignacio Juarez for helpful discussions on the CD8 project.

I would like to give my most sincere thanks to everybody in the Tsokos Lab- thank you all so much for your great mentorship, friendship and encouragement along the way.

I would like to thank Drs. Olivier Kocher, Emmanuel Maverakis and Ioannis Vlachos for their kind collaborations. I would also like to thank Dr. Yered Pita-Juarez and Xanthi-Lida Katopodi, and everybody in the Vlachos lab for their friendship and the wonderful time we had together during the collaboration and beyond.

I would like to thank my dear friends in the CLS animal facility- Andrew Sumski, William Valle, and Nancy Jean Parker for all the help they have provided throughout my time working with animals. It is always a wonderful time working and chatting with them. They always try their best to help me no matter my problem is animal related or not. I cannot thank them enough for connecting me with people who can further help me. Andrew always takes great care with every animal order I put, and always warms my heart with his lovely emails and encouragement. Whenever I say thank you, William and Andrew always reply with, “come on, that’s what friends do.”

I would like to thank Dr. Shinobu Matsuura for her mentorship and support throughout my graduate studies. I would like to thank Dr. Getulio Oliveira Pereira De Oliveira Jr for his support and friendship and for teaching me how to analyze RNA-sequencing data. I would like to thank Dr. Shulin Lu and Dr. Haibin Wang for teaching me clinical cases.

I would also like to thank Danka Chartland for being a relentless advocate for the students to voice their rights. No matter how busy she is, she is always willing to listen to

our concerns and tries her best to help us solve the problems. I would also like to thank Sharon Sankey for all the help she has offered to ease the administrative tasks.

I would like to thank Dr. Judith Schotland, for giving me the opportunity to join this program and providing me with different teaching assistantship opportunities available to help me grow in all aspects during my time in the program. I would like to thank Dr. Nancy O'Hare and Dr. Dustin Allen for providing the opportunity to teach and for their guidance in developing my teaching skills during my tenure as their teaching assistant.

I would like to thank Cindy Cabral, Nicole Jones, and Marilyn Messier for their friendship, help and support during my time in different divisions.

I would like to thank Tony, Danny, and Hector from the Discovery Café for always brightens up my day in the morning, and for cheering me up every time I felt down, with coffee, fruits, and lollipops.

I would like to thank Brendan McDermott for reviewing my dissertation, and Dr. Sarah Garibova for providing all the resources to help me with my thesis.

I would like to thank my family and friends for their love and support during difficult times.

People always say that during graduate school it is easy to get overwhelmed by the workload, but I am so fortunate to be showered by the love and support of all my friends and colleagues in Boston. I love you all.

ROLE OF IMPAIRED LIPID METABOLISM AND

IMMUNE DYSREGULATION IN THE PATHOGENESIS

OF CARDIOVASCULAR DISEASE

SHI SU

Boston University Sargent College of Health and Rehabilitation Sciences, 2022

Major Professors: Peter Kang, Associate Professor of Medicine, Harvard Medical School

and

Vassilis Zannis, Professor *Emeritus* of Biochemistry and Medicine, Boston University School of Medicine

ABSTRACT

Cardiovascular disease is the leading cause of death worldwide. Altered lipid metabolism significantly contributes to pathogenesis of cardiovascular disease. Hypercholesterolemia also contributes to elevated oxidative stress, which leads to tissue damage. In my studies, I sought to gain a better understanding on the development of cardiovascular disease in a novel mouse model that mimics human coronary artery disease. This mouse model developed spontaneous occlusive atherosclerosis when placed on atherogenic diet. I found that dual therapy using a nanoparticle carrying an antioxidant agent together with an antiplatelet drug could significantly ameliorate disease progression, compared with groups treated with antioxidant or antiplatelet alone.

In addition to lipid accumulation and oxidative stress, immune modulation has also gained significant attention in the development of cardiovascular disease. Specifically, it has been long observed that cardiovascular disease is one of the major complications in patients with autoimmune disease. To further understand how impaired

immune cell functions lead to cardiac dysfunction, I used mouse models of autoimmunity. I found that regulatory T cell (Treg)-specific deletion of a splicing gene, Srsf1, leads to dysfunctional Tregs, which significantly contribute to cardiac dysfunction. I also found that heterozygous deletion of the Srsf1 gene in Tregs significantly delayed disease recovery in a toxin-induced multiple sclerosis model. Transcriptomic analysis of T cells with Srsf1 deficiency showed enrichment in differentially expressed genes that are associated with fatty acid oxidation and lipid metabolism pathways. Using a virus infection model, I also found that Srsf1 deletion in total T cells compromised $CD8^+$ T cell function and monocyte migration. These findings have implications for the role of the splicing gene on cardiovascular disease.

TABLE OF CONTENTS

LIST OF FIGURES

LIST OF ABBREVIATIONS

ABCA1 .....ATP-binding cassette transporter A1

Angptl2 .....Angiopoietin-like 2

ApoA-I ..... Apolipoprotein A-I

ApoB ..... Apolipoprotein B

ApoE ..... Apolipoprotein E

CAD ..... Coronary artery disease

CETP..... Cholesteryl-ester transfer protein

CREKA .....Cys-Arg-Glu-Lys-Ala

CVD .....Cardiovascular disease

DEG ..... Differentially expressed gene

EAE.....Experimental autoimmune encephalomyelitis

FoxP3 .....Forkhead box P3

GEO ..... Gene Expression Omnibus

GO.....Gene Ontology

GpIIb/IIIa .....Glycoprotein IIb/IIIa

HDL .....High-density lipoprotein

HMGCR..... 3-Hydroxy-3-methylglutaryl coenzyme A reductase

hnRNP.....Heterogeneous nuclear ribonucleoproteins

hypoE ..... Hypomorphic apolipoprotein E

KEGG .....Kyoto encyclopedia of genes and genomes

LCMV .....Lymphocytic choriomeningitis virus

LDL.....Low-density lipoprotein

LDX-1..... Lectin-like oxidized low-density lipoprotein receptor-1

oxLDL.....Oxidized Low-density lipoprotein

PDGF ..... Platelet-derived growth factor

PVAX..... coPolyoXalate incorporated with Vanillyl Alcohol

RA..... Rheumatoid Arthritis

ROS.....Reactive oxygen species

Scd1..... Stearoyl-CoA desaturase 1

SLE .....Systemic Lupus Erythematosus

SR-BI .....Scavenger receptor class B type I

SRSF1 ..... Serine/arginine-rich splicing factor 1

TPM .....Tirofiban carrying PVAX incorporated Micellular nanocomplex

Treg.....Regulatory T cells

VA..... Vanillyl Alcohol

VLDL.....Very-low-density lipoprotein

VLDLR ..... Very-low-density lipoprotein receptor

CHAPTER ONE: INTRODUCTION

1.1 Lipid Metabolism and Cardiovascular Disease

Many risk factors, including hyperlipidemia, hyperglycemia, and inflammation, contribute to the pathophysiology of cardiovascular disease[1–3]. Different murine models have been established for the investigation of how different factors contribute to the homeostasis of cardiac health. It has been shown that atherosclerosis is a lipid-driven disease that arises from the accumulation of low-density lipoprotein (LDL) and remnant lipoprotein particles in the arteries[4]. In addition, inflammation connects aberrant lipid profile with dysfunctional cells in CVD[5]. Hypercholesterolemia is one of the best understood risk factors for atherosclerosis[6,7]. The development of atherosclerosis starts with lipid accumulation in the intima of the vessels, which leads to recruitment of monocytes, which later become foam cells that generate the fatty streak[8,9]. The fatty streak evolves into atherosclerotic plaque. Unstable plaques may erupt to form thrombus that occludes the artery[8,9].

Evidence from clinical trials and Mendelian randomization studies support the epidemiologic observation that LDL is the cause of atherosclerotic cardiovascular disease[10]. High density lipoprotein (HDL) has long been recognized as a biomarker that is inversely correlated with the coronary heart disease event rate[11]. However, the results of the mendelian randomization study showed that HDL levels are not causally related to decreased disease risk[12]. It has been observed that individuals deficient in cholesteryl-ester transfer protein (CETP), an enzyme that catalyzes the transfer of cholesteryl esters from HDL to other lipoproteins[13,14], had higher HDL levels[15]. However, despite

promising preclinical studies in mouse models[16–18], clinical trials designed to increase HDL levels by inhibition of CETP were unsuccessful due to adverse effects[18]. These studies suggest that increasing the concentration of HDL cholesterol alone may not be sufficient for cardiac protective purposes. Indeed, HDL has several cardioprotective functions, including anti-inflammatory, anti-thrombotic, antioxidant, and anti-diabetic properties[19,20]. In addition to promoting cholesterol efflux, HDL also enhances endothelial functions, promotes endothelial repair, and promotes angiogenesis in ischemia[20]. HDL can lose its cardioprotective functions and becomes dysfunctional under certain conditions such as infection, inflammation and diabetes[21]. The possible factors that contribute to the dysfunctional HDL include changes in the protein compositions of HDL as well as changes in the HDL-associated lipids[21].

Apolipoprotein A-I (apoA-I) is the major protein of HDL[22]. HDL metabolism starts with apoA-I being released from the liver and intestine[23]. Lipid free apoA-I interacts functionally with ATP-binding cassette transporter A1 (ABCA1) on the cell surface and leads to the synthesis of HDL and cholesterol efflux from the cells[22,24]. The removal of excess cholesterol from peripheral tissues via apoA-I and HDL and their transport to the liver for excretion has been widely known as “reverse cholesterol transport” [22–24]. HDL containing apoA-I or apoE also interacts with scavenger receptor class B type I (SR-BI), which results in selective uptake of cholesterol ester by the cells[22,25].

SR-BI is an 82-kDa membrane glycoprotein with one large extracellular domain and two transmembrane domains with short cytoplasmic amino- and carboxy-terminal

domains[26]. SR-BI is abundantly expressed on the surface of hepatocytes and nonplacental steroidogenic tissues[27]. SR-BI is a multiligand membrane receptor protein and can bind with high affinity to HDL, as well as LDL and VLDL[28]. SR-BI is also important for LDL transcytosis in endothelial cells[29]. Efflux of free cholesterol from macrophages to HDL can also be facilitated by SR-BI[30]. It has been shown that the carboxyl terminus of SR-BI interacts with a docking protein named PDZK, which stabilizes the cell surface expression of SR-BI in the liver[31]. Therefore, targeted disruption of the PDZK1 gene in mice can cause tissue-specific depletion of the SR-BI, altering lipoprotein metabolism[32].

Investigations in the functions of SR-BI showed that both abnormal lipid levels and dysfunctional HDL contribute to the pathogenesis of coronary heart disease[33,34]. In addition, a recent human genetic study showed that rare variant that causes loss of function of SR-BI raises HDL cholesterol level and increases risk of coronary heart disease[35]. These lines of evidence have collectively demonstrated the important role of SR-BI in the pathogenesis of coronary artery disease, suggesting that manipulating the gene encoding SR-BI (Scarb1) in the mouse models can be a promising way to mimic human coronary heart disease[36]. The major drawback of mouse models with whole body SR-BI deletion, however, is the female infertility[37], creating significant burden on colony management.

1.2 Cholesterol Accumulation and Oxidative Stress

Oxidative stress and cholesterol accumulation coexist and synergize in the progression of cardiovascular disease [38–41]. Regarding atherosclerosis, it has also been reported that oxidized LDL (oxLDL) is involved in the initiation of plaque formation[42].

OxLDL is a chemoattractant for monocytes and lymphocytes[43,44]. Binding of oxLDL on lectin-like oxidized low-density lipoprotein receptor-1 (LDX-1) enhances its uptake in different cell types and triggers a series of downstream events. These include endothelial cell dysfunction and cell death[42]. Oxidative stress in the vasculature is determined by the imbalance of pro-oxidant and antioxidant state that favors the former[45]. Overproduction of reactive oxygen species (ROS) plays an important role in the progression of atherosclerosis[46], which relies on a vicious cycle between oxidative stress and inflammation[47]. Inflammation caused by overt oxidative stress is therefore a process that connects aberrant lipid profile with dysfunctional cells in CVD[5].

1.3 Animal Models for the Investigation of Atherosclerosis

In humans, subendothelial lipoprotein retention constitutes the initiating process in atherosclerosis[48]. There is also evidence showing endocytosis and transcytosis of LDL in the arterial endothelium[49]. Based on these findings, a large number of animal models have been developed to study the mechanisms of atherosclerosis. Apolipoprotein E (apoE) is a ligand for receptors that clear remnants of chylomicrons and very low density (VLDL) lipoproteins[50]. LDL receptor (LDLR) is essential for receptor-mediated cholesterol endocytosis, and it has been proven that its deficiency leads to atherosclerosis[6,7,51]. Therefore, apoE-/- and LDLR-/- mice are the two most widely used models for atherosclerosis research[5253]. Although these two mouse models can develop atherosclerosis in aortic root and along the aorta tree, they seldom develop any coronary aortic atherosclerosis. In order to better mimic human manifestation of coronary heart disease, which has plaque developing in the coronary arteries, increasing numbers of

animal models with different genetic and diet manipulations have been developed, including the manipulation of the SR-BI gene[36].

High availability of free cholesterol drives the tissue pathology in SR-BI-/- mice[54], even though SR-BI-/- mice do not develop spontaneous atherosclerosis on chow diet[55]. Studies in the function of SR-BI showed that both abnormal lipid levels and dysfunctional HDL contribute to the pathogenesis of coronary heart disease. It has been demonstrated that SR-BI deficient mice have dysfunctional HDL characterized by compromised anti-inflammatory function[56,57]. Previous studies have shown that loss of SR-BI expression leads to early onset of occlusive atherosclerotic coronary artery disease, spontaneous myocardial infarction, severe cardiac dysfunctions, and premature death in apoE-/- mice[58,59]. Since both SR-BI and LDL receptor contribute to cholesterol clearance, SR-BI ablation in LDLR-/- mice also led to more plaque development on high fat Western diet[60]. Overexpression of SR-BI can reduce atherosclerosis in LDLR-/- mice[61].

Recently, Drs. Kocher and Krieger generated another mouse model that lacks the carboxyl terminus of SR-BI[62]. This model was generated by introduction of a 507Ala/STOP mutation into the SR-BI gene to produce a truncated receptor, SR-BIΔCT[62]. The truncated SR-BI disrupts the interaction between SR-BI and its docking protein PDZK1, leading to more than >95% reduction of cell surface expression of SR-BI in the liver[62]. When the SR-BIΔCT mice were crossed with apoE-/- mice, the SR-BIΔCT/apoE-/- mice exhibited hypercholesterolemia and rapid-onset and fatal occlusive coronary arterial atherosclerosis on chow diet[62]. Measurements of the cardiac

hemodynamic parameters also showed impaired cardiac functions resulted from the occlusive coronary arterial atherosclerosis[62]. However, it is not clear whether similar phenotypes can be observed in SR-BIΔCT/LDLR-/- mice. In this dissertation, I characterized the phenotypes of SR-BIΔCT/LDLR-/-mice and their susceptibility to coronary artery disease.

1.4 Antioxidant Therapy in Coronary Artery Disease

Oxidative stress has been closely related to the pathogenesis of heart disease[63–66]. It has been shown that in lipid metabolism, oxidized lipids, including oxLDL, contribute to plaque formation[43,67]. Oxidative stress results from the overproduction of reactive oxidative species (ROS)[66]. Under normal conditions, HDL prevents the oxidation of LDL[68,69]. However, these functions are lost in animals with dysfunctional HDL such as the SR-BI deficient mice[56,57].

Dietary interventions with antioxidant ingredients that decrease oxidative stress have been tried in an effort to reduce the cardiovascular risks[70,71]. However, results from clinical trials using administration of antioxidants have been inconclusive[72]. There are also other strategies aiming to reduce the damage caused by oxidative stress. For example, some pharmaceutical interventions as well as gene therapies have been explored by altering the enzymes or molecules involved in the oxidative stress-activated signaling pathway to alleviate downstream tissue damage[73,74]. However, because ROS act as signaling molecules in health, antioxidant treatments primarily targeting the pathogenic effects of oxidative stress in a targeted manner is most desirable[75]. In this dissertation, I

demonstrated that targeted antioxidant therapy could ameliorate the disease progression of atherosclerosis.

1.5 Thrombosis and Antiplatelet Therapy in Coronary Artery Disease

Atherosclerosis starts with endothelial activation that leads to the expression of adhesion molecules on the endothelial surface[76]. This allows binding of monocytes and subsequent migration into the subendothelial space. LDL also enters the subendothelial space and turns into oxLDL. Monocytes within the subendothelial space differentiate into macrophages, which express various scavenger receptors, such as SR-AI, SR-AII, and CD36 that take up oxLDL[77]. Macrophages take up oxLDL and convert into foam cells, which form the early atherosclerotic lesion, also known as fatty streak[78]. The excessive uptake of cholesterol and oxLDL by macrophages results in their death, and the cholesterol they carry is deposited, along with other cell debris, to form a necrotic core that constitutes the atherosclerotic plaque[78].

Additional progression of the atherosclerotic lesion involves smooth muscle cell migration that is stimulated by platelet-derived growth factor (PDGF)[79]. The smooth muscle cells secrete extracellular matrix molecules that cover the necrotic core, forming fibrous cap, that promotes intimal thickening that may impede blood flow to various degrees[80]. Stabilization of the fibrous cap is compromised by secretion of matrix metalloproteinases (MMPs) secreted by the macrophages[81]. Rupture of the weakened fibrous cap may be accompanied by platelet activation and adhesion that combinedly may cause thrombosis[79].

Because platelet activation and aggregation in response to endothelial injury are

important parts of the pathophysiology of acute coronary syndrome, antiplatelet therapy has been widely used in the management and prevention of cardiovascular disease[82–84]. Many types of antiplatelet drugs are clinically available. Glycoprotein IIb/IIIa antagonists, such as tirofiban, are administered intravenously to prevent platelet-to-platelet aggregation via the fibrinogen receptor[85,86]. Inhibition of GpIIb/IIIa has been shown to reduce the complications in patients with acute coronary syndrome[87]. However, because tirofiban is poorly soluble and functions in a dose-dependent manner and has a short half-life (~2-2.5hrs), it is challenging to manage its dosage to prevent adverse bleeding events[88]. To improve the therapeutic efficacy, a targeted therapy approach is desired.

1.6 Nanomedicine in Coronary Artery Disease

Nanomedicine is an emerging area of research that has been extensively applied in cancer research. Due to the similarities between atherosclerosis and cancer[89,90], such as elevated oxidative stress, inflammation, cell proliferation and apoptosis, efforts to apply nanotechnology-based interventions have been made for the therapy of cardiovascular disease[91]. It has been demonstrated by electron microscopic images that nanoparticles can translocate across the endothelium of the atherosclerotic aortas due to increased permeability of the vessles[92]. VE-cadherin is the major component of adherens junctions, which are tightly regulated protein complexes that join adjacent endothelial cells and prevent leukocyte migration and vascular leak[93]. Leaky vasculatures are a result of the absence of VE-cadherin. Inflammatory mediators such as vascular endothelial growth factor can cause p120-catenin and VE-cadherin to dissociate, leading to internalization of

VE-cadherin[93]. During inflammation, the permeability of vessels increases and allows for nanoparticle distribution in different organs[94]. In addition, there are various processes via which nanoparticles can be taken up by the cells, including endocytosis, phagocytosis, passive diffusion/ direct transmembrane transport[95].

Nanomedicine has great potential in CVD therapies due to their many advantages such as small size, tissue/cell targeting capacity, and longer half-life[96]. An important advantage of nanomedicine is that multiple nanoparticles can be assembled to form a multi-functional nano complex. Such modifications can be applied to improve the targeting capacity and therapeutic efficiency of nanomedicine. For example, PEGylation of nanoparticles is a classic strategy to provide a hydrating layer to the nanoparticle, which can hinder the adsorption of plasma proteins on the surface of the nanoparticles[97].

CREKA (Cys-Arg-Glu-Lys-Ala) was first designed as a tumor targeting peptide as it has high affinity to fibrin[98]. Because of the similarity between tumor and atherosclerotic plaque, using apoE$^{-/-}$ mice, it has also been shown that CREKA is also a plaque homing peptide[99]. In recent years, increased application of CREKA has been incorporated in the nanocarrier drug delivery system[100,101]. Especially, Zhang et al. demonstrated that CREKA can work together with a platelet inhibitor for cancer therapy[100].

Based on the materials that are used for their synthesis, there are polymeric, micellular, liposomal, metal and carbon-based nanoparticles[102]. Polymers and micelles are two of the most commonly used materials for the synthesis of nanoparticles[103–105]. Biodegradable polymers such as polyoxalate and copolyoxalate were developed in the

1970s and have been used in biomedical applications such as suture coating due to their biocompatibility and biodegradability[106]. It has been shown that vanillin, which is the primary component of the extract of the vanilla bean, as well as its main metabolites, vanillic acid and vanillyl alcohol, all have antioxidant properties[107]. We have previously synthesized a nanoparticle which is copolyoxalate incorporated with Vanillyl Alcohol (VA) that we named PVAX[108]. This design makes the nanoparticle sensitive and responsive to oxidative stress because their backbone structure contains peroxalate ester bonds that hydrolyzes in the presence of high concentration of H_2O_2[108,109]. Hydrolysis of the peroxalate ester bonds releases the VA that is incorporated in the nanoparticle[110]. We demonstrated that this nanoparticle is effective in the amelioration of surgically induced ischemia reperfusion models[110–113].

1.6a Description of the nano-micelle complex

In this dissertation, we generated a nano micelle complex that includes the plaque homing peptide CREKA (Cys-Arg-Glu-Lys-Ala), and an antioxidant nanoparticle PVAX that we have previously developed[108]. In addition, this nano complex encapsulates an antiplatelet agent Tirofiban. We named this nano complex, **T**irofiban carrying **P**VAX incorporated **M**icellular nanocomplex (TPM).

The outside shell of the micelle complex contains pluronic F-127 polymers bound with mPEG-PCL blocks. Pluronic F-127 is a triblock copolymer consisting of two hydrophilic tails and one hydrophobic head. mPEG-PCL is an amphiphilic diblock in which PCL acts as the hydrophobic core that binds to the hydrophilic mPEG. In solution, the blocks self-assemble in a way that the synthesized complex shell presents hydrophilic

properties on the outer surface and hydrophobic properties on the inner surface. PVAX was incorporated in the shell of the micelle and the antiplatelet tirofiban was encapsulated in the hydrophobic core (**Figure 1**).

Figure 1

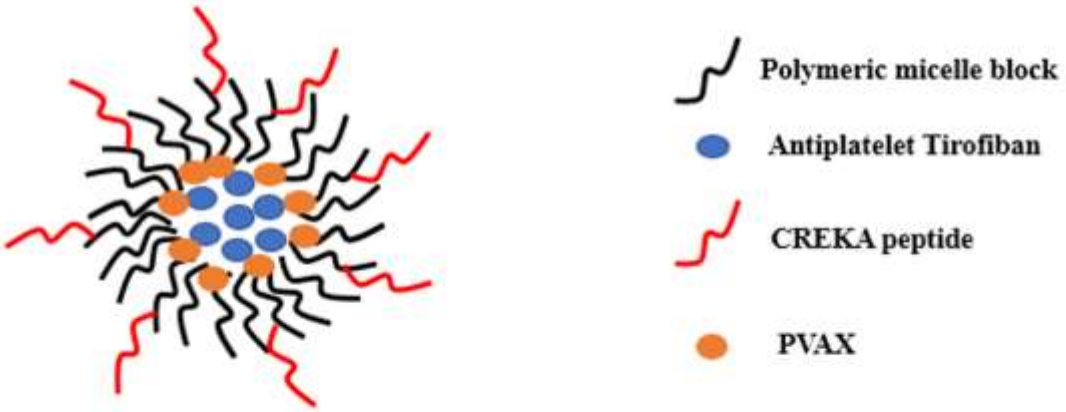

Figure 1. Schematic illustration of the tirofiban carrying PVAX-incorporated micellular nanocomplex.

The objective of the nanoparticle section in this dissertation was to demonstrate the proof-of-concept pre-clinical use of the SR-BIΔCT/LDLR-/- mouse model by employing the nanoparticle assisted antioxidant and antiplatelet therapy to ameliorate diet-induced cardiac dysfunction caused by occlusive atherosclerosis in this mouse model. I hypothesized that tissue targeted antioxidant and anti-platelet treatment can preserve the cardiac functions in SR-BIΔCT/LDLR-/- mice compared to their non-treated counterparts.

1.7 Immunity and Cardiovascular Health

Cardiovascular disease is a major complication in many diseases, including diabetes, viral infection, chronic kidney disease, and chronic obstructive pulmonary disease[114–117]. In addition to the traditional risk factors, it has been recently appreciated that immune cells play a critical role in the pathogenesis of cardiovascular disease[118,119]. This is evident in the increased prevalence of cardiovascular disease in patients with autoimmune diseases. For example, a number of autoimmune diseases, such as systemic lupus erythematosus (SLE), rheumatoid arthritis (RA) and psoriasis, are known to increase the risk of cardiovascular disease[120–122]. Specifically, the CVD risk among SLE patients is at least doubled compared to the general population[123]. It has been found in the Framingham Heart Study that women in the 35- to 44-year age group with lupus were over 50 times more likely to have a myocardial infarction than were women of similar age[124]. There are more factors that play a role in the accelerated atherosclerosis in the SLE patients that cannot be explained by the traditional Framingham risk factors[125]. The traditional risk factors of CVD based on the Framingham Heart Study include age, sex, elevated total serum cholesterol and LDL cholesterol, decreased HDL cholesterol, elevated diastolic and systolic blood pressure, left ventricular hypertrophy, diabetes mellitus, and cigarette smoking.

While traditional cardiovascular risk factors such as hypercholesterolemia are more prevalent in SLE patients, lipid lowering therapy failed to halt the progression of atherosclerosis[126,127]. In addition to the traditional risk factors, there are multiple immune factors that contribute to the accelerated cardiovascular disease in patients with SLE,

including autoantibodies such as anti-oxLDL antibodies and anti-apoA-I antibodies[120]. Autoantibodies are those that attack self-antigens[128]. Increasing evidence has suggested that the presence of autoantibodies is not limited to autoimmune disease. For example, autoantibodies against oxLDL have been found in patients with carotid atherosclerosis[129]. These antibodies are also elevated in children with familial hypercholesterolemia[130]. Circulating autoantibodies to oxLDL are also correlated to the arterial accumulation of oxLDL in LDLR-/- mice[131].

Modified LDL, apoB peptide and modified HDL can all affect adaptive immunity and innate immunity[132,133]. It has been increasingly apparent that atherosclerosis is an inflammatory disorder that involves many immune cells[134,135]. Recent immune cell atlas of murine mouse models showed transcriptional changes in aortic lesions[136,137]. Both innate immunity and adaptive immunity are involved in the pathogenesis of atherosclerosis[134]. In innate immunity, macrophages produce proinflammatory cytokines, such as TNFα, IL-1β and IFNα/β, matrix degrading enzyme and growth factors[138]. Interferon regulatory factor-5 has been found to regulate CD11c+ macrophages in the formation of rupture–prone atherosclerotic plaques[139]. In adaptive immunity, T and B cell respond to antigens such as modified lipoproteins, and produce cytokines such as IFNγ[140]. The combined effects can induce expression of adhesion molecules on endothelial cells and smooth muscle cells, that facilitate immune cell recruitment, and contribute to the disease progression[76]. It has been shown that apoB100, the only apolipoprotein component of LDL particle, is an autoantigen that drives the generation of pathogenic T helper cell type 1 (Th1) with proinflammatory cytokine secretion[141].

Immunohistological staining of murine atherosclerotic specimens showed that $CD4^+$ T cells were prominent in the fibrous cap and the subendothelial space in atherosclerosis prone apoE-/- mice, whereas $CD8^+$ T cells were sparse [142]. Different T cell subsets have different functions in atherosclerosis[143]. For example, it has been demonstrated that while tail vein transfer of $CD4^+$ T cells aggravates atherosclerosis in immunodeficient $apoE^{-/-}$ mice[144], a specific subset of $CD4^+$ T cells, natural regulatory T cells (Tregs), prevented the development of atherosclerosis in mice[145].

Tregs control the immune response to self and foreign antigens and help prevent autoimmune disease[146]. Tregs produced by normal thymus are termed natural Tregs, and those formed by differentiation of naive T cells outside the thymus, either in the periphery or in cell culture are called adaptive or induced Tregs[147]. Natural Tregs are characterized as expressing both CD4 T cell coreceptor and CD25, a component of the IL-2 receptor[148]. The natural Tregs, without pathogenic stimulation which drives it to acquire pathogenic properties, express the nuclear transcription factor Forkhead box P3 (FoxP3)[147]. Naturally occurring Treg mutation in the FOXP3 gene causes immunodysregulation, polyendocrinopathy and enteropathy X-linked (IPEX) syndrome in humans and the x-linked lymphoproliferative disease in mice (also known as scurfy mice)[149].

Low numbers of $FoxP3^+$ Tregs are found in all stages of human atherosclerotic lesions[150]. The levels of regulatory T cells are linked to diet-induced hypercholesterolemia[151]. Atherosclerosis-driven Treg plasticity produces a subset of dysfunctional IFNγ+ Th1/Tregs[152]. Th1 cells produce proinflammatory cytokines [153]. On

the other hand, depletion of FoxP3$^+$ Tregs promotes hypercholesterolemia and atherosclerosis[154]. Additionally, dysfunctional and proinflammatory Tregs are essential for adverse cardiac remodeling in ischemic cardiomyopathy[155]. CCL17 chemokine suppresses the recruitment of Tregs and aggravates myocardial infarction[156]. It has also been found that Tregs can promote atherosclerosis regression[157]. Conversion of anti-inflammatory Tregs to pro-inflammatory Th17 like cells during the progression of atherosclerosis with loss of FoxP3 has been observed in a lineage tracing study in apoE-/- mice[158]. These studies demonstrate the importance of Tregs in the suppression of cardiovascular disease.

While many factors are involved in controlling the function of Tregs[159], it has been increasingly apparent that alternative splicing also affects Treg functions[160]. It has been observed in humans that alternative splicing of FOXP3 controls the effector functions of Tregs and is associated with human atherosclerotic plaque stability[161]. The alternative splicing of FOXP3 can be induced by IL-1β, which promotes Th17 differentiation[162].

These studies prompted us to further investigate how defective Tregs might exacerbate the progression of atherosclerosis, and how alternative splicing plays a role in the process.

1.8 Alternative Splicing

During the characterization of the SR-BIΔCT mice, it was observed that SR-BII expression was increased as a compensatory response[62]. SR-BII is an alternative spliced isoform of SR-BI that also mediates HDL cholesterol uptake [163,164]. The carboxyl

terminus of the SR-BII is different from that of SR-BI[165]. These observations led us to investigate the relationship between alternative splicing and cholesterol metabolism.

Alternative splicing is a naturally occurring event that promotes protein diversity[166]. However, alternatively spliced gene products may possess different functions compared with the constitutively spliced gene products[167]. In humans, it has been found that alternative splicing of HMGCR(3-Hydroxy-3-methylglutaryl coenzyme A reductase), the rate-limiting enzyme for cholesterol biosynthesis and the direct target of statins, reduces responsiveness to statin treatment[168]. Regulation of alternative splicing has also been observed in cell cultures and animal studies[169]. Further analyses have shown that heterogeneous nuclear ribonucleoprotein A1 (hnRNPA1) regulates HMGCR alternative splicing and modulates cellular cholesterol metabolism[170].

There are several splicing factors that control alternative splicing. Among them are two major classes of splicing factors: serine-arginine (SR) proteins and heterogeneous nuclear ribonucleoproteins (hnRNP). Serine and Arginine Rich Splicing Factor 1 (SRSF1) is one of the major SR proteins involved in alternative splicing[171], and works opposite to HRNNPA1[172]. SRSF1 promotes splicing by recruiting spliceosomes whereas HRNNPA1 interferes with spliceosome binding[173].

Increased expression of SRSF1 has been associated with cancer[174]. In cardiomyocyte-specific Srsf1 knockout mice, it was observed that Srsf1 regulates the alternative splicing of CaMKIIδ, which temporally reprograms excitation-contraction coupling in cardiac muscle[175]. SRSF1 was then further found to be involved in vascular aging[176]. Srsf1 also promotes vascular smooth muscle cell proliferation through a

Δ133p53/EGR1/KLF5 pathway[177], and it is also important for the postnatal maturation of neuromuscular junctions in mice[178].

Other splicing genes are also important in lipid metabolism. For example, SRSF11 can stabilize apoE[179]. Aberrant alternative splicing can produce dysfunctional cells, including Tregs[160]. Data from human patients showed that alternative splicing of FoxP3 controls the effector functions of Tregs and is associated with human atherosclerotic plaque stability[161].

SR-BII is an alternatively spliced isoform of SR-BI[163]. Specifically, SR-BII arises from an exon skipping process that a 129-nucleotide exon is spliced out, generating an alternative carboxyl terminus than SR-BI[163]. It has been shown that SR-BII also functions for HDL uptake, although less efficient than SR-BI[163,164]. The SR-BII expression was increased in mice with truncated carboxyl terminus of SR-BI[62]. In humans macrophages, it has been demonstrated that SR-BII contains cytoplasmic signaling motifs and localizes to caveolae[180]. The mechanisms by which SR-BII contributes to the pathogenesis of atherosclerosis is still unclear as the ability of SR-BII stimulating cholesterol efflux does not reflect enhanced hydrolysis of stored cholesteryl esters[180]. In humans, SR-BI, SR-BII, and a newly discovered isoform SR-BIII have been detected[181]. Transgenic mouse models overexpressing human SR-BI and SR-BII respectively showed that SR-BII promoted more inflammation than SR-BI in lipopolysaccharide-induced injury in liver and kidney[182].

Alternative splicing, lipid metabolism, and immune regulation may be interconnected in the pathogenesis of atherosclerosis. On the one hand, it has been

reported that Srsf1 is an important splicing factor that is involved in the SR-B splicing machinery[183], and SR-BI is critical in maintaining normal T cell development and enhancing thymus regeneration[184]. On the other hand, SRSF1 is also crucial for normal T cell and Treg functions[185,186].

The objective of the Treg immunology section of this dissertation was to determine whether insufficient expression of Srsf1 in Tregs also affects Treg functions. The results of this study may have implications in the accelerated cardiovascular disease observed in patients with autoimmune diseases.

1.9 Infection and Alternative Splicing

In addition to chronic inflammation, infection also increases the risk of CVD[187]. T lymphocytes might be the link that connects these conditions, as T cells act as mediators in both conventional CVD and infection[188]. Increased mortality due to cardiovascular disease has been associated with influenza. It has been reported that there is a significant association between respiratory infections, especially influenza, and acute myocardial infarction[189]. While there are abundant epidemiological evidence regarding association between viral infection and increased risk of cardiovascular disease[190], the exact mechanisms remain unclear.

Adaptive immune cells, such as T lymphocytes and B lymphocytes, can recognize pathogens and develop immunological memory for rapid and effective response upon second encounter to the same pathogen[191]. In recent years, it has been observed that innate immune cells, such as monocytes, macrophages, and natural killer cells, also exhibit memory characteristics[192]. The process by which innate immune system shows

enhanced responsiveness to subsequent stimuli after initial activation is termed "trained immunity[193]." Trained immunity has been proposed as a novel mechanism linking infection and the development of atherosclerosis because monocytes, the most abundant immune cells that contribute to the development of atherosclerotic plaques, can develop a long-lasting proinflammatory phenotype after brief stimulation with micro-organisms or microbial products[194]. In addition, it is the oxLDL, rather than LDL, that induces trained immunity in monocytes, leading to long-term inflammatory cytokine production and foam cell formation[195]. Following acute myocardial infarction, cytotoxic $CD8^+$ T cells are recruited to infarction site to release Granzyme B, leading to cardiomyocyte apoptosis, adverse ventricular remodeling and cardiac dysfunction[196]. It has been demonstrated that the pro-inflammatory response to hypercholesterolemia in apoE-/- mice was started by the activation of $CD8^+$ T cells rather than $CD4^+$ T cells[197]. In addition, HDL loses its anti-inflammatory properties during acute influenza infection[198].

In this dissertation, we focused on the effects of SRSF1 deficiency on the function of $CD8^+$ T cells. Cytotoxic $CD8^+$ T cells are crucial for the host antigen-specific immune response to viral pathogens[199]. Using a lymphocytic choriomeningitis virus (LCMV) infection model, we evaluated the $CD8^+$ T cell homeostasis and function *in vivo*, and found that SRSF1 deficiency impaired the antiviral capacity of $CD8^+$ T cells. Specifically, SRSF1 is necessary for the maintenance of normal $CD8^+$ T lymphocyte numbers in the lymphoid compartment, and for the proliferative capacity and cytotoxic function of $CD8^+$ T cells. Transcriptome analyses of Srsf1-deficient T cells showed association of SRSF1 with regulation of cell cycle, MAP kinase signaling and IFN

signaling pathways after viral infection. Mechanistically, SRSF1 controls the expression and activity of the Mnk2/p38-MAPK axis at the molecular level. Our findings identified novel roles for SRSF1 in the physiology and function of cytotoxic $CD8^+$ T lymphocytes.

1.10 Alternative Splicing and Il-17 Expression

The transcriptomic studies also showed that the Tregs derived from Srsf1 deficient T cells had elevated mRNA levels of *Il-17a* and *Il-17f*[185,186]. Many factors regulate the expression of IL-17, including RORγt, RUNX1, STAT3, NF-κB, as well as certain microRNAs[200]. IL-17A expression is also regulated by alternative splicing, a regulatory process that enables the generation of protein isoforms from a single gene[185,186,201,202]. SRSF1 has been shown to influence Th17 differentiation[185,203]. SRSF1 is a multi-functional serine arginine protein that not only controls pre-mRNA splicing, but also regulates many other splicing independent activities such as nonsense-mediated mRNA decay, nuclear export of mRNA, and mTOR activation[204–207]. It has been suggested that SRSF1 plays an important role in autoimmunity[185,186,208]. On the other hand, IL-17 has been shown to enhance the stability of CXCL1 mRNA by inhibiting the interaction between SRSF1 and CXCL1 in the TRAF cascade, which mediates IL17 signaling[209,210]. These studies collectively suggest that SRSF1 might be involved in multiple steps in the IL-17 signaling pathway.

Myeloid-derived suppressor cells (MDSCs) constitute a specific population of cells that can expand and suppress T cell responses during inflammation and infection. In mice, there are two types of MDSCs characterized by the co-expression of CD11B and either Ly6G (in $Ly6G^+Ly6C^-$ granulocytes) or LY6C (in $Ly6G^-Ly6C^+$ monocytes) [211].

Monocytic MDSCs have been found to suppress $CD8^+$ T cells in the spleen [212]. MDSCs suppress T-cell function by down-regulating the expression of CD3 ζ chain in T cells [213]. Interestingly, SRSF1 also regulates mRNA expression of CD3 ζ chain in T cells as well as its transcriptional activation [214]. In the acute infection study described in this dissertation, we identified a potential mechanism that implicates SRSF1 in innate immune responses through MDSCs.

CHAPTER TWO: METHODS AND MATERIALS

Materials of nanoparticle

Pluronic F-127 polymers, Tirofiban hydrochloric monohydrate, Tetrahydrofuran, and 100% ethanol were purchased from Sigma-Aldrich (Saint Louis, MO). mPEG-PCL micelle blocks and PVAX nanoparticles were synthesized as previously reported and provided by Dr. Dongwon Lee (Chonbuk National University, Korea)[108].

Animals and diets

The SR-BIΔCT mouse line was generated as previously described[62]. The LDLR-/- mice were purchased from Jackson Labs (JAX002207). The SR-BIΔCT/LDLR-/- mouse model was generated by crossing SR-BIΔCT with LDLR-/-. The SR-BIΔCT/LDLR-/- mice are fertile.

For phenotypical analyses, 6-week-old mice were placed on normal chow or Paigen diet and followed up for four weeks since the beginning of the diet. Age and sex matched SR-BIΔCT/LDLR-/- and LDLR-/- mice were placed on normal chow or an atherogenic Paigen diet (TD.88051) at 6-week, 18-week, or 30-week of age for survival rate analysis. For the therapeutic intervention, four groups of age- and sex-matched SR-BIΔCT/LDLR-/- mice (n=10/group) were placed on an atherogenic Paigen diet for one week. Starting from week two of the diet intervention, we administered via intraperitoneal (i.p.) injection with 50µl of PBS, PVAX, Tirofiban or Tirofiban carrying PVAX incorporated Micellular nanocomplex (TPM) daily for two weeks. All mice underwent weekly echocardiographic assessment. The bodyweight and food intake of the mice were monitored daily. Fasting glucose levels were measured on the day the mice

started diet intervention and on the day of sacrifice.

At the end of each treatment intervention, animals were euthanized, and tissues were collected.

B6.Srsf1.$^{fl/fl}$ mice were generated[186] and B6.dLck^{cre} (stock 012837) mice were purchased from the Jackson Laboratory (Bar Harbor, ME, USA). The two strains were crossed to generate the B6. Srsf1.$^{fl/fl}$ dLck^{cre} strain.

B6.Foxp3$^{YFP\text{-}cre}$ (stock 016959) were purchased from the Jackson Laboratory (Bar Harbor, Maine). B6.Srsf1$^{fl/fl}$ mice were generated by backcrossing the B6.129S4-Srsf1 $^{fl/fl}$ mice with C57BL/6J mice for twelve generations [215]. B6.Srsf1$^{fl/fl}$ mice were crossed with B6.Foxp3$^{YFP\text{-}cre}$ to generate Srsf1$^{fl/fl}$.Foxp3$^{YFP\text{-}cre}$ mice.

All procedures were performed in accordance with protocols reviewed and approved by the Beth Israel Deaconess Medical Center Institutional Animal Care and Use Committee.

Echocardiogram

Echocardiographic studies were performed with a Vevo2100 system (VisualSonics Inc., Toronto, Canada). Mice were anesthetized with continuous 1.5% isoflurane inhalation while placed onto the warm plate with embedded EKG leads in the supine position. A MS400 (18-38 MHz) transducer was applied to the left hemithorax. Two-dimensional targeted M-mode imaging was obtained from the short-axis view at the level of the largest left ventricular diameter. M-mode measurements of left ventricular end-diastolic and end-systolic diameter and left ventricular anterior- and posterior-wall thickness were made from images recorded on videotape using Vevo Lab analysis

software. Left ventricular ejection fraction (LVEF) was calculated using LVEF (%) = stroke volume (SV)/end diastolic volume (EDV). Left ventricular fractional shortening (LVFS) was calculated using LVFS (%) = [(LVEDD – LVESD)/LVEDD] × 100, where LVEDD and LVESD indicate left ventricular end-diastolic and end-systolic diameter, respectively.

The same method can be applied in 3-wk-old mice as juvenile mice and adult mice showed no significant differences in their EF and FS[216].

Hemodynamic Studies

Cardiac function was evaluated in SR-BIΔCT/LDLR-/-and $LDLr^{-/-}$ mice on chow diet or atherogenic Paigen diet for various lengths using left ventricular pressure-volume (PV) loop measurements. Mice were anesthetized under continuous 2% isoflurane inhalation and their LV hemodynamic parameters were measured using a 1.0 Fr. micro-tip pressure-volume catheter (Scisense Inc., Ontario, Canada) inserted into the right common carotid artery and then gently advanced into the left ventricle. Data were recorded using a Powerlab system (ADInstruments, Colorado Springs, CO), and beat by beat pressure-volume parameters, including stroke volume, cardiac output, maximum and minimum left ventricular volumes, change in pressure with time (dP/dt) and contractility were measured and analyzed using CardioSoft Pro software (CardioSoft, Houston, TX).

Histology

Formalin-fixed tissues that underwent tissue processing were embedded in paraffin blocks. Six μm paraffin sections were stained with hematoxylin and eosin (H&E) for morphology analysis or Masson's trichrome staining that stains the collagens for

fibrosis analysis. Images were obtained by KEYENCE BZ-X700 microscope.

On 14 days of the EAE experiment, mice were sacrificed for spinal histological analyses. Mice were perfused from the apex of the left ventricle and the spinal cords were flushed out by 1xPBS using a 22G needle at the time of sacrifice. The spinal cords were fixed in 10% formalin and embedded in paraffin. 6μm short-axis serial sections were made from the paraffin blocks and stained with hematoxylin and eosin (H&E).

Oil-Red-O Staining

Hearts were mounted in Tissue-Tek OCT compounds (Sakura) and froze on dry ice. Serial 6μm short-axis cryo-sections of the heart were obtained. The sections were fixed in 4% paraformaldehyde in 1× PBS for 5 minutes at room temperature. Incubating the slides with 60% isopropanol for 5 minutes, the slides were stained with freshly prepared Oil Red O (0.5% in triethylphophate) working solution for 10 minutes. Then, the slides were rinsed with 60% isopropanol for 2 minutes repeatedly, following the hematoxylin and eosin staining for 10 seconds. The slides were rinsed with 1× TBS for 3 times and with distilled water before mounting a coverslip onto the slides with warmed glycerol gelatin. Images were obtained by KEYENCE BZ-X700 microscope.

Wright-Giemsa Staining

Blood smears were fixed with methanol and stained using Wright-Giemsa solution (Sigma-Aldrich) according to the manufacturer's instructions for histopathologic analysis. Images were obtained using a KEYENCE BZ-X700 microscope.

Hematological analysis

Blood was collected by cardiac puncture into Microvette® EDTA tubes (Sarstedt).

Complete blood count analyses were determined using Hemavet® 850 analyzer (Drew Scientific).

Synthesis of Micelle Complex

Micelle surfactants (MPEG-PCL and F-127, 8:2 ratio) and PVAX (10% of w/v of micelle) were dissolved in tetrahydrofuran and mixed by vortexing. Clot-binding peptide CREKA (Cys-Arg-Glu-Lys-Ala) (10% of w/v of micelle) was dissolved in 100% ethanol. Therapeutic dose of tirofiban (0.1mg/g body weight) was dissolved in 100% ethanol. The above components are mixed with vortex. 1X Phosphate-buffered Solution (PBS) was added to the mixture. Five minutes of low-speed vortex was necessary to generate micelle complex with desired characteristics. When the solvents were evaporated, the micelle solution was filtered through a 0.2µm portable filter to remove clumps of individual components or aggregated micelles. For imaging purposes, the encapsulated moiety was Nile Red (Sigma)[217] instead of tirofiban.

Fasting glucose measurement

Mice were withheld from food overnight prior to glucose measurement. Tail vein blood glucose level was measured using a FreeStyle Glucometer and strips.

Hematological profiling

Tail vein blood was collected weekly and the complete blood count profiles were generated using Hemavet® 850 analyzer (Drew Scientific).

Study design

Four groups of age- and sex-matched SR- $BI^{\Delta CT}$. $LDLr^{-/-}$ mice (n=10/group) were placed on an atherogenic Paigen diet (TD.88051) for one week. Starting from week two

of the diet intervention, we administered via intraperitoneal (i.p.) injection with 50µl of PBS, PVAX, Tirofiban or Tirofiban carrying PVAX incorperated Micellular nanocomplex (TPM) daily for two weeks. The bodyweight and food intake of the mice were monitored daily. Fasting glucose levels were measured at baseline and at the end of study.

Primers

Primers were purchased from Eurofins Genomics. Primer sequences are:

Foxp3 Cre WT Forward 5'-CCTAGCCCCTAGTTCCAACC-3'

Foxp3 Cre WT Reverse 5'-AAGGTTCCAGTGCTGTTGCT-3'

Foxp3 Cre Mut Forward 5'-AGGATGTGAGGGACTACCTCCTGTA-3'

Foxp3 Cre Mut Reverse 5'-TCCTTCACTCTGATTCTGGCAATTT-3'

Srsf1 Flox Forward 5'-GGGACTAATGTGGGAAGAATG-3'

Srsf1 Flox Reverse 5'-AACCTAAACTATTGCTCCCATCTG-3'

Mnk2 forward 5'-GCTGCGACCTGTGGAGCCTGGG-3'.

Mnk2a reverse 5'-GATGGGAGGGTCAGGCGTGGTC-3'.

Mnk2b reverse 5'-GAGGAGGAAGTGACTGTCCCAC-3'.

LCMV-GP reverse 5'-GCAACTGCTGTGTTCCCGAAAC-3'.

LCMV-GP forward 5'-CATTCACCTGGACTTTGTCAGACTC-3'

Experimental Autoimmune Encephalomyelitis (EAE) Model

On day 0 of the experiment, 8 wk-old mice were immunized subcutaneously using 200 µg MOG_{35-55} peptide (AnaSpec) emulsified in the complete Freund's adjuvant containing 4 mg/mL Mycobacterium tuberculosis extract (H37Ra) (Chondrex). In addition, each

mouse was subjected to 200 ng of pertussis toxin (List Labs, Campbell) injection intraperitoneally on days 0 and 2 of the experiment. Mice were monitored and weighed daily until day 28 of the experiment. The following 5 clinical scores were used: 1, limp tail; 2, hind-limb paresis; 3, hind-limb paralysis; 4, tetraplegia; and 5, moribund[218].

EAE priming cell experiment

On day 7 of the EAE experiment, mice were sacrificed and the inguinal lymph nodes of the mice were collected. Cells were subjected to 3, 10, or 30μg/ml MOG_{35-55} peptide and incubated for 3 days.

ELISA

Supernatant of the *ex vivo* EAE priming cells after 3 days of incubation was collected for ELISA. ELISA MAX Deluxe SET Mouse IL-17A (BioLegend), ELISA MAX Deluxe SET Mouse IFN-γ (BioLegend) were used. All procedures were performed according to the manufacturer's instructions. Each assay was performed in duplicate independently.

Plasma lipid measurement

Plasma of the mice was used to measure their cholesterol and triglyceride contents using Infinity™ total cholesterol solution and triglycerides liquid stable reagent (Thermo Fisher) according to the manufacturer's instructions. Cholesterol content of HDL and non-HDL fraction was measured by Cholesterol Assay Kit - HDL and LDL/VLDL (ab65390).

Antibodies and Reagents

Flow cytometry antibodies and other reagents: anti-mouse CD90.2 (53-2.1,

BioLegend), 7-AAD and Annexin-V (BioLegend, San Diego, CA, USA), CD3 (145-2C11, BioLegend), CD4 (GK1.5, Invitrogen), CD8a (53-6.7, BioLegend), CD25 (PC61, BioLegend), CD127 (A7R34, BioLegend), IL-17A (TC11-18H10.1, BioLegend), IL-17F (9D3.1C8, BioLegend), FOXP3 (MF-14, BioLegend), RORγt (B2D, BioLegend), Ly6C (HK1.4, BioLegend), Ly6G (1A8, BioLegend), CD11B (M1/70, BioLegend). Western blot antibodies: anti-phospho-p38 MAPK (Thr180/Tyr182) (Cell Signaling) (D3F9), anti-beta-actin (AC-74) (Merck) and goat anti-rabbit IgG-horse-radish peroxidase (HRP) and goat anti-mouse IgG-HRP were purchased from Thermo Fisher Scientific (Waltham, MA, USA) and Ammonium-Chloride-Potassium (ACK) lysing buffer was obtained from Fisher Scientific (Pittsburgh, PA, USA).

Lymphocytic Choriomeningitis Virus (LCMV) infection

The LCMV-Armstrong strain was a generous gift from Dr. John Teijaro (The Scripps Research Institute). Eight to twelve-week-old WT and $Srsf1^{fl/f}.dLck^{cre}$ mice were infected via intraperitoneal injection (i.p.) with 10^5 PFU and maintained for 8 days in the Animal Research facility at BIDMC..Age- and sex-matched mice injected with PBS served as controls. For CD8 study, on day 8 post infection, mice were euthanized, and tissues were collected for downstream procedures. For MDSC study, bone marrow and splenocytes were harvested at 24hrs post-infection for flow cytometric analyses.

Tissue processing and Cell isolation

Spleens and mesenteric lymph nodes were homogenized using a syringe plunger and 70μm cell strainer. RBC lysis was performed with ACK lysing buffer for 3 min. All cell cultures used in RPMI complete medium (RPMI supplemented with 10% FBS plus

penicillin and streptomycin antibiotics).

Flow cytometry

Flow cytometry was performed using a CytoFLEX LX Flow Cytometer (Beckman Coulter) and analyzed using FlowJo. Single cell suspension of mouse bone marrow cells or splenocytes were collected for flow cytometric analyses. ZombieNIR Viability Kit (BioLegend) or zombie aqua viability dye staining was performed for live/dead cell staining. Surface staining was performed in PBS with Fc block at 4°C for 30 minutes. Surface staining was performed in FACS staining buffer (PBS containing 2% FBS) on ice for 30 minutes with Fc block.

For intracellular cytokine staining, cells were stimulated for 4 hours in culture medium with PMA (1mM, Sigma-Aldrich), Ionomycin (1μM, Sigma-Aldrich) and monensin (1μL/mL, BD Biosciences). After cell surface staining, cytofix/Cytoperm and Perm/Wash buffer (BD Biosciences) were used for fixation and permeabilization. Appropriate antibodies were used for intracellular staining for cytokines or transcription factors according to manufacturer's instructions.

On 14 days of the EAE experiment, mice were sacrificed, and their spinal cords were harvested for flow cytometric analyses. The spinal cords were digested in 20 mg/mL collagenase D (MilliporeSigma 11088882001) and 20 μg/mL DNase I (MilliporeSigma 10104159001) at 37°C for 30 min. Following enzymatic digestion, spinal cords were mechanically processed by passage through a 70-μm cell strainer. Spinal cord homogenates were then subjected to Opt-Prep Density Gradient Medium (Sigma) for gradient centrifugation. The cells located at the interphase were collected and

washed with complete RPMI medium and resuspended in HBSS. The single cell suspensions were incubated with anti-CD16/32 (Biolegend 93) at a 1:100 dilution on ice for 20 min prior to conjugated antibody staining. Cells were then stained with the following conjugated antibodies (antibodies used in this study were purchased from Biolegend if not otherwise indicated) at 4°C for 20 min: CD25 (clone PC61, 1:100), CD45 (clone 30-F11, 1:100), CD90.2 (clone 53-2.1, 1:100), IL-17A (clone JC11-18H10.1, 1:50), IFNγ (clone XMG1.2, 1:50) (Thermo Fisher).

Cytotoxicity assays

CD8+ T cells were isolated from Srsf1$^{fl/fl}$ and Srsf1$^{fl/fl}$.dLck^{cre} mice using MACS as CD8+ effector T cells. The murine lymphoblastoid T cell line EL4 was cultured in DMEM complete medium (supplemented with 10% FBS and 1% penicillin/streptomycin) and cocultured with the isolated CD8+ effector T cells with the following Effector:Target ratios: 10:1, 5:1, 2.5:1, 1.25:1 and 0.63:1. The cells were incubated at 37°C with 5% CO2 for 4 hours to induce cell cytotoxicity. The cytotoxicity was measured using the CytoTox 96 Non-radioactive cytotoxicity assay LDH detection kit (Promega) according to the manufacturer's instructions.

RNA-sequencing

Total T cells were isolated from spleens by magnetic assisted cell sorting (MACS), using the Pan T cell isolation kit (Miltenyi Biotech). Total RNA was extracted using the RNeasy mini kit (Qiagen) and submitted for RNA sequencing to the Molecular Biology Core Facilities at the Dana-Farber Cancer Institute (DFCI). Libraries were prepared using Roche Kapa mRNA HyperPrep strand specific sample preparation kits

from 200ng of purified total RNA according to the manufacturer's protocol on a Beckman Coulter Biomek i7. The finished dsDNA libraries were quantified by Qubit fluorometer and Agilent TapeStation 4200. Uniquely dual indexed libraries were pooled in an equimolar ratio and shallowly sequenced on an Illumina MiSeq to further evaluate library quality and pool balance. The final pool was sequenced on an Illumina NovaSeq 6000 targeting 40 million 150bp read pairs per library at the Dana-Farber Cancer Institute Molecular Biology Core Facilities. Sequenced reads were aligned to the UCSC mm10 reference genome assembly and gene counts were quantified using STAR (v2.7.3a). Differential gene expression testing was performed by DESeq2 (v1.22.1). RNAseq analysis was performed using the VIPER snakemake pipeline.

Transfections

Healthy donor deidentified blood samples were obtained from the Kraft donor center at Dana Farber Cancer Institute. All studies were approved by the institutional review board. T cells were isolated from blood using the Rosette Sep T cell isolation kit (Stem Cell Technologies). Human T cells were transfected using the Amaxa human T cell nucleofector kit (Lonza, Cologne, Germany), following the manufacturer's instructions. Briefly, 3×10^6 to 6×10^6 cells were resuspended in 100 μL nucleofector solution. Plasmid DNA pcDNA3.1 empty vector or pcDNA3.1-Srsf1 (0.5 μg/10^6 cells) was added, and cells were transferred into a cuvette and electroporated using the U-014 program in the nucleofector device. Cells were immediately rescued into prewarmed medium and cultured overnight.

RT-qPCR

mRNA was isolated using the RNeasy mini kit (Qiagen) and reverse transcribed into cDNA using the ecodry oligo dT RNA to cDNA premix (Clontech). Real-time quantitative PCR amplification was carried out with SYBR Green I mastermix using a LightCycler 480 (Roche) instrument, following the program: initial denaturation at 95 ºC for 5 min; 40 cycles of amplification (denaturation at 95 ºC for 15 s, annealing at 60 ºC for 15 s, extension at 72 ºC for 30 s); one cycle of melting curves (95 ºC for 15 s, 65ºC for 2 min and 97 ºC continuous), with a final cooling step at 37 ºC. Threshold cycle values were used to calculate relative mRNA expression by the ΔCt relative quantification method.

Western Blot

Total protein was extracted using RIPA buffer (Boston Bioproducts) and electrophoresed on NuPAGE 4–12% Bis-Tris gels (Life Technologies). Proteins were transferred to PVDF membranes, blocked with 5% (wt/vol) non-fat milk in Tris-buffered saline with 0.05% Tween 20 (TBS-T) for 1 h, followed by an incubation with primary antibody 1:1000 dilution (1:10000 for β-actin antibody) in TBS-T 5% milk at 4 ºC overnight (room temperature for 1h for β-actin antibody). Membranes were washed with TBS-T, incubated with HRP-conjugated secondary antibody for 1 h, washed with TBS-T, developed with enhanced chemiluminescence (ECL) reagents (1:4000 ECL prime; GE Healthcare). Retrieved bands were visualized by a ChemiDoc XRS imager (Bio-Rad). Densitometry was performed using Image Lab (Bio-Rad).

RNA-Seq Analysis

RNA-Seq data of natural regulatory T cells (nTregs) of WT and Srsf1$^{fl/f}$.dLck^{cre} mice were acquired from the NCBI Gene Expression Omnibus (GEO) from the series under accession number: GSE136286.

Bioinformatic Analyses

Raw sequencing data were acquired in FASTQ format. Data quality was evaluated using FastQC[219] and data were pre-processed with Cutadapt [220] for adapter removal following best practices [221]. Alignment of sequencing reads to the reference genome (GRCh38 and GRCm38 for human and mouse, respectively) was performed using STAR[222], and the quantification of reads was carried out with the SubRead package [223]. Gene expression level normalization and differential expression analysis was carried out using the DESeq2 Bioconductor R package (version 1.6.3) [224], while ClusterProfiler [225] was utilized for downstream functional investigations and pathway enrichment analyses. Differential expression p-values were corrected for multiple testing using the false discovery rate (FDR) and Storey's q- value [226]. Genes with adjusted $p < 0.05$ were considered as differentially expressed.

Differential exon usage analysis was performed with DEXSeq (v1.34.1) [227,228]. First, the exon annotation was created based on the GRCm38 Ensembl v98 gene annotation. Differential exon usage p-values were corrected for multiple testing using FDR method. Plots were generated in R using ggplot2 (v3.3.3) [229] ComplexHeatmap (v2.6.2) [230], and ggsashimi (v1.1.0) [231].

Statistical Analysis

Comparisons between two different groups were done by two-tailed Student's t-test. Comparison among groups of different treatment was analyzed using one-way ANOVA with post hoc Tukey test. Statistical analyses were performed with GraphPad Prism 9.0 software (GraphPad Software). Data are shown as mean ± SEM. P values < 0.05 were considered significant.

CHAPTER THREE: RESULTS

3.1 SR-BIΔCT/LDLR-/-mice develop atherosclerotic cardiovascular disease in a diet dependent manner

3.1a. Atherogenic diet induced organ enlargement in SR-BIΔCT/LDLR-/-mice

At the end of the four-week diet intervention, we observed that while there was no significant body weight differences between two groups (**Figure 1A**), SR-BIΔCT/LDLR-/-mice had significantly increased heart weight and lung weight compared to LDLR-/-mice (**Figure 1B&C**), both of which are surrogate markers of potential heart failure [232]. In addition, SR-BIΔCT/LDLR-/-mice showed significant hepatosplenomegaly (**Figure 1D-F**).

Figure 1

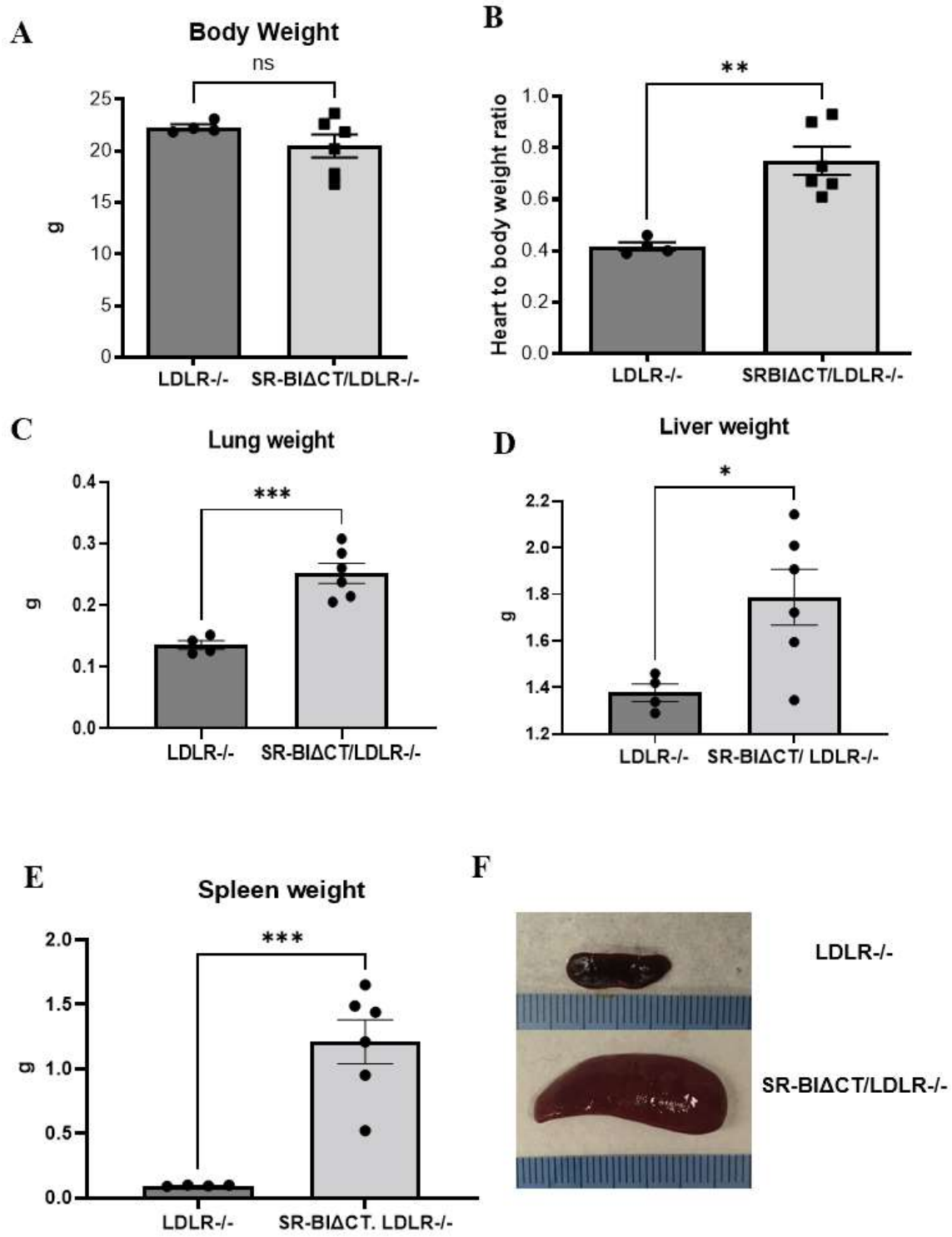
A
Body Weight
ns
g
25
20
15
10
5
0
LDLR-/-
SR-BIΔCT/LDLR-/-
B
**
Heart to body weight ratio
1.0
0.8
0.6
0.4
0.2
0.0
LDLR-/-
SRBIΔCT/LDLR-/-
C
Lung weight
***
g
0.4
0.3
0.2
0.1
0.0
LDLR-/-
SR-BIΔCT/LDLR-/-
D
Liver weight
*
g
2.2
2.0
1.8
1.6
1.4
1.2
LDLR-/-
SR-BIΔCT/ LDLR-/-
E
Spleen weight
***
g
2.0
1.5
1.0
0.5
0.0
LDLR-/-
SR-BIΔCT. LDLR-/-
F
LDLR-/-
SR-BIΔCT/LDLR-/-

Figure 1. Atherogenic diet induced organ enlargement in SR-BIΔCT/ LDLR-/- mice. Body weight **(A),** heart weight **(B),** lung weight **(C),** liver weight **(D),** and spleen weight **(E) of** SR-BIΔCT. LDLR-/- (n=6) and LDLR-/- (n=4) mice after four weeks of atherogenic diet. (Unpaired student t test, *, $p<0.05$, **, $p<0.01$, ***, $p<0.001$). **(F)**. Representative gross organ images showing the spleen of LDLR-/- and SR-BIΔCT/ LDLR-/- after four weeks of atherogenic diet.

3.1b. SR-BIΔCT/LDLR-/-mice showed accelerated lipid accumulation in tissues after atherogenic diet intervention

In order to further investigate the morphological changes induced by the atherogenic diet, we performed histological analyses of the tissue sections. At the end of diet intervention, SR-BIΔCT/LDLR-/-mice showed significantly elevated lipid accumulation in the heart and liver compared to LDLR-/- mice (**Figure 2A**). In addition, the SR-BIΔCT/LDLR-/-heart also showed massive immune cell infiltration. Moreover, both the liver and the spleen of SR-BIΔCT/LDLR-/- showed signs of extramedullary hematopoiesis with the increased number of hematopoietic cells (**Figure 2A**). Oil-Red-O staining showed that there was increased neutral lipid accumulation in the heart of SR-BIΔCT/LDLR-/- after 3 weeks of atherogenic diet intervention compared with their chow diet counterparts (**Figure 2B**).

In order to determine there was tissue damage in the heart, we performed Masson's trichrome staining of the sections of the heart tissue to visualize cardiac fibrosis. We found that on chow diet, the SR-BIΔCT/LDLR-/-mice did not develop any fibrotic tissues in the heart (**Figure 2C**). However, severe cardiac healing fibrosis was observed in SR-BIΔCT/LDLR-/-mice four weeks after atherogenic diet challenge. The fibrotic tissue was absent in the heart of the LDLR-/- mice on the same atherogenic diet for the same duration.

Figure 2

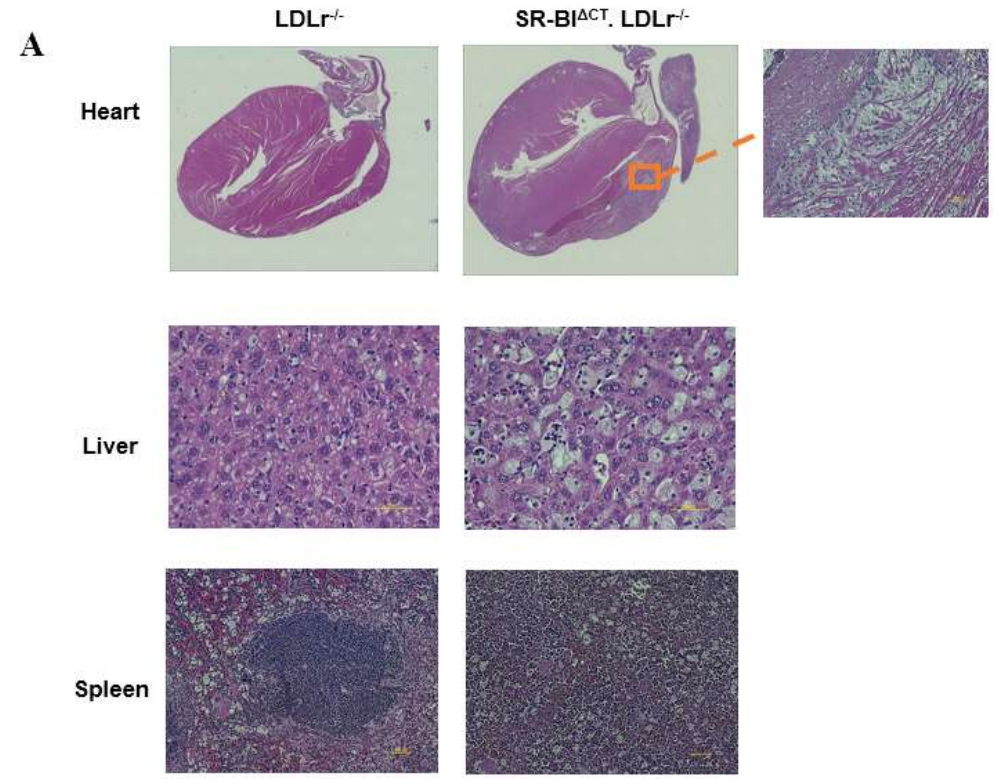
A
LDLr-/-
SR-BIΔCT. LDLr-/-
Heart
Liver
Spleen
B
SR-BIΔCT. LDLr-/-
Chow Diet
SR-BIΔCT. LDLr-/-
Paigen Diet
C
LDLr-/-
Paigen Diet
SR-BIΔCT. LDLr-/-
Chow Diet
SR-BIΔCT. LDLr-/-
Paigen Diet

Figure 2. Atherogenic diet induced lipidation on SR-BIΔCT/ LDLR-/- tissues. (A). H &E staining showing morphology changes in heart, liver and spleen of SR-BIΔCT/ LDLR-/- and LDLR-/- after four weeks of atherogenic diet intervention. **(B).** Oil-Red-O staining showing neutral lipid accumulation (red area) in the heart of SR-BIΔCT/ LDLR-/- on chow diet and atherogenic diet for three weeks. **C.** Masson's trichrome staining showing fibrosis of the hearts of SR-BIΔCT/ LDLR-/- and LDLR-/- on chow diet or atherogenic diet for four weeks.

3.1c. Atherogenic diet impaired the cardiac functions of SR-BIΔCT/LDLR-/-mice

In order to determine whether the accelerated lipid accumulation also affects the cardiac functions of the animals, we performed echocardiography and pressure volume loop measurements in SR-BIΔCT/LDLR-/-and LDLR-/- mice. Our echocardiographic data showed that the first two weeks of atherogenic diet did not significantly change the cardiac parameters of the mice (**Figure 3A&B**). However, after three weeks of atherogenic diet, SR-BIΔCT/LDLR-/-mice had significantly decreased ejection fraction (**Figure 3A**), which is the percentage of blood that leaves the left ventricle every time the heart beats, and fractional shortening (**Figure 3B**), which is the percentage change in left ventricular diameter during the period of contraction (systole).

Additionally, when we compared the cardiac functions of the SR-BIΔCT/LDLR-/-mice with the LDLR-/- mice after three weeks of atherogenic diet, we found that the SR-BIΔCT/LDLR-/-mice showed significantly lower stroke volume (**Figure 3C**), which leads to significantly lower cardiac output (**Figure 3D**), as the cardiac output is the production of heart rate multiplied by stroke volume. When we measured the maximum change of pressure over time (maximum dP/dt) of these mice, which is a parameter for cardiac contractility, we found that SR-BIΔCT/LDLR-/-mice had a lower maximum dP/dt, suggesting these mice had a weaker contractility compared to the LDLR-/- mice

(**Figure 3E**). The minimum change of pressure over time (minimum dP/dt) of SR-BIΔCT/LDLR-/-mice was also significantly lower than the LDLR-/- mice, suggesting worsened diastolic function in the SR-BIΔCT/LDLR-/-mice (**Figure 3F**).

Taken together, these data suggested that three weeks of atherogenic diet could significantly impair the cardiac functions of the SR-BIΔCT/LDLR-/-mice and the cardiac deterioration was worse than the classical LDLR-/- mice.

Figure 3

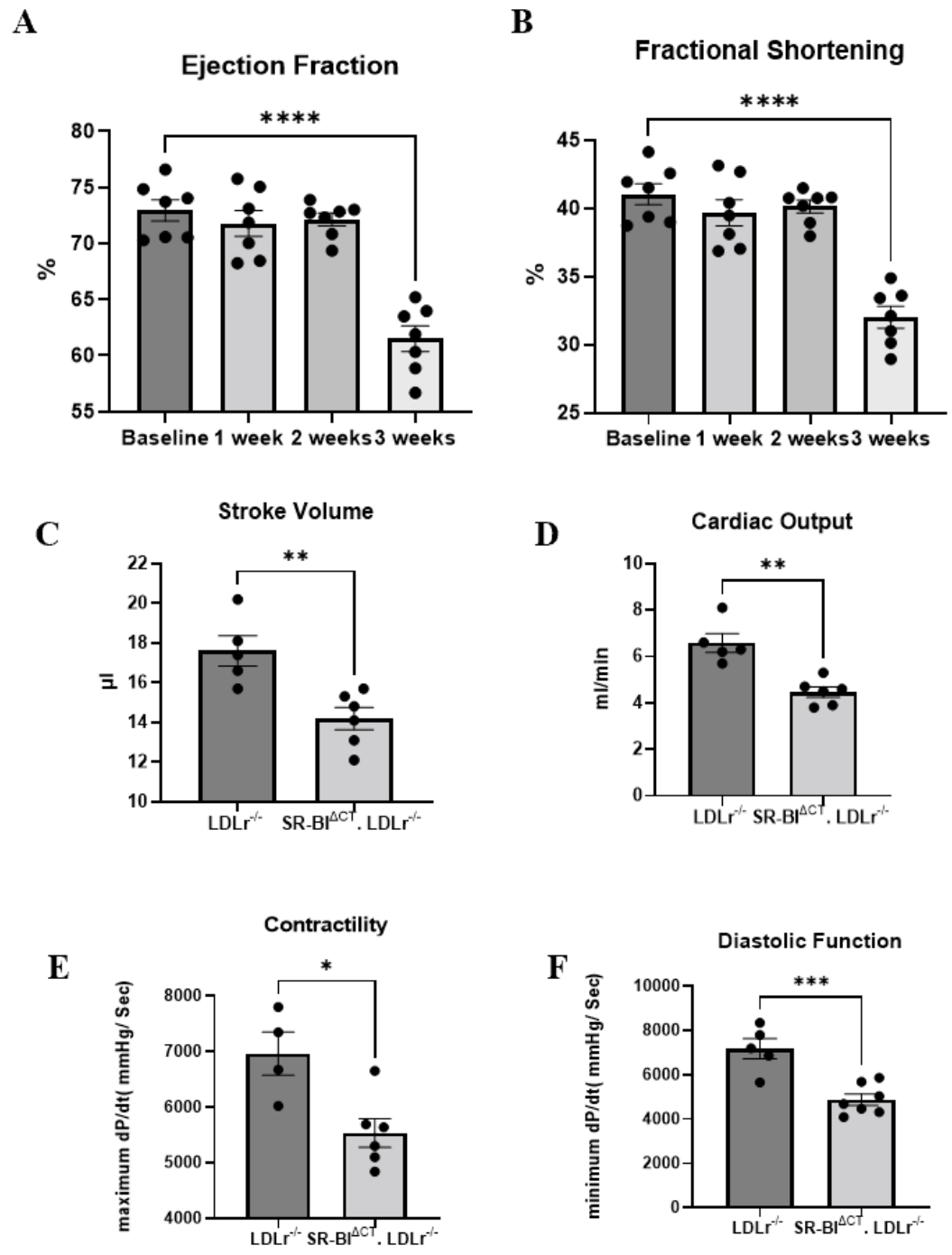
A
Ejection Fraction
****
%
80
75
70
65
60
55
Baseline 1 week 2 weeks 3 weeks
B
Fractional Shortening
****
%
45
40
35
30
25
Baseline 1 week 2 weeks 3 weeks
C
Stroke Volume
**
µl
22
20
18
16
14
12
10
LDLr-/-
SR-BI ΔCT. LDLr-/-
D
Cardiac Output
**
ml/min
10
8
6
4
2
0
LDLr-/-
SR-BI ΔCT. LDLr-/-
E
Contractility
*
maximum dP/dt(mmHg/ Sec)
8000
7000
6000
5000
4000
LDLr-/-
SR-BI ΔCT. LDLr-/-
F
Diastolic Function
***
minimum dP/dt(mmHg/ Sec)
10000
8000
6000
4000
2000
0
LDLr-/-
SR-BI ΔCT. LDLr-/-

Figure 3. Atherogenic diet impairs the cardiac functions of SR-BIΔCT/ LDLR-/- mice. Ejection Fraction **(A)** and Fractional Shortening **(B)** of the SR-BIΔCT/ LDLR-/- mice (n=7) at baseline and 1,2, and 3 weeks after atherogenic diet. (Paired student t test, ****, p<0.0001). Stroke Volume **(C),** Cardiac Output **(D),** Cardiac Contractility **(E)** and Diastolic Function **(F)** of the LDLR-/- (n=4-5) and SR-BIΔCT/ LDLR-/- (n=6) mice after 3 weeks of atherogenic diet. (Unpaired student t test, *, p<0.05, **, p<0.01, ***, p<0.001)

3.1d. Atherogenic diet altered the hematological profiles of SR-BIΔCT/LDLR-/-mice

In order to determine whether the atherogenic diet also change the hematological profiles of the SR-BIΔCT/LDLR-/-mice, we collected the tail vein blood of the mice on a weekly basis and performed hematological analyses. We found that two weeks after the start of diet intervention, the SR-BIΔCT/LDLR-/-mice had significantly elevated circulating cell counts in total white blood cell (leukocytosis), neutrophil (neutrophilia) and lymphocyte (lymphocytosis) (**Figure 4A-C**). This phenotype was not observed in LDLR-/- mice even after four weeks of atherogenic diet intervention.

In addition, the diet induced an anemic phenotype in SR-BIΔCT/LDLR-/- mice but not LDLR-/- mice starting at week two of the diet intervention (**Figure 4D**). Blood smears also showed that three weeks after diet intervention, the red blood cells of the SR-BIΔCT/LDLR-/-mice were morphologically abnormal compared to their chow diet counterparts, or LDLR-/- mice on the same atherogenic diet (**Figure 4E**). In order to further investigate whether there is a hematopoietic defect in SR-BIΔCT/LDLR-/-mice after high cholesterol diet intervention, we examined the histology of the bone marrow. We found that after four weeks of atherogenic diet, the bone marrow of SR-BIΔCT/LDLR-/-mice had apparently less mature red blood cells in the bone marrow, while the bone marrows of the LDLR-/- mice on the same diet and SR-BIΔCT/LDLR-/-

mice on chow diet showed normal appearance of mature red blood cells (**Figure 4F**). These data correspond with our observation of increased extramedullary hematopoiesis in the liver and spleen of the SR-BIΔCT/LDLR-/-mice following the switch to atherogenic diet (**Figure 2A**).

Figure 4

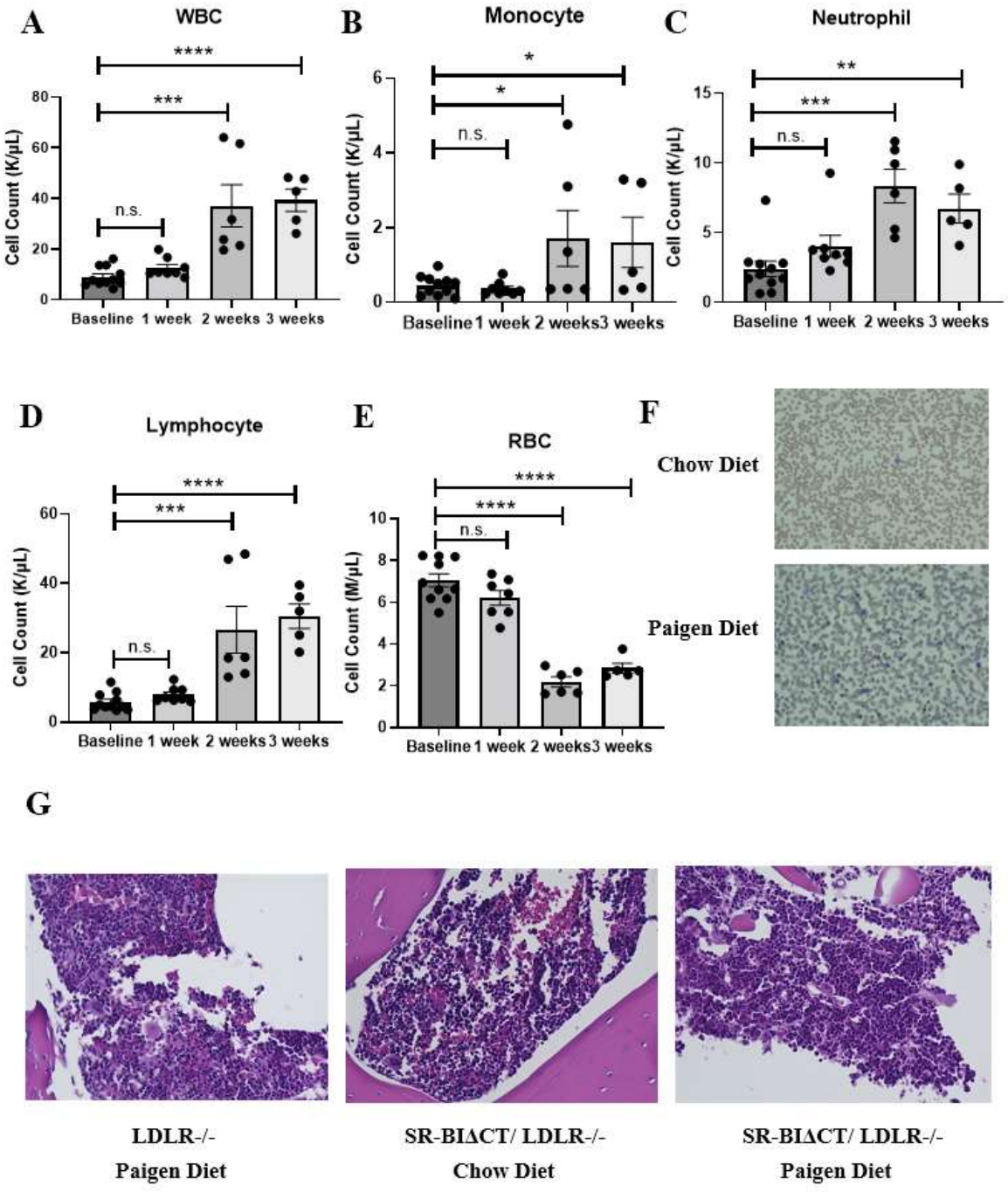
A
WBC
Cell Count (K/μL)
Baseline 1 week 2 weeks 3 weeks
B
Monocyte
Cell Count (K/μL)
Baseline 1 week 2 weeks 3 weeks
C
Neutrophil
Cell Count (K/μL)
Baseline 1 week 2 weeks 3 weeks
D
Lymphocyte
Cell Count (K/μL)
Baseline 1 week 2 weeks 3 weeks
E
RBC
Cell Count (M/μL)
Baseline 1 week 2 weeks 3 weeks
F
Chow Diet
Paigen Diet
G
LDLR-/-
Paigen Diet
SR-BIΔCT/ LDLR-/-
Chow Diet
SR-BIΔCT/ LDLR-/-
Paigen Diet

Figure 4. Atherogenic diet alters the hematological profiles of SR-BIΔCT/ LDLR-/- mice. Cell counts of total white blood cells **(A)** monocytes **(B)** neutrophils **(C),** lymphocytes **(D),** and red blood cells **(E)** of the SR-BIΔCT/ LDLR-/- (n=6) mice at baseline and after 1, 2, and 3 weeks of atherogenic diet. (Paired student t test, *, $p<0.05$, **, $p<0.01$, ***, $p<0.001$, ****, $p<0.0001$). **(F)** Representative blood smears of the SR-BIΔCT/ LDLR-/- mice after three weeks of chow or atherogenic Paigen diet (40x). **(G)** Representative H&E staining images of the bone marrow of LDLR-/- and SR-BIΔCT/ LDLR-/- on either chow diet or atherogenic Paigen diet for four weeks (40x).

3.1e. Atherogenic diet shortened the life span of SR-BIΔCT/LDLR-/-mice

On chow diet, SR-BIΔCT/LDLR-/-mice showed similar body weight, behaviors and coat colors compared to LDLR-/- mice. Since SR-BIΔCT/ apoE-/- mice die prematurely on chow diet[62], in order to determine whether diet intervention as well as the age starting diet will affect the life span of the SR-BIΔCT/LDLR-/-mice, we started atherogenic diet at 6-week-old **(Figure 5A)**, 18-week-old **(Figure 5B)** and 30-week-old **(Figure 5C)** of both SR-BIΔCT/LDLR-/-and LDLR-/- mice. We found that SR-BIΔCT/LDLR-/-mice, regardless of their age, began to die at around 20 days and died within 60 days after the initiation of diet, with the majority died between 25 to 35 days of diet **(Figure 5D)**. However, the overall lifespan was significantly shorter in SR-BIΔCT/LDLR-/- mice starting diet at 6-week-old. There was no statistically significant difference between the lifespans of SR-BIΔCT/LDLR-/- mice starting diet at 18-week-old or 30-week-old. In addition, male SR-BIΔCT/LDLR-/- mice had longer lifespan following the initiation of atherogenic diet than female SR-BIΔCT/LDLR-/-mice (**Figure 5E**). In comparison, the survival rate of LDLR-/- mice was not affected by diet intervention.

It has been previously shown that the CREKA (Cys-Arg-Glu-Lys-Ala) can home to the atherosclerotic plaque[233]. In our previous models with SR-BI background, it has been demonstrated that fibrin presents in the plaque of both SR-BI-/-/apoE-/- mice on chow diet and SR-BI-/-/LDLR-/- mice fed with high cholesterol Paigen diet [234235]. PVAX works in areas with elevated level of H_2O_2 [110]. It has been demonstrated that aged LDLR-/- have elevated oxidative stress[236]. Specifically, the oxidative stress is high in aged aorta[237]. Based on our age-related survival rate data, to ensure highest survival rate during the study period, as well as clinical relevance, we decided to start nano-therapy intervention in 30-week-old SR-BIΔCT/LDLR-/- mice placed on high cholesterol atherogenic diet.

Figure 5

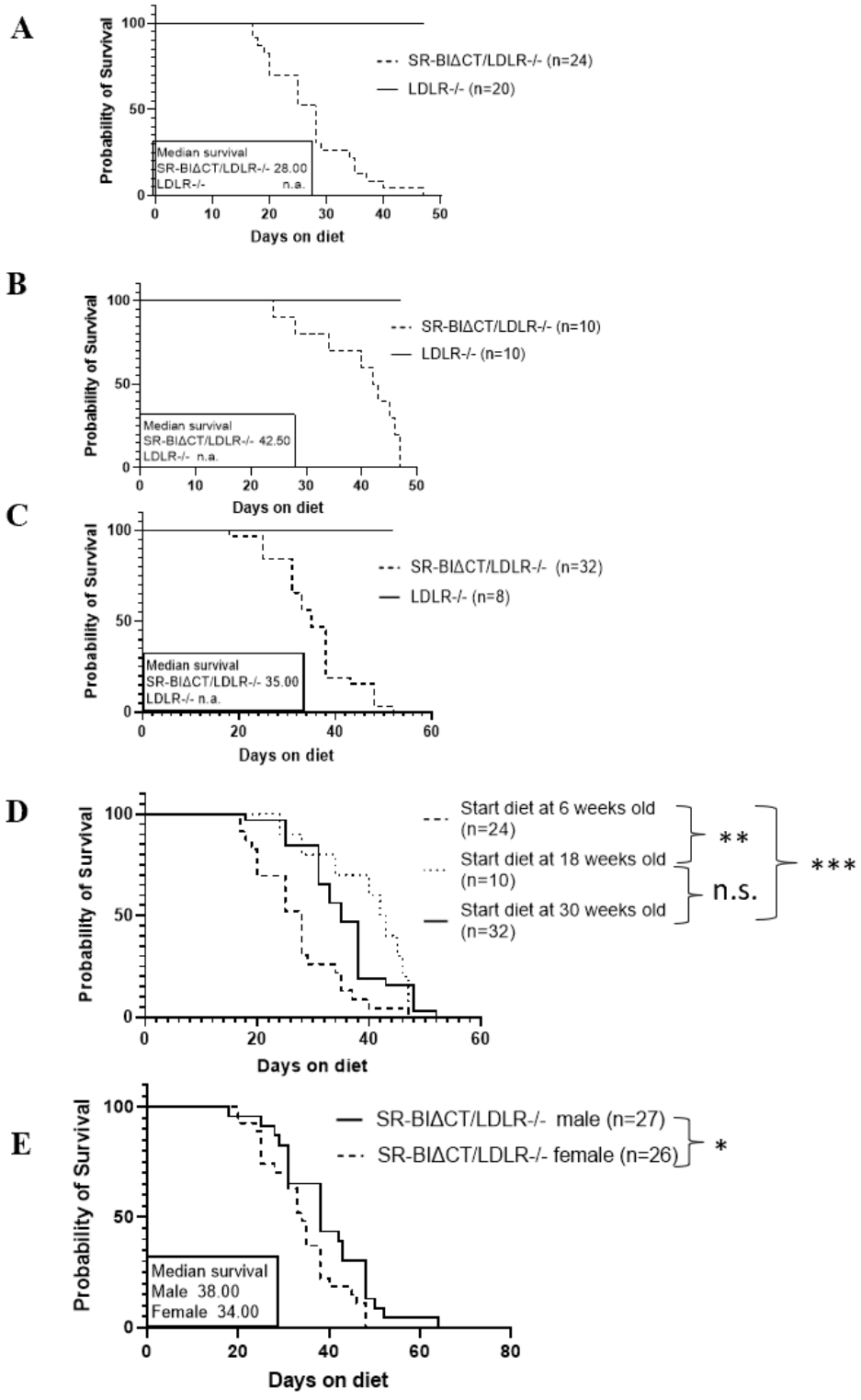
A
Probability of Survival
100
50
0
0 10 20 30 40 50
Days on diet
SR-BIΔCT/LDLR-/- (n=24)
LDLR-/- (n=20)
Median survival
SR-BIΔCT/LDLR-/- 28.00
LDLR-/- n.a.
B
Probability of Survival
100
50
0
0 10 20 30 40 50
Days on diet
SR-BIΔCT/LDLR-/- (n=10)
LDLR-/- (n=10)
Median survival
SR-BIΔCT/LDLR-/- 42.50
LDLR-/- n.a.
C
Probability of Survival
100
50
0
0 20 40 60
Days on diet
SR-BIΔCT/LDLR-/- (n=32)
LDLR-/- (n=8)
Median survival
SR-BIΔCT/LDLR-/- 35.00
LDLR-/- n.a.
D
Probability of Survival
100
50
0
0 20 40 60
Days on diet
Start diet at 6 weeks old (n=24)
Start diet at 18 weeks old (n=10)
Start diet at 30 weeks old (n=32)
**
n.s.
***
E
Probability of Survival
100
50
0
0 20 40 60 80
Days on diet
SR-BIΔCT/LDLR-/- male (n=27)
SR-BIΔCT/LDLR-/- female (n=26)
*
Median survival
Male 38.00
Female 34.00

Figure 5. Atherogenic diet shortened the lifespan of SR-BIΔCT/ LDLR-/- mice. Kaplan-Meier survival curves of 6-wk-old **(A),** 18-week-old **(B)** and 30-week-old **(C)** SR-BIΔCT/LDLR-/- and LDLR-/- mice after atherogenic diet intervention. **D.** Kaplan-Meier survival curves of SR-BIΔCT/LDLR-/- mice starting atherogenic diet intervention at 6 weeks old, 18 weeks old or 30 weeks old. **E.** Kaplan-Meier survival curves of male and female SR-BIΔCT/LDLR-/- mice after starting atherogenic diet. (Kaplan–Meier survival analysis, *, $p<0.05$, **, $p<0.01$, ***, $p<0.001$.)

3.2 Nanomedicine and the amelioration of cardiovascular disease

3.2.a. Nanocomplex assisted antioxidant and antiplatelet treatment preserved the cardiac functions of the SR-BIΔCT/LDLR-/- mice on atherogenic diet.

In order to investigate whether antiplatelet, antioxidant, or a combination of the two therapies could have different effects on the cardiac functions of the mice, we monitored the cardiac functions weekly using echocardiography. Based on our data that the first two weeks of diet did not significantly change the cardiac functions of the mice but the SR-BIΔCT/LDLR-/- mice started to show significant cardiac functional impairment on the third week of diet. We found that at the end of three-week atherogenic diet intervention, PBS and tirofiban groups failed to preserve their cardiac functions (**Figure 6A-C**). However, mice treated with PVAX had less profound decrease in ejection fraction and mostly preserved their fractional shortening. In comparison, TPM treatment showed superiority to other groups with the best preservation of ejection fraction and fractional shortening.

Figure 6

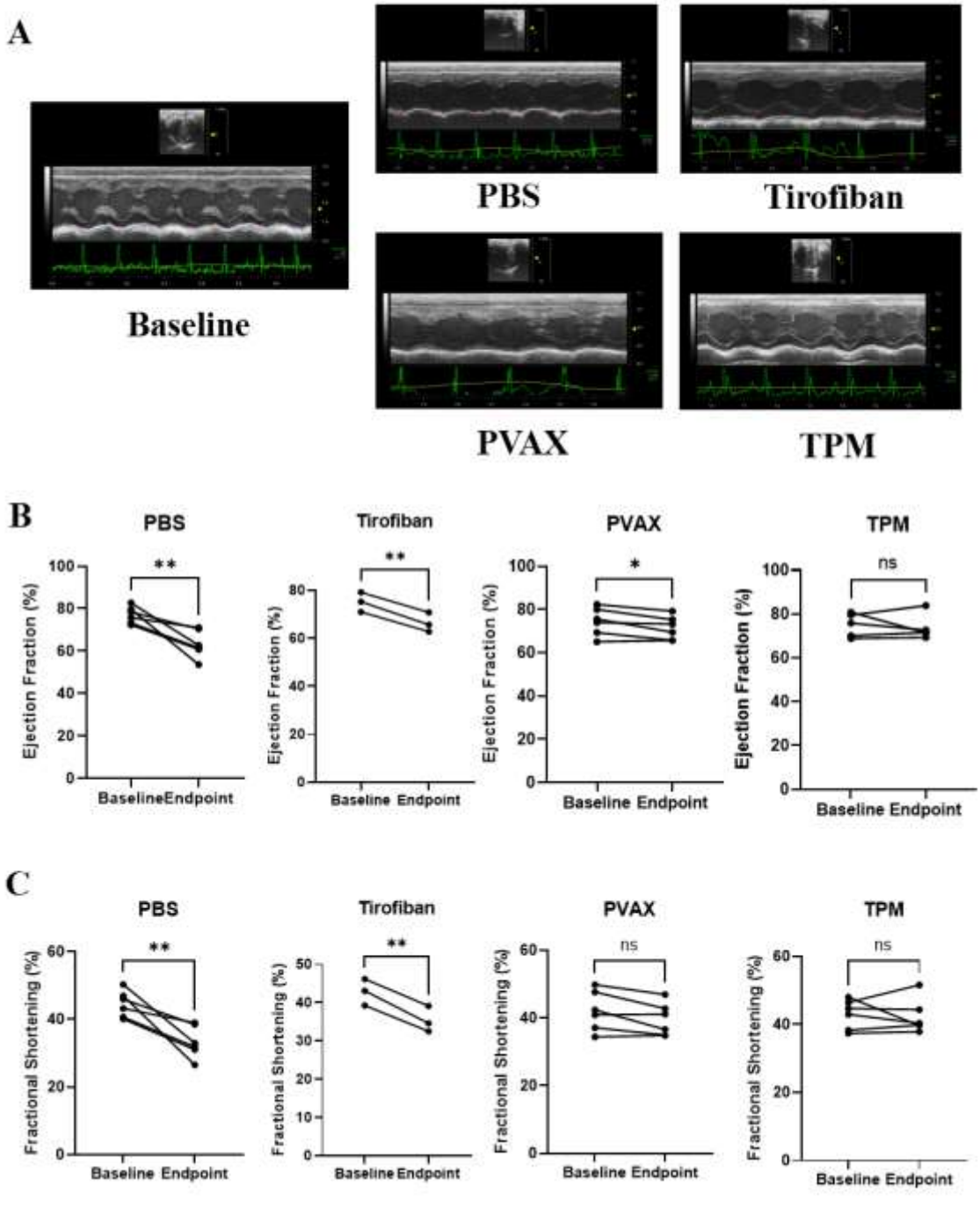
A
Baseline
PBS
Tirofiban
PVAX
TPM
B
PBS
Tirofiban
PVAX
TPM
Ejection Fraction (%)
**
*
ns
Baseline
Endpoint
C
Fractional Shortening (%)
**
ns
Baseline
Endpoint

Figure 6. Cardiac functional changes in SR-BIΔCT/LDLR-/- mice after receiving different treatments. (A) Representative M-mode echocardiographic still images of SR-BIΔCT/LDLR-/- mice at baseline and after atherogenic diet intervention receiving PBS, tirofiban, PVAX, or tirofiban carrying PVAX-incorporated micellular nanocomplex (TPM). Ejection Fraction **(B)** and Fractional Shortening **(C)** changes between baseline and endpoint (3wks after atherogenic diet) in mice subjected to PBS (n=6), tirofiban (n=3), PVAX (n=6), or tirofiban carrying PVAX-incorporated micellular nanocomplex (TPM) (n=6) treatment. (paired student t test. *, $p<0.05$, **<0.01)

3.2.b. Nanoparticle assisted antioxidant treatment improved hematological profiles of the SR-BIΔCT/LDLR-/- mice induced by atherogenic diet.

Because after three weeks of atherogenic diet, the SR-BIΔCT/LDLR-/- mice exhibited profound leukocytosis, neutrophilia, lymphocytosis, and severe anemia, in order to assess whether the nanoparticle assisted treatment would rectify these abnormalities, we determined the complete blood count of these mice following different treatments. We found that PVAX antioxidant treatment could hinder the expansion of the circulating neutrophils and lymphocytes and improved the anemic phenotype (**Figure 7A-D**). The TPM treatment was able to rectify all parameters of the hematological profile. The mice that were treated with only the antiplatelet tirofiban did not show any improvement in their hematological profiles.

Figure 7

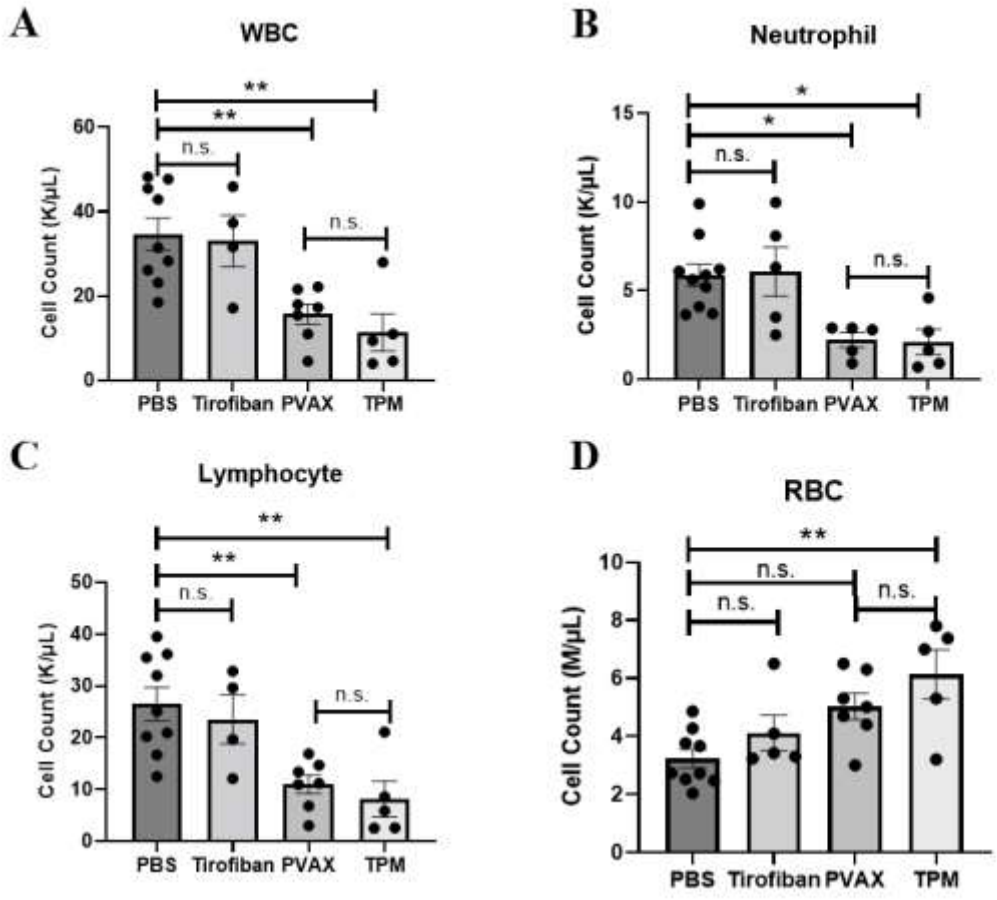

Figure 7. Hematological profiles of SR-BIΔCT/LDLR-/- mice receiving different treatments. Cell counts of total white blood cells **(A)**, neutrophils **(B)**, lymphocytes **(C)**, and red blood cells **(D)** of the SR-BIΔCT/LDLR-/- mice after atherogenic diet intervention while receiving PBS (n=9), tirofiban (n=5), PVAX (n=7), or tirofiban carrying PVAX-incorporated micellular nanocomplex (TPM) (n=5). (One Way ANOVA. *, $p<0.05$, **, $p<0.01$).

3.2.c. Nanoparticle assisted antioxidant and antiplatelet dual treatment did not alter the lipid profiles in SR-BIΔCT/LDLR-/- mice during the treatment period.

In order to determine whether the therapeutic effects of nanoparticle treatment were related to the lipid content in the plasma, we measured the plasma total cholesterol and free cholesterol of SR-BIΔCT/LDLR-/- mice after different treatments. We found that the lipid profiles were not altered by the treatments (**Figure 8 A-D**).

Figure 8

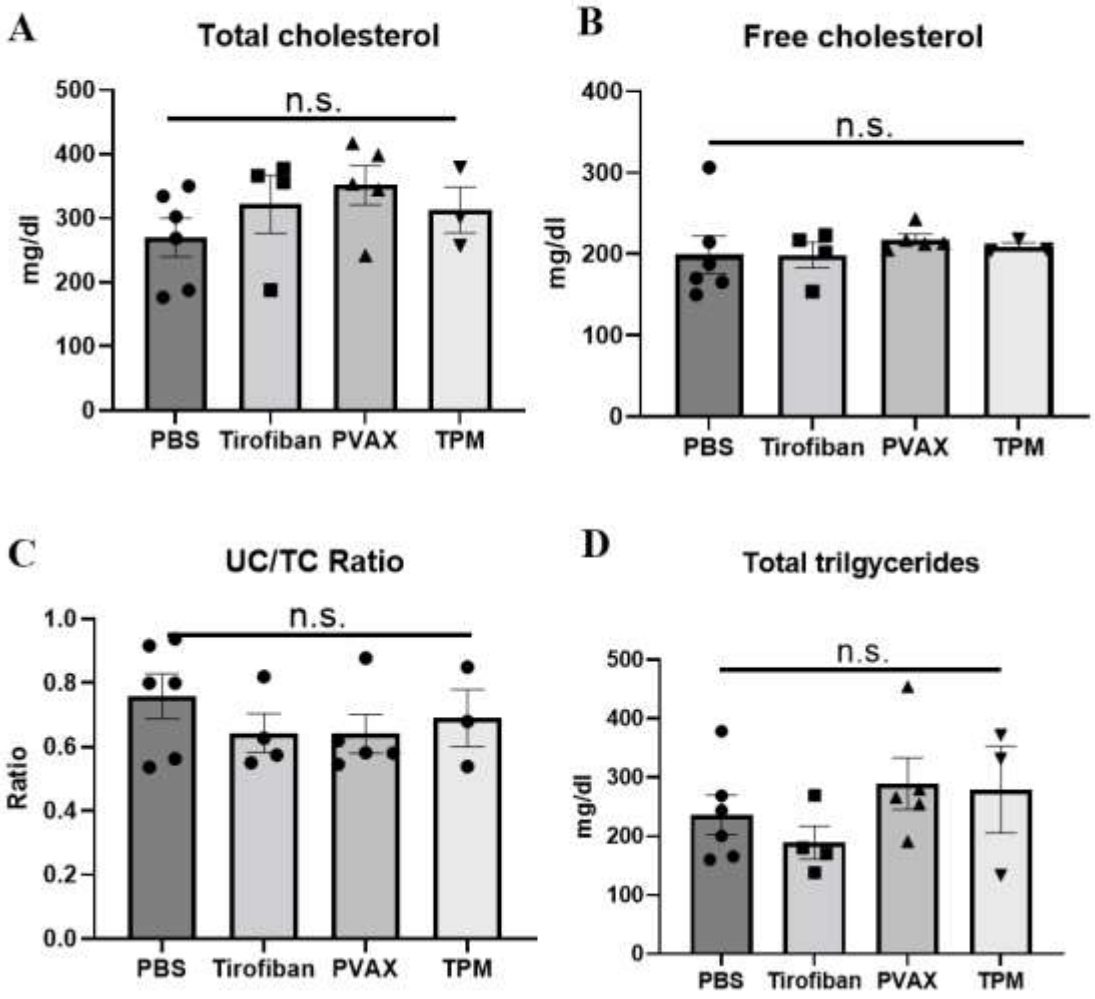

Figure 8. lipid profiles of SR-BIΔCT/LDLR-/- mice receiving different treatments. Plasma concentration of total cholesterol **(A),** free cholesterol **(B),** unesterified cholesterol (UC) to total cholesterol (TC) ratio **(C),** and total triglycerides **(D),** of the SR-BIΔCT/LDLR-/- mice after atherogenic diet intervention while receiving PBS (n=5), tirofiban (n=4), PVAX (n=3), or tirofiban carrying PVAX-incorporated micellular nanocomplex (TPM) (n=3). (One way ANOVA)

3.2.d. Nanoparticle assisted antioxidant treatment decreased fasting glucose

In order to evaluate whether antioxidant treatments could have an impact on the glucose regulation, an important risk factor of cardiovascular disease, we measured the fasting glucose level of mice subjected to different treatments after three weeks of atherogenic diet challenge. We found that mice that received PVAX and TPM had significantly lower fasting glucose levels compared to the groups that received PBS and tirofiban (**Figure 9**).

Figure 9

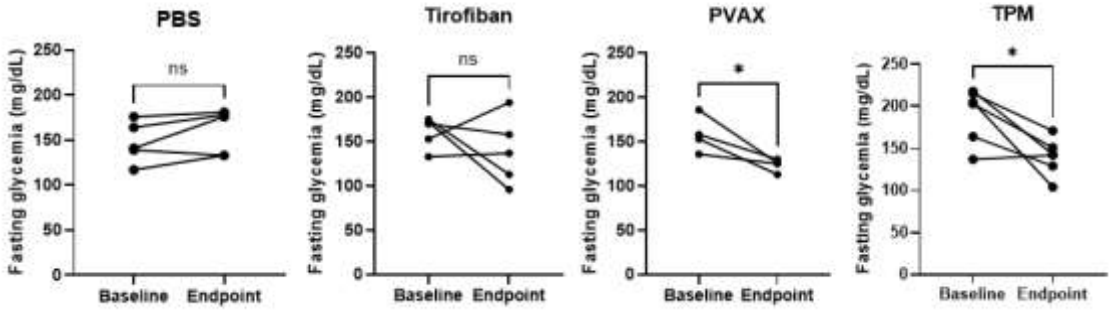

Figure 9. Fasting glucose levels of SR-BIΔCT/LDLR-/- mice receiving different treatments. (A) Fasting glucose levels of SR-BIΔCT/LDLR-/- mice at baseline and after atherogenic diet intervention while receiving PBS (**A**) (n=4), tirofiban (**B**) (n=5), PVAX (**C**) (n=4), or tirofiban carrying PVAX-incorporated micellular nanocomplex (TPM) (**D**) (n=4). (paired student t test. *, $p<0.05$)

3.3 Treg specific SRSF1 abnormality links autoimmune disease and cardiovascular disease

3.3.a. Treg specific Srsf1 deficiency impairs the cardiac function in mice

It has been previously shown that the $Srsf1^{fl/fl}.Foxp3^{cre}$ mice died around weaning age[215]. In order to investigate whether the cardiac function was impaired by the Treg specific Srsf1 deficiency, which led to the immature death of the knockout mice, I compared the ejection fraction and fractional shortening among the $Srsf1^{+/+}.Foxp3^{cre}$, $Srsf1^{fl/+}.Foxp3^{cre}$, and $Srsf1^{fl/fl}.Foxp3^{cre}$ mice. I found that the heterozygous $Srsf1^{fl/+}.Foxp3^{cre}$ mice had similar ejection fraction and fractional shortening compared to the $Srsf1^{+/+}.Foxp3^{cre}$ mice (**Figure 10**). However, these cardiac functional parameters were significantly decreased in the $Srsf1^{fl/fl}.Foxp3^{cre}$ mice.

Figure 10

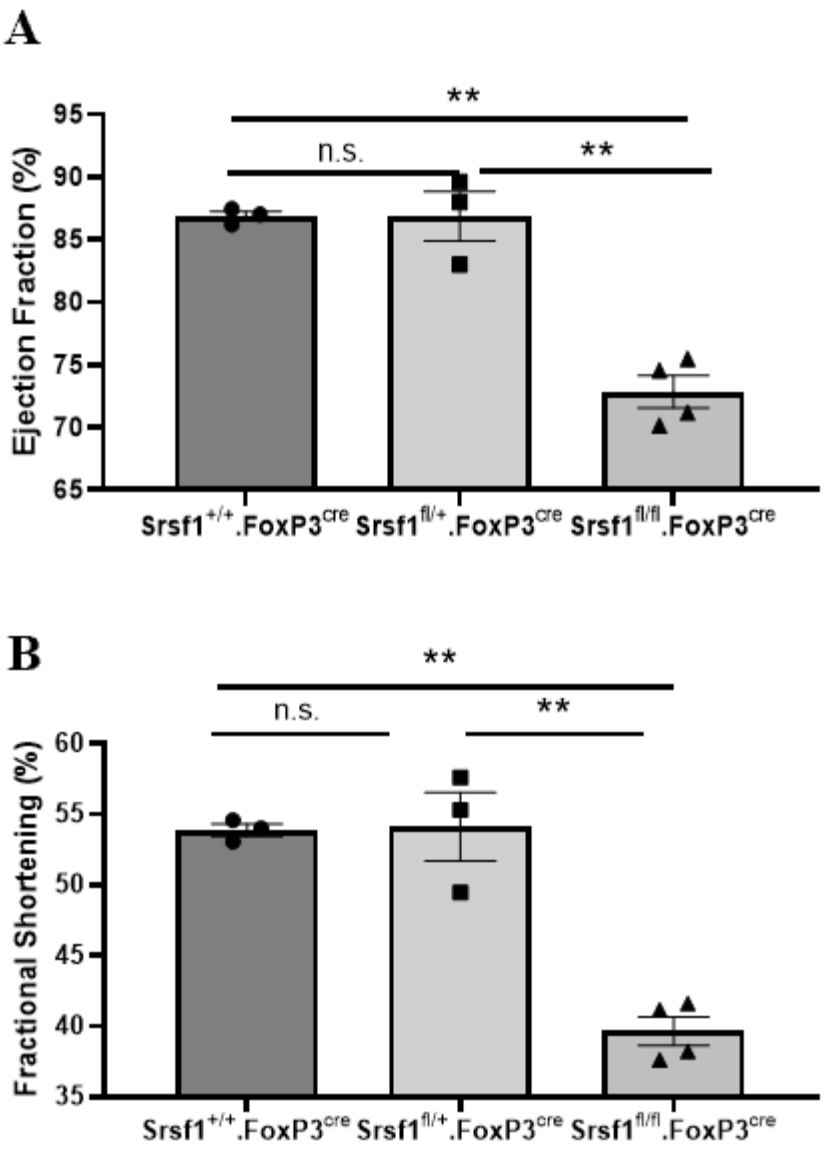

Figure 10. Srsf1$^{fl/fl}$.Foxp3^{cre} mice showed impaired cardiac functions. At 3 weeks of age, the ejection fraction (**A**) and fractional shortening (**B**) of Srsf1$^{+/+}$.Foxp3^{cre}, Srsf1$^{fl/+}$.Foxp3^{cre}, and Srsf1$^{fl/fl}$.Foxp3^{cre} mice were assessed by echocardiogram (mean ± SEM, n = 3-4/group). (One way ANOVA. **, $p<0.01$).

3.3.b. Treg specific Srsf1 deficiency does not alter the plasma cholesterol level, but decreases the plasma triglyceride level

In order to determine whether Treg specific Srsf1 knockout will affect the circulating lipid contents, I measured the total cholesterol and triglyceride contents in the plasma of $Srsf1^{+/+}.Foxp3^{cre}$, $Srsf1^{fl/+}.Foxp3^{cre}$, and $Srsf1^{fl/fl}.Foxp3^{cre}$ mice. I found that the cholesterol levels of the mice were not affected by the absence of Srsf1 in Tregs (**Figure 11A**). However, Treg specific deficiency of Srsf1 significantly lowered the circulating triglyceride level **(Figure 11B)**.

Figure 11

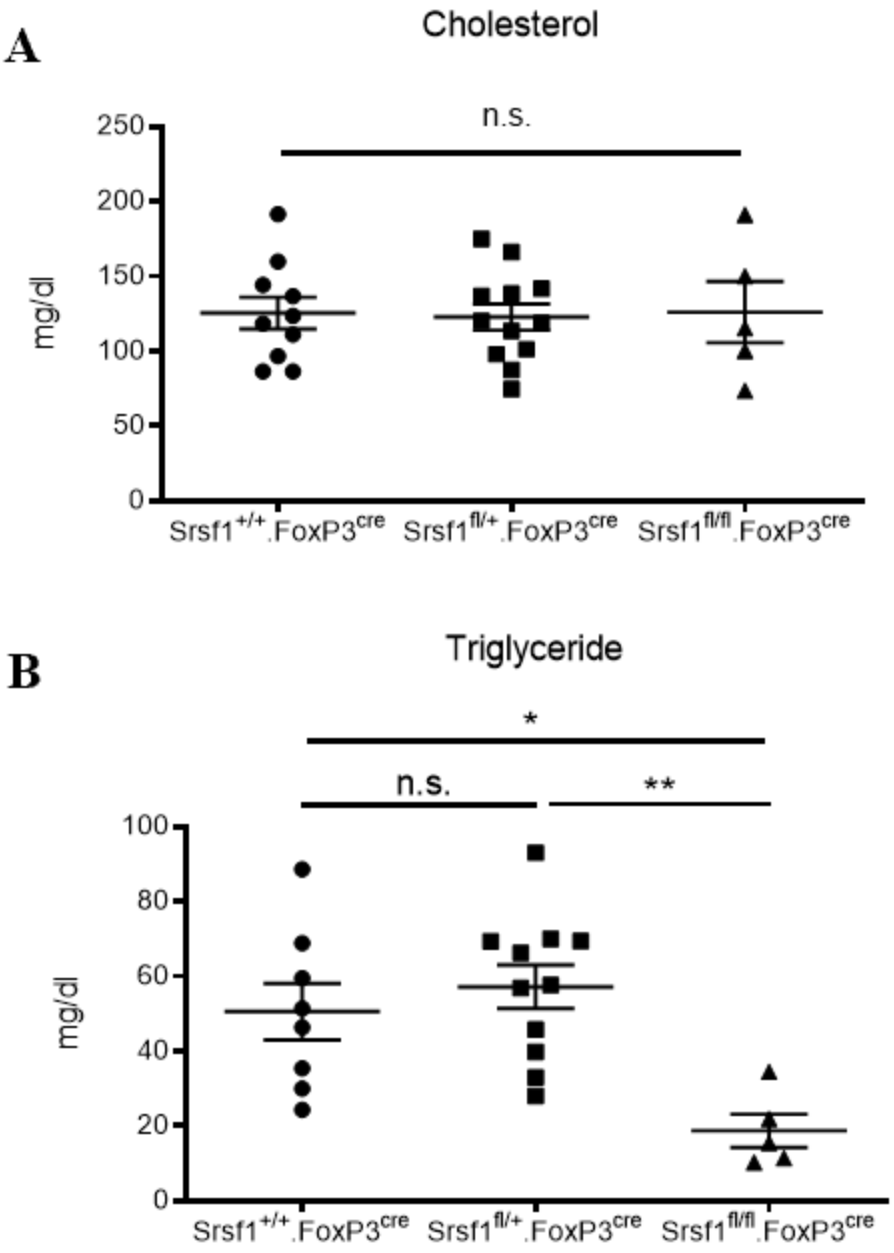

Figure 11. Srsf1$^{fl/fl}$.Foxp3^{cre} mice showed decreased circulating triglyceride level. At 3 weeks of age, the circulating cholesterol (**A**) and triglyceride (**B**) level of Srsf1$^{+/+}$.Foxp3^{cre} , Srsf1$^{fl/+}$.Foxp3^{cre} , and Srsf1$^{fl/fl}$.Foxp3^{cre} mice were measured (mean ± SEM, n = 5-12/group). (One Way ANOVA. *, $p<0.05$, **, $p<0.01$).

3.3.c. Heterozygous Treg-specific Srsf1 knockout mice showed dysfunctional Tregs following induction of inflammation

Due to the premature death of the Srsf1$^{fl/fl}$.Foxp3^{cre} mice, we compared the heterozygous Srsf1$^{fl/+}$.Foxp3^{cre} mice with the WT Srsf1$^{+/+}$.Foxp3^{cre} mice to examine the Treg suppressing function on an experimental autoimmune encephalomyelitis (EAE) murine model of multiple sclerosis. It has been shown that Tregs are involved in the recovery phase of the disease course and dysfunctional Tregs hinder its recovery[238,239]. We found that the HET mice experienced impaired disease recovery by showing higher clinical scores compared to the WT mice (**Figure 12**).

Figure 12

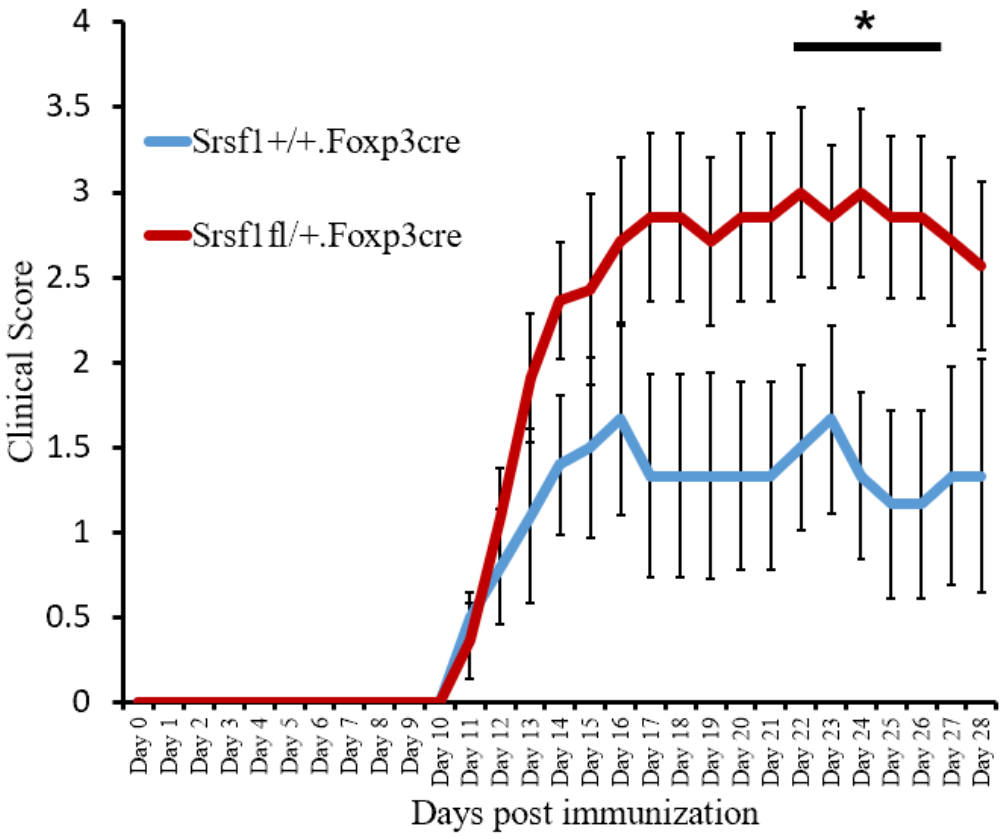

Figure 12. Srsf1$^{fl/+}$·Foxp3^{cre} mice showed worsened disease progression upon EAE induction. At 8 weeks of age, EAE was induced in Srsf1$^{+/+}$.Foxp3^{cre} and Srsf1$^{fl/+}$.Foxp3^{cre} mice by immunization with $MOG_{35–55}$ emulsified in the complete Freund's adjuvant. Daily clinical scores were measured. Cumulative results of two independent experiments are shown (mean ± SEM, n = 6-7/group). (unpaired student t test. *, $p<0.05$).

In addition, on day 14 of the EAE, we assessed the immune cell infiltration in the spinal cord using H&E staining. The H&E staining showed that Srsf1$^{fl/+}$.Foxp3^{cre} mice exhibited increased immune cell infiltration in the spinal core after EAE (**Figure 13**).

Figure 13

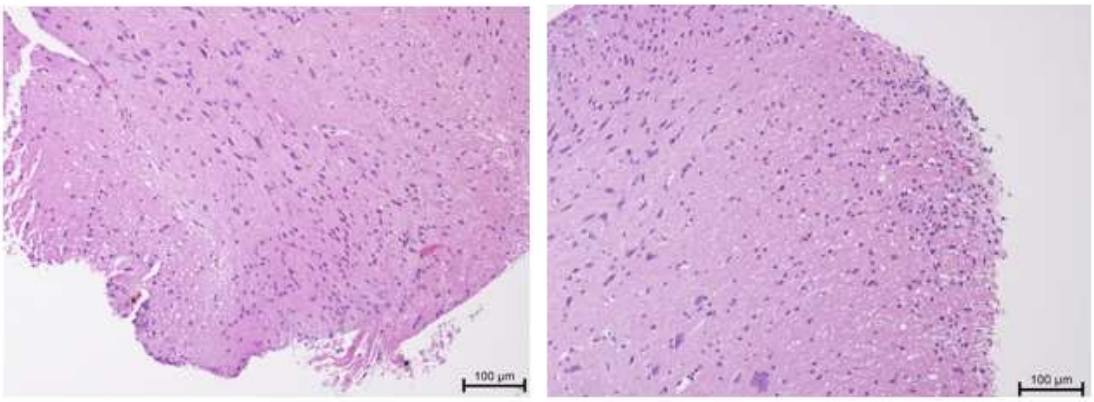

Figure 13. Srsf1$^{fl/+}$·Foxp3^{cre} mice showed increased inflammation in the spinal cord after EAE. H&E staining images showing spinal cords of Srsf1$^{+/+}$.Foxp3^{cre} and Srsf1$^{fl/+}$.Foxp3^{cre} harvested on day 14 of the EAE experiment.

In order to determine the specific cell type of the immune cells infiltrated in the spinal cord, on day 14 after immunization, we assessed the immune cells infiltrated in the spinal cords of the $Srsf1^{+/+}$.$Foxp3^{cre}$ and $Srsf1^{fl/+}$.$Foxp3^{cre}$ mice and found a significant increase in cell counts of lymphocyte, T cells, $CD4^+$ T cells, and the IFNγ producing $CD4^+$ T cells (**Figure 14**). In addition, there was a trend towards elevated $CD8^+$ T cells and IL-17A producing $CD4^+$ T cells in the $Srsf1^{fl/+}$.$Foxp3^{cre}$ spinal cords. These data suggested worsened inflammation in the $Srsf1^{fl/+}$.$Foxp3^{cre}$ mice.

Figure 14

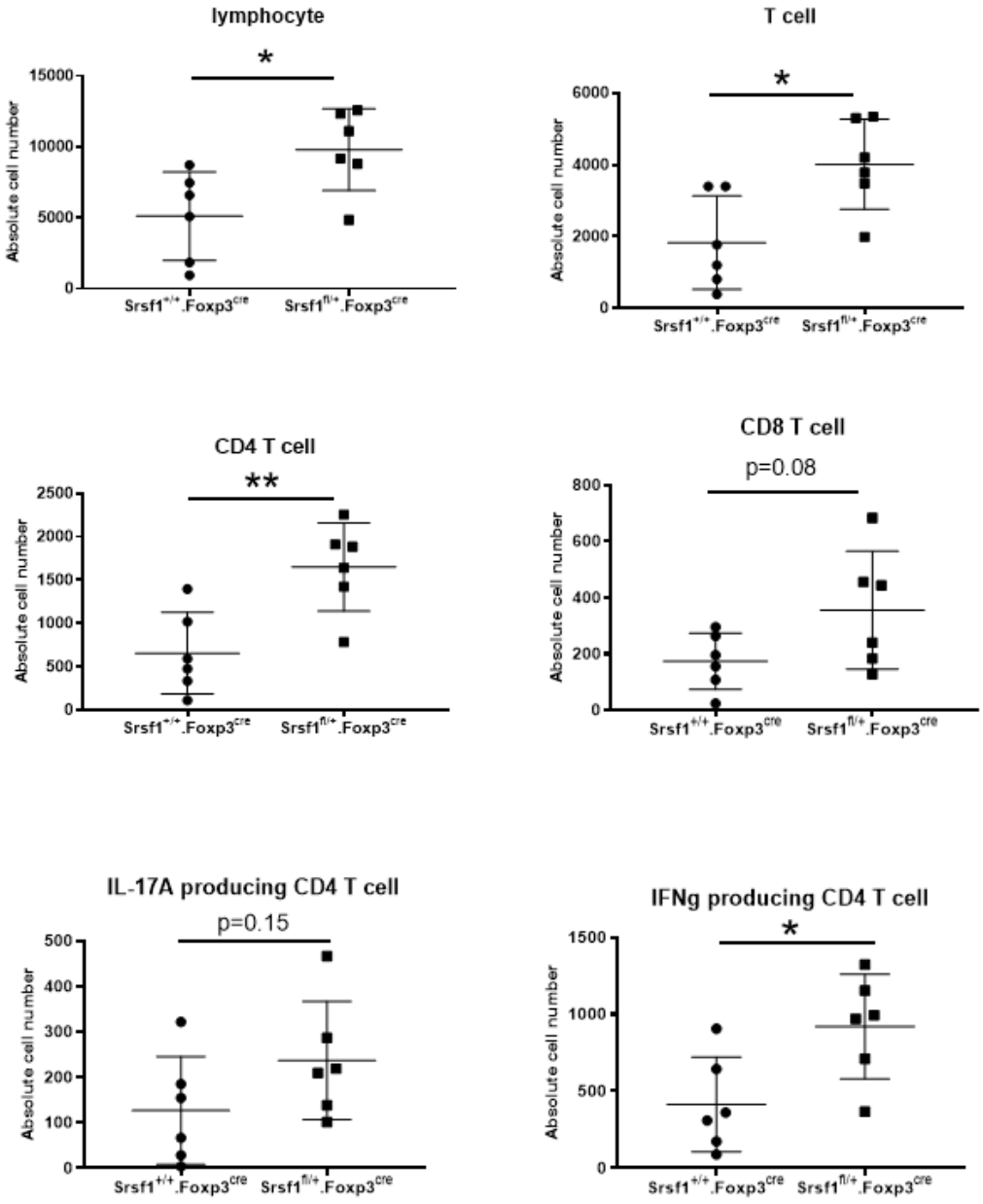

Figure 14. Srsf1$^{fl/+}$·Foxp3^{cre} mice showed increased inflammatory cell infiltration in the spinal cord after EAE. Absolute cell numbers of spinal cord–infiltrated CD4$^+$ T cells, CD8$^+$ T cells, IL-17A–producing CD4$^+$ T cells, and IFNγ-producing CD4$^+$ T cells were evaluated by flow cytometry on day 14 after EAE. Cumulative data are shown (mean ± SEM, n = 6/group).

In order to determine the specific cell type of the immune cells infiltrated in the spinal cord, on day 14 after immunization, we assessed the immune cells infiltrated in the spinal cords of the Srsf1$^{+/+}$.Foxp3^{cre} and Srsf1$^{fl/+}$.Foxp3^{cre} mice and found a significant increase in cell counts of lymphocyte, T cells, CD4^{+} T cells, and the IFNγ producing CD4^{+} T cells (**Figure 14**). In addition, there was a trend towards elevated CD8^{+} T cells and IL-17A producing CD4^{+} T cells in the Srsf1$^{fl/+}$.Foxp3^{cre} spinal cords. These data suggested worsened inflammation in the Srsf1$^{fl/+}$.Foxp3^{cre} mice.

Figure 15

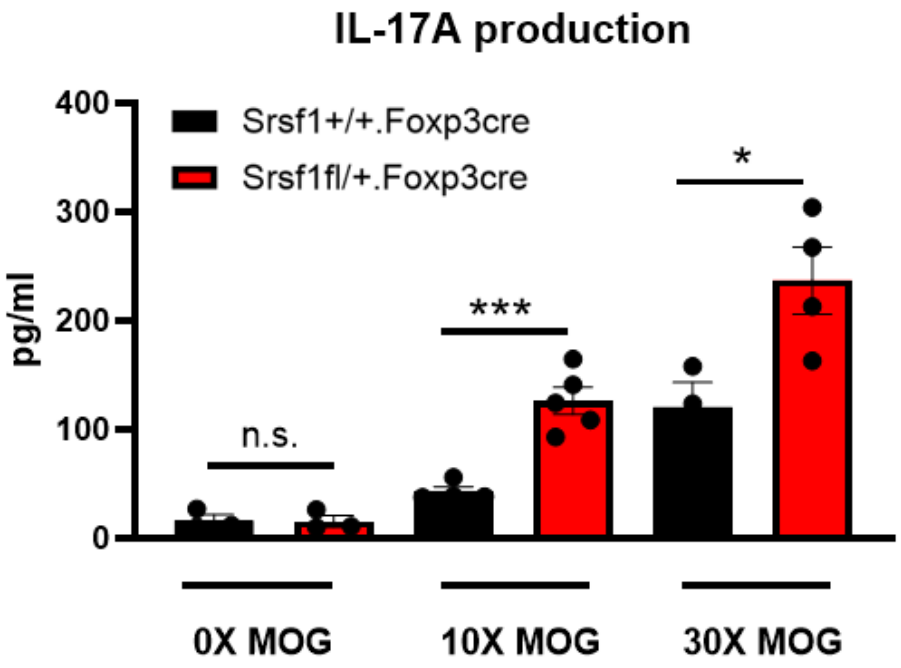

Figure 15. Lymphocytes from Srsf1$^{fl/+}$·Foxp3^{cre} showed elevated IL17-A production upon EAE immunization. Mononuclear cells harvested from inguinal lymph nodes on day 7 were activated in vitro with different concentrations of MOG$_{35–55}$ for 3 days. IL-17A concentrations were measured by ELISA. Cumulative data are shown (mean ± SEM, n = 3-6/group). (unpaired student t test. *, $p<0.05$, ***,$p<0.001$).

3.3.d. Loss of SRSF1 alters molecular pathways and gene signatures involved in lipid metabolism

In order to explore the molecular pathways that might be involved in the lipid metabolism of dysfunctional Tregs, we reanalyzed the RNA-seq data of Tregs derived from T cell specific Srsf1 deficient mice[186]. Pathway analysis of the RNA-seq data of the Tregs isolated from the complete T cell knockout model showed that pathways such as fatty acid activation and fatty acid beta oxidation were significantly enriched (**Figure 16A**). In addition, in the volcano plot, we also found several gene signatures related to lipid metabolism that were significantly altered, including down-regulation of Stearoyl-CoA desaturase 1 (Scd1), Fatty Acid Desaturase 2 (FASD2), VLDLR, and up-regulation of Angiopoietin-like 2 (Angptl2) indicating Treg specific insufficiency of SRSF1 may also be associated with impaired lipid metabolism (**Figure 16B**).

Figure 16

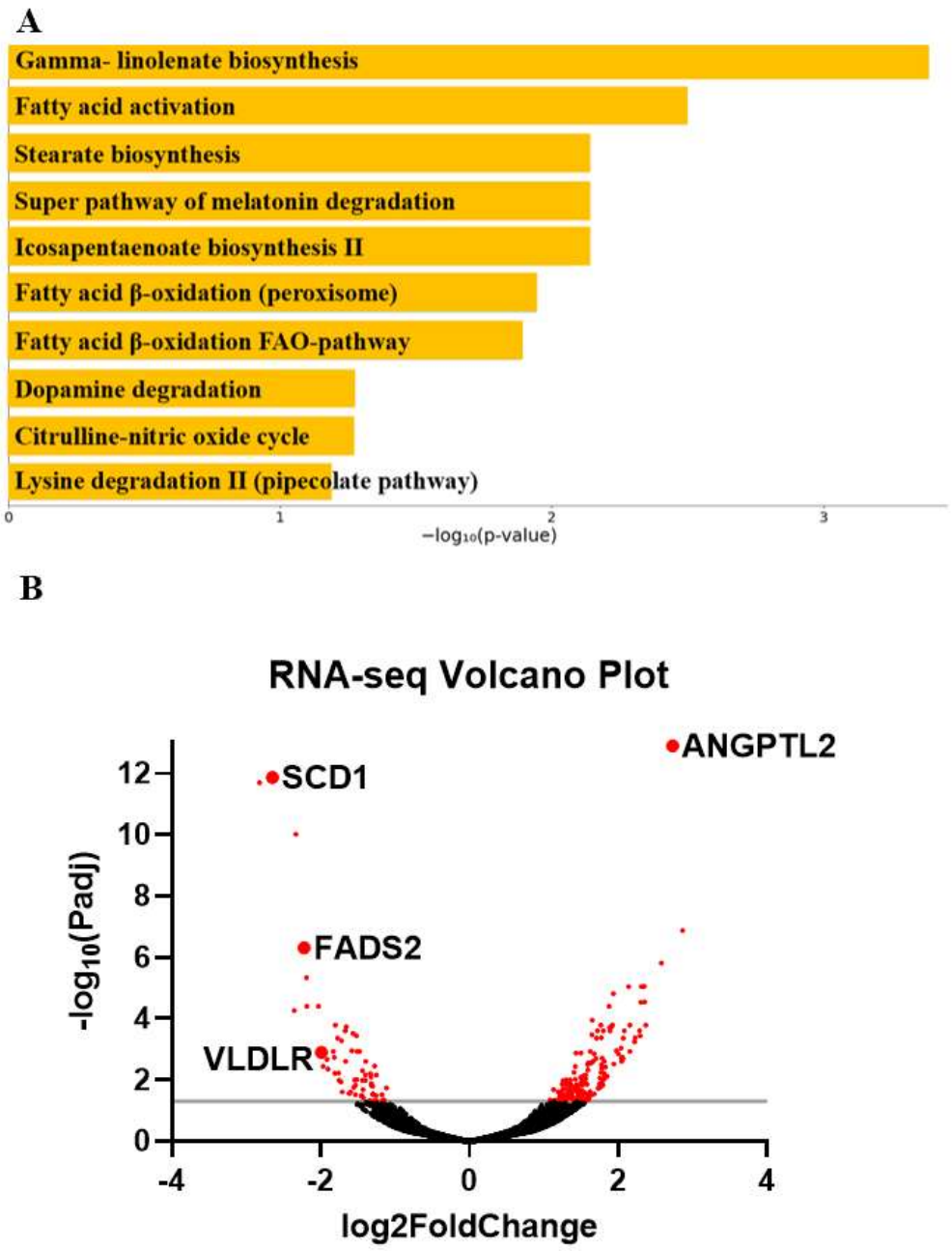

Figure 16. RNA-seq analyses in lipid metabolism in Tregs derived from T cell-specific Srsf1 deficient mice. RNA-seq data (GEO: GSE173268) were extracted and analyzed. (**A**) enriched pathways of the RNA-seq data, (**B**) volcano plot showing differentially expressed genes

3.4. The regulation of Srsf1 on CD8 functions and its implications in cardiovascular disease.

Using the T cell conditional knockout mice ($Srsf1^{fl/fl}$.$dLck^{cre}$) that lack SRSF1 selectively in T cells[185], we examined the role of SRSF1 in CD8 T cells in these Srsf1-conditional knockout (cKO) mice. While the frequencies of both CD4 and CD8 T cells were reduced in the $Srsf1^{fl/fl}$.$dLck^{cre}$ mice, the CD8 T cell compartment was profoundly depleted (18.9% n=10) with 2-3-fold reduced frequencies compared to the wild-type (WT) mice (29.6% n=10) **(Figure 17A and B)**. The proportions of CD8:CD4 T cell populations were significantly altered from normal ratios of 0.64 in WT mice to 0.4 in the $Srsf1^{fl/fl}$.$dLck^{cre}$ mice **(Figure 17B)**. We further evaluated the functional capacity of the CD8 T cells using the effector-to-target cell cytotoxicity luminescence assays. $Srsf1^{fl/fl}$.$dLck^{cre}$ CD8 T cells displayed significantly reduced ability to kill target cells as evidenced by decreased luminescent signals indicative of cell lysis in the 10:1, 5:1 and 2.5:1 effector: target ratios ($p<0.05$) compared to CD8 T cells from WT mice **(Figure 17C)**. Altogether, these results indicate that SRSF1 is essential for the homeostasis, proliferative capacity, and cytotoxic function of CD8 T cells.

Figure 17

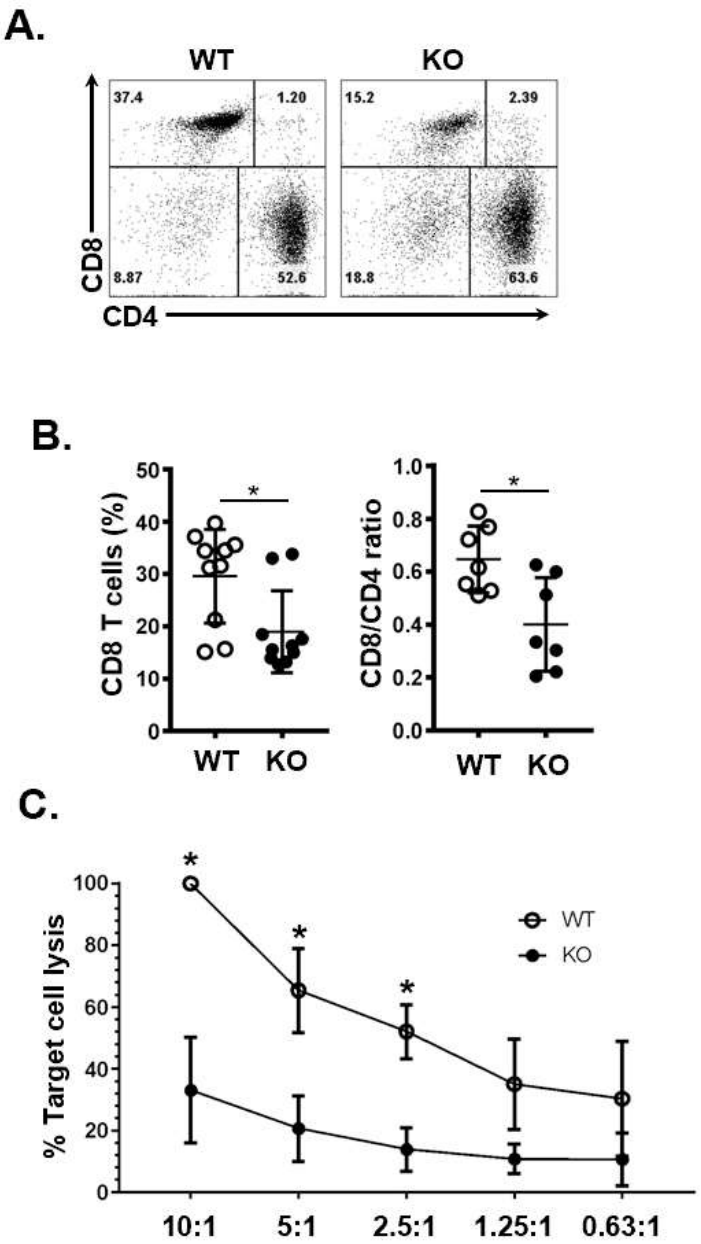

Figure 17. Lower frequency and impaired cytotoxicity activity of CD8 T lymphocytes in Srsf1$^{fl/fl}$.dLck^{cre}. (A) Flow cytometry dot plots show *ex vivo* frequencies of CD8 and CD4 T cells from the spleens of WT and Srsf1$^{fl/fl}$.dLck^{cre} (KO) mice **(B)** Graphs show percentage of CD8 T cells and CD8/CD4 ratio (n=7). **(C)** Graph shows percentage of target cell lysis after coculture with CD8 T cells from WT (n=3) or Srsf1$^{fl/fl}$.dLck^{cre} (KO) mice (n=4), at different effector: target ratios. Graphs show mean±SEM. *, $p<0.05$)

3.4.a. Lower Srsf1$^{fl/fl}$.dLck^{cre} CD8 T cells during the immune response to viral infection

To evaluate the role of SRSF1 in CD8 T cells in response to viral infection, we assessed the CD8 T cell populations in the LCMV-infected WT and Srsf1$^{fl/fl}$.dLck^{cre} mice. We found that Srsf1$^{fl/fl}$.dLck^{cre} mice had a lower frequency of CD8 T cells in the spleen (33.2%) (n=5) compared to the WT mice (48.1%, p=0.0001, n=3). The low number of CD8 cells was not accompanied by CD4 lymphopenia, as shown by the decreased CD8/CD4 ratio in the spleen (7.7) (n=3) of Srsf1$^{fl/fl}$.dLck^{cre} mice compared to WT mice (1.3, p=0.0009) **(Figure 18A and B)**. We also observed a significant increase of double negative (DN) T cells in Srsf1$^{fl/fl}$.dLck^{cre} mice spleen (20.6%) compared to WT mice (2.4%, p=0.0002). These results show that deficiency of SRSF1 may lead to aberrant T cell compartmentalization during the viral immune response.

Figure 18

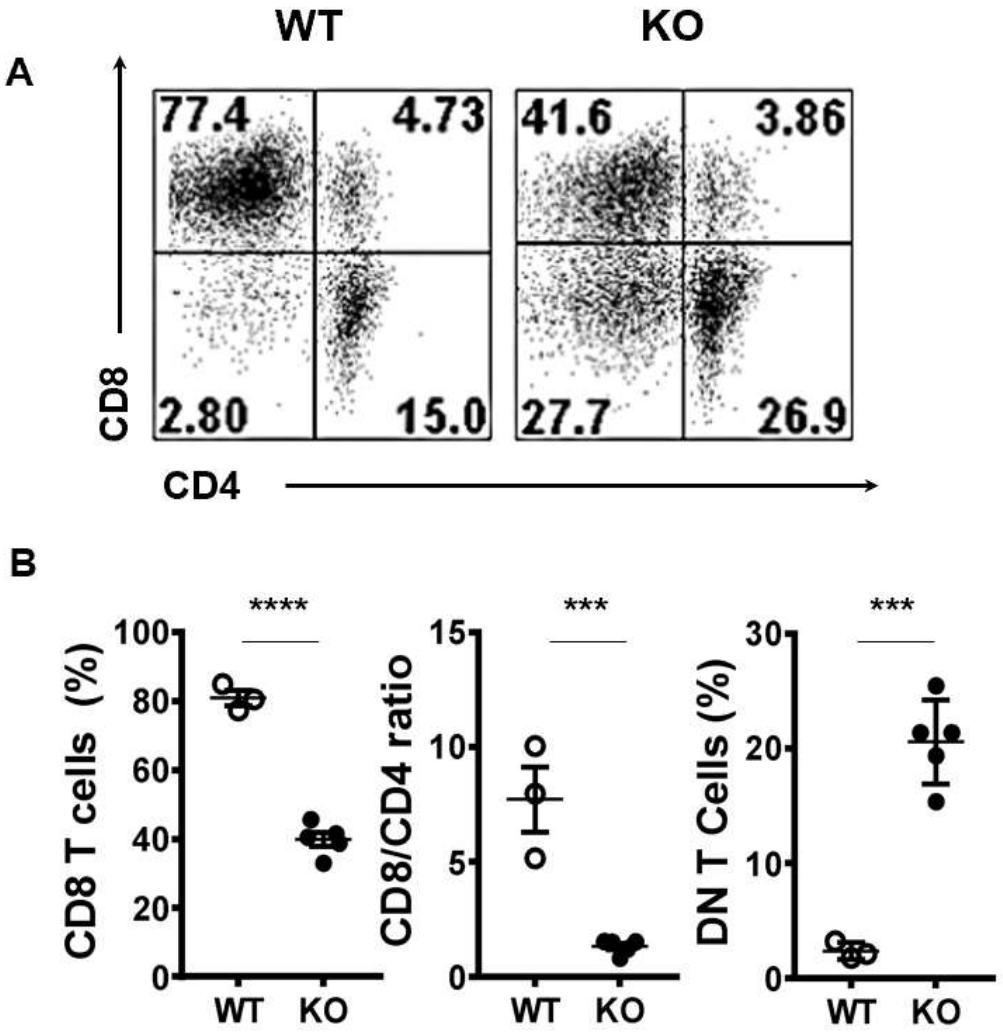

Figure 18. Altered phenotype of Srsf1-cKO CD8 T cells during the immune response to viral infection. *Srsf1*-cKO (KO) or WT mice were infected with LCMV Armstrong strain by IP injection. After 8 days of infection, spleens were collected for T cell phenotyping A) Plots show the frequency of CD8, CD4 and CD4-CD8- double negative (DN) T cells gated on live Thy1.2+ T cells. B) Graphs show the percentages of CD8 T cells, CD8/CD4 ratio and DN in the spleen of WT (n=3) and KO (n=5) mice. (Graphs show mean±SEM. ***, $p<0.005$, ****, $p<0.001$.)

3.4.b. SRSF1 is necessary for CD8 T cell survival and viral clearance

Impaired proliferation and cell cycle arrest eventually lead to cellular apoptosis[240]. It is known that SRSF1 is important for cell cycle progression, and its deficiency leads to impaired proliferation[205]. Therefore, we examined whether SRSF1 controls the anti-apoptotic effects in T cells during the antiviral response. We measured the frequencies of early and late apoptotic T cells post LCMV infection. We found that total T cells and CD8 T cells from the spleen of $Srsf1^{fl/fl}$.$dLck^{cre}$ mice had higher frequencies of early (Annexin V+ 7-AAD-) (20.3% and 13.9%, respectively) and late (Annexin V+ 7-AAD+) (21.1% and 18.3%, respectively) apoptotic cells compared to those from the WT mice (early 13.9% and 4.7%, late 18.3% and 10.7%, respectively, $p<0.01$ and $p<0.05$, respectively) **(Figure 19A and B)**.

In addition to the CD8 T cell defects herein explained, we also quantified by qPCR the LCMV viral load in the spleen and liver, two of the main target tissues of this virus. We found that the $Srsf1^{fl/fl}$.$dLck^{cre}$ mice had significantly higher LCMV viral loads (10-fold in spleen and 100-fold in liver) compared to WT mice after 8 days of LCMV infection **(Figure 19C)**. These data suggest an impaired viral clearance ability of the $Srsf1^{fl/fl}$.$dLck^{cre}$ mice.

Figure 19

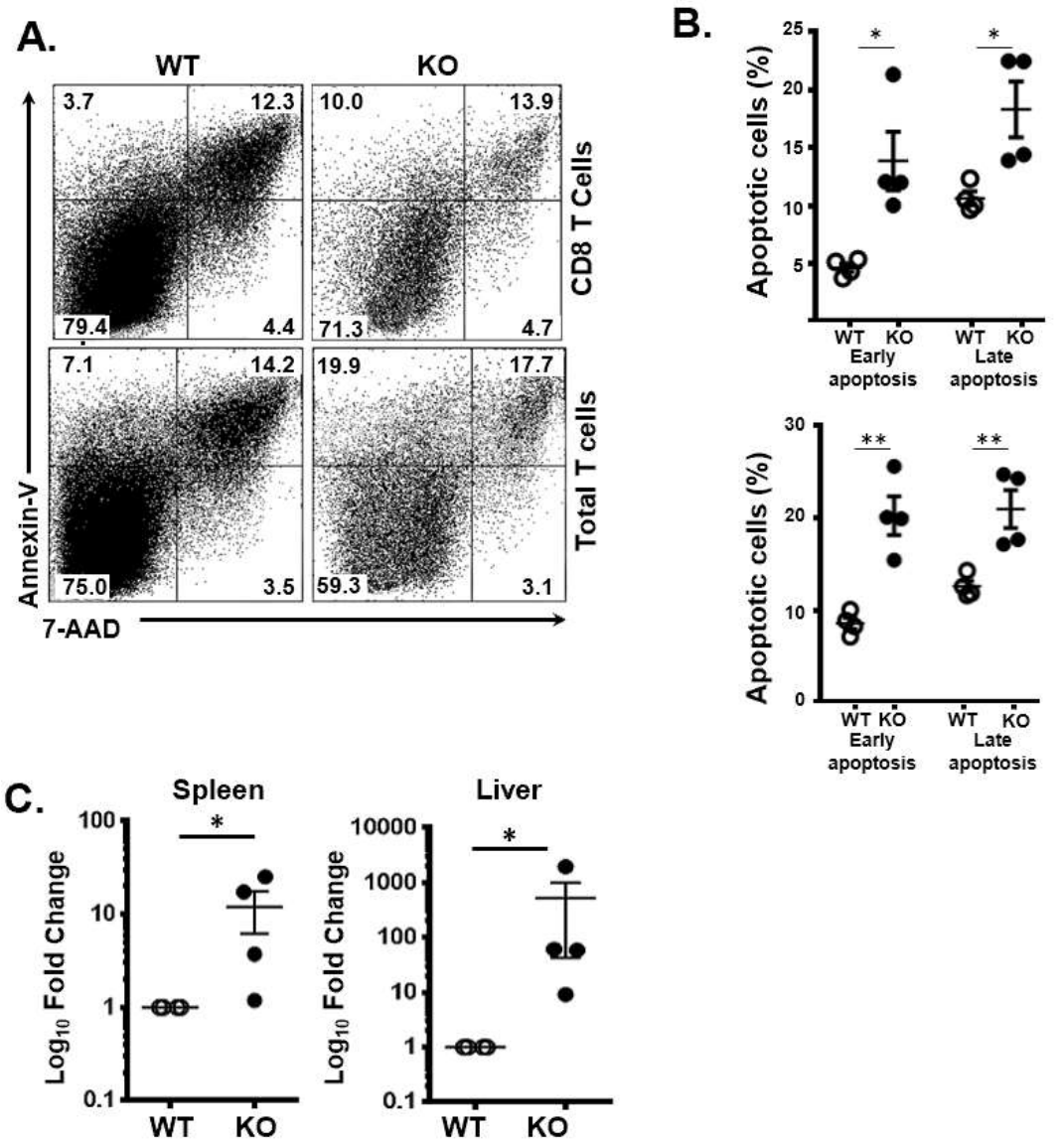

Figure 19. SRSF1 is necessary for CD8 T cell survival and viral clearance. *Srsf1*-cKO (KO) or WT mice were infected with LCMV Armstrong strain by IP injection. On day 8 post infection, spleens were collected for analysis of apoptotic cells. Spleen and liver were evaluated for LCMV viral load. A) Plots show apoptotic cells gated on CD8 and Thy1.2^{+} T cells from spleens of mice infected with LCMV (n=4/group) B) Graphs show frequencies of early (Annexin V^{+} 7-AAD^{-}) and late Annexin V^{+} 7-AAD^{+}) apoptotic cells. C) LCMV GP mRNA expression in spleen and liver cells was measured by real-time RT-qPCR. Graphs show relative expression (n=4 mice/group). (Graphs show mean±SEM.*, $p<0.05$, **, $p<0.01$)

3.4.c. Transcriptomic profiling showed that SRSF1 controls antiviral cytokine signaling and apoptotic pathways in T cells

To better understand how SRSF1 affects the biological processes in the context of viral infection, we performed RNA sequencing of spleen T cells from WT and $Srsf1^{fl/fl.}dLck^{cre}$ mice on day 8 post LCMV infection. Our transcriptomics data show that Srsf1 controls a large number of genes during the antiviral immune response. A total of 1894 genes were differentially expressed (DE) in KO compared to WT T cells, with 711 upregulated genes and 755 downregulated genes at the 2-fold cutoff and 186 upregulated genes and 242 downregulated genes at the 4-fold cutoff ($p < 0.05$) **(Figure 20A)**. The volcano plot shows the DE genes in the T cells from $Srsf1^{fl/fl.}dLck^{cre}$ mice compared to WT mice **(Figure 20B)**. Gene Ontology (GO) terms and Kyoto encyclopedia of genes and genomes (KEGG) enrichment analysis detected pathways involved in response to IFN-γ and the signaling pathways they mediate. Other pathways include T cell activation, cytokine-mediated signaling, and regulation of cytokine production **(Figure 20C and D)**. Several genes associated with the enriched pathways based on the pathway analysis were downregulated in $Srsf1^{fl/fl.}dLck^{cre}$ mice, including those in the MAPK pathway **(Figure 20E)**. These findings suggest that SRSF1 controls genes and molecular pathways important for the host antiviral immune response.

Figure 20

A.

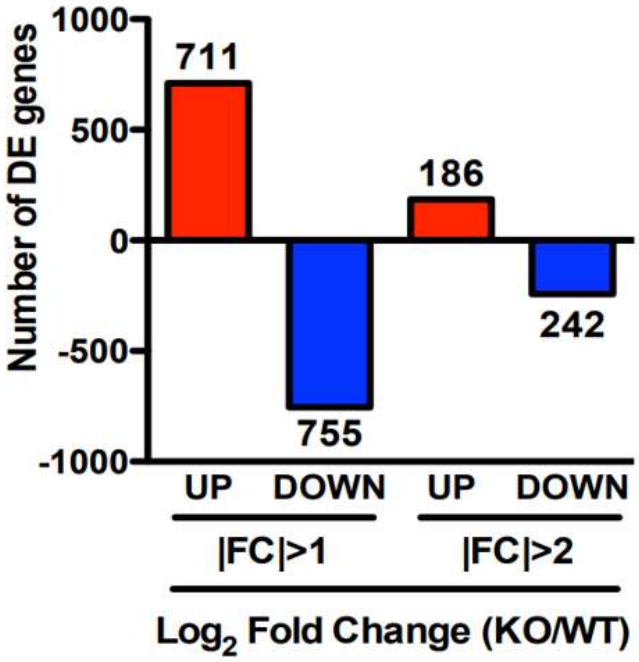
Number of DE genes
1000
500
0
-500
-1000
711
755
186
242
UP
DOWN
UP
DOWN
|FC|>1
|FC|>2
Log2 Fold Change (KO/WT)

B.

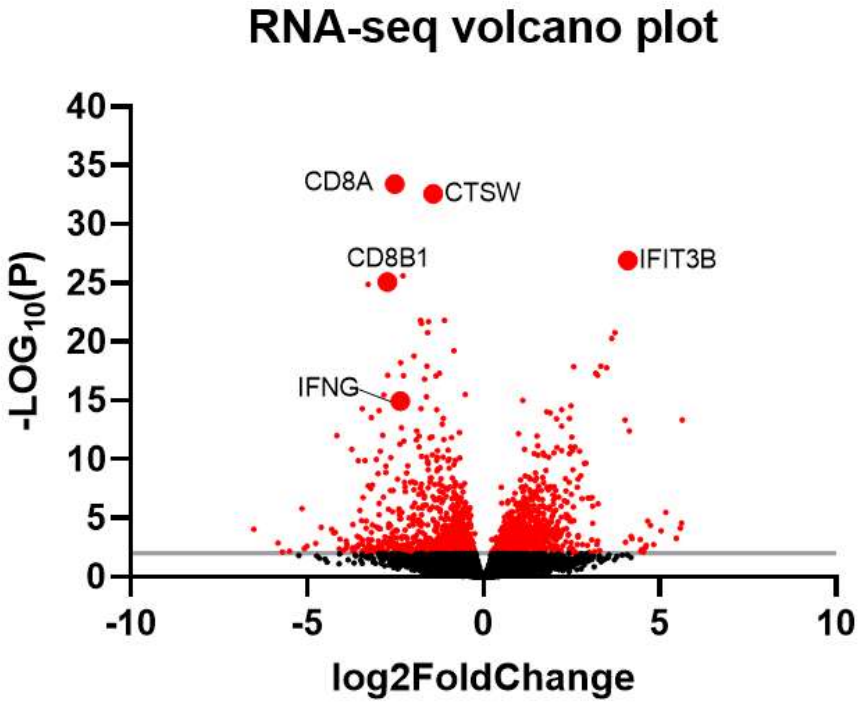
RNA-seq volcano plot
-LOG10(P)
40
35
30
25
20
15
10
5
0
CD8A
CTSW
CD8B1
IFIT3B
IFNG
-10
-5
0
5
10
log2FoldChange

Figure 20

C.

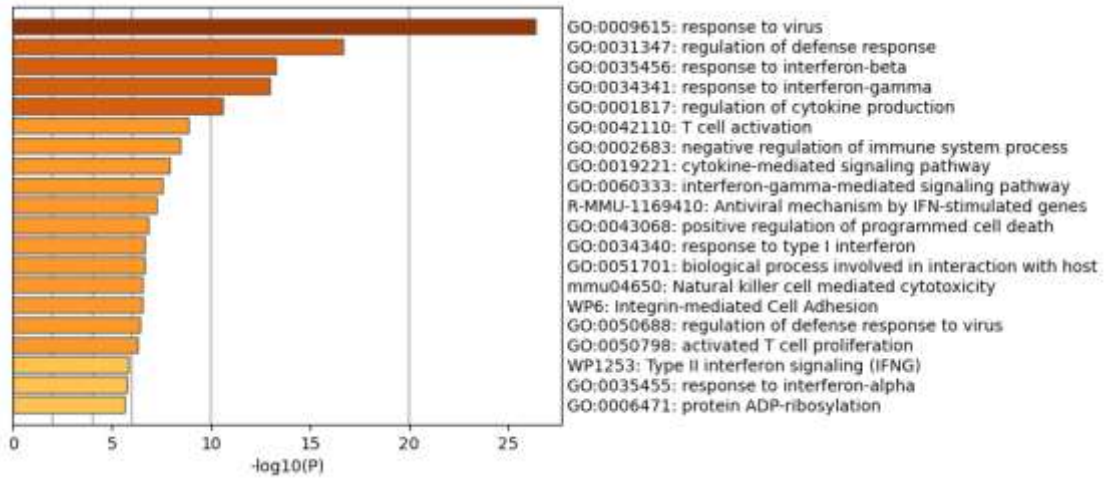
GO:0009615: response to virus
GO:0031347: regulation of defense response
GO:0035456: response to interferon-beta
GO:0034341: response to interferon-gamma
GO:0001817: regulation of cytokine production
GO:0042110: T cell activation
GO:0002683: negative regulation of immune system process
GO:0019221: cytokine-mediated signaling pathway
GO:0060333: interferon-gamma-mediated signaling pathway
R-MMU-1169410: Antiviral mechanism by IFN-stimulated genes
GO:0043068: positive regulation of programmed cell death
GO:0034340: response to type I interferon
GO:0051701: biological process involved in interaction with host
mmu04650: Natural killer cell mediated cytotoxicity
WP6: Integrin-mediated Cell Adhesion
GO:0050688: regulation of defense response to virus
GO:0050798: activated T cell proliferation
WP1253: Type II interferon signaling (IFNG)
GO:0035455: response to interferon-alpha
GO:0006471: protein ADP-ribosylation
0
5
10
15
20
25
-log10(P)

Figure 20

D.

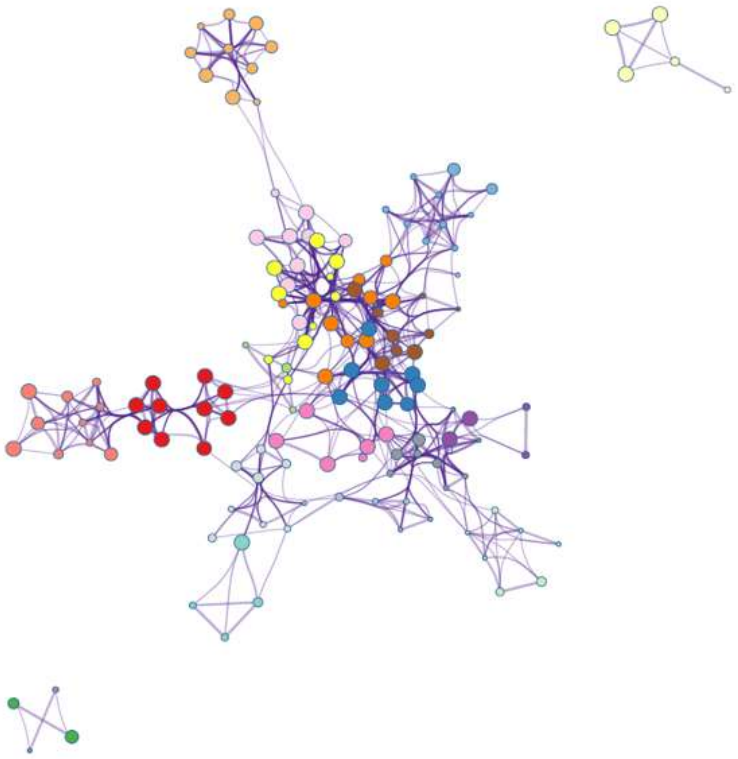

response to virus
regulation of defense response
response to interferon-beta
response to interferon-gamma
regulation of cytokine production
T cell activation
negative regulation of immune system process
cytokine-mediated signaling pathway
interferon-gamma-mediated signaling pathway
Antiviral mechanism by IFN-stimulated genes
positive regulation of programmed cell death
response to type I interferon
biological process involved in interaction with host
Natural killer cell mediated cytotoxicity
Integrin-mediated Cell Adhesion
regulation of defense response to virus
activated T cell proliferation
Type II interferon signaling (IFNG)
response to interferon-alpha
protein ADP-ribosylation

Figure 20

E

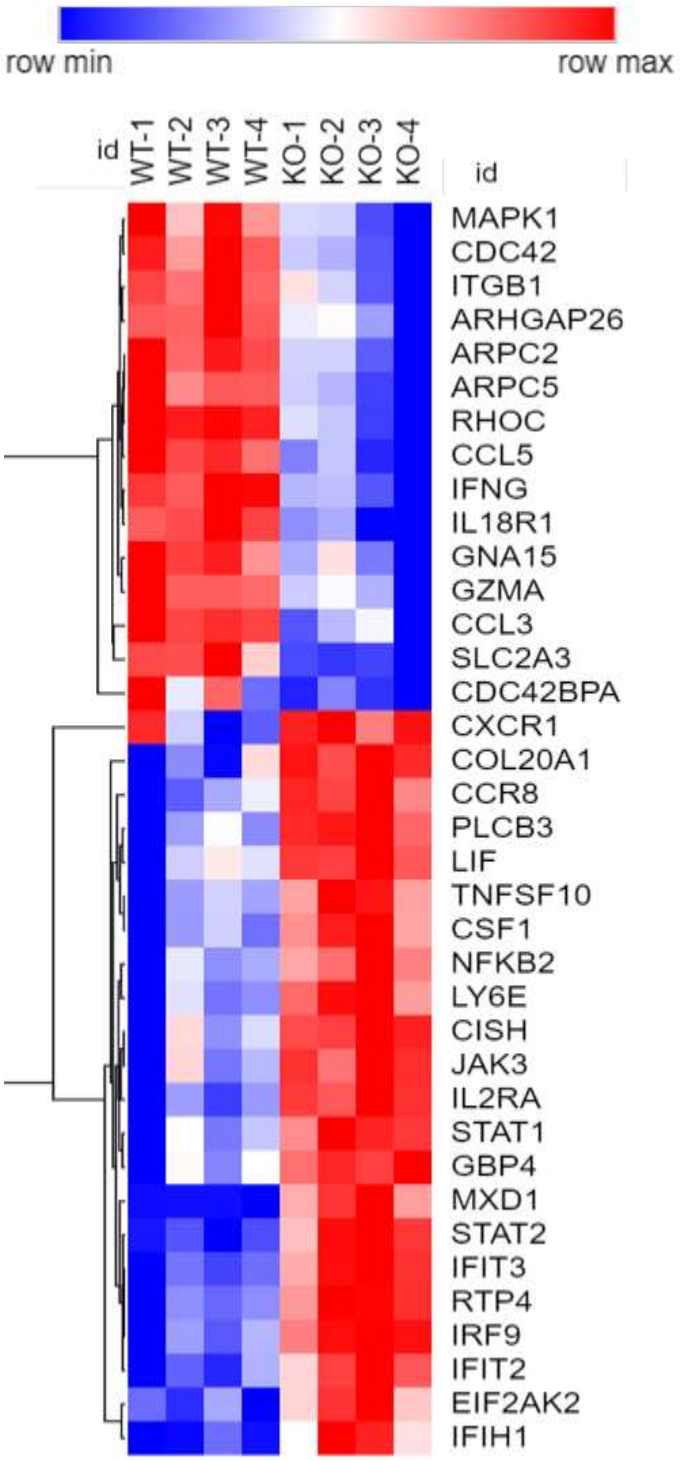
row min
row max
id
WT-1
WT-2
WT-3
WT-4
KO-1
KO-2
KO-3
KO-4
id
MAPK1
CDC42
ITGB1
ARHGAP26
ARPC2
ARPC5
RHOC
CCL5
IFNG
IL18R1
GNA15
GZMA
CCL3
SLC2A3
CDC42BPA
CXCR1
COL20A1
CCR8
PLCB3
LIF
TNFSF10
CSF1
NFKB2
LY6E
CISH
JAK3
IL2RA
STAT1
GBP4
MXD1
STAT2
IFIT3
RTP4
IRF9
IFIT2
EIF2AK2
IFIH1

Figure 20. RNA-Seq Transcriptomics Analysis of T cells from LCMV infected mice. Total T cells were isolated from spleens of LCMV infected WT and KO mice (n=4/group). **(A)** RNA-sequencing data analysis shows differentially expressed (DE) genes with log_2fold change (FC) differences at $p<0.05$. **(B)** Volcano plot showing upregulated and downregulated genes in KO T cells after LCMV infection. **(C)** Bar graph of top 40 enriched terms, colored by p-values. **(D)** GO terms enrichment map shows clusters of top 20 pathways. **(E)** Heat map showing average expression of selected DE genes associated with enriched terms.

3.4.d. SRSF1 controls Mnk2 expression and activity of the p38 MAPK pathway

Based on its roles in cellular proliferation/apoptosis and cytokine signaling, we investigated the relationship between SRSF1 and activity of the p38-MAPK signaling pathway. We stimulated spleen T cells with CD3/CD28 and examined the expression of phosphorylated p38 protein. We found that activated $Srsf1^{fl/fl}$.$dLck^{cre}$ T cells had lower levels of phosphorylated p38 protein expression compared to WT T cells **(Figure 21A and B)**. To evaluate if SRSF1 is sufficient to modulate the p38 pathway, and to test this in human T cells, we overexpressed SRSF1 by transient transfection of Srsf1-expressing plasmid vector in peripheral blood T cells and assessed the expression of phosphorylated p38 protein. We found an increase of phosphorylated p38 expression in T cells overexpressing SRSF1, compared to control transfected cells **(Figures 21C and D)**. We hypothesized that SRSF1 controls the expression of Mnk2, which further controls the activation of p38. To test this hypothesis, we overexpressed SRSF1 in T cells and measured the mRNA expression of Mnk2a, the isoform of Mnk2 that activates p38 mediated cell death. We found that cells overexpressing Srsf1 had significantly lower Mnk2a mRNA levels **(Figure 21E)**. Our results suggest that SRSF1 controls the Mnk2/p38-MAPK axis which may contribute to its role in cell proliferation/survival and cytokine mediated function.

Figure 21

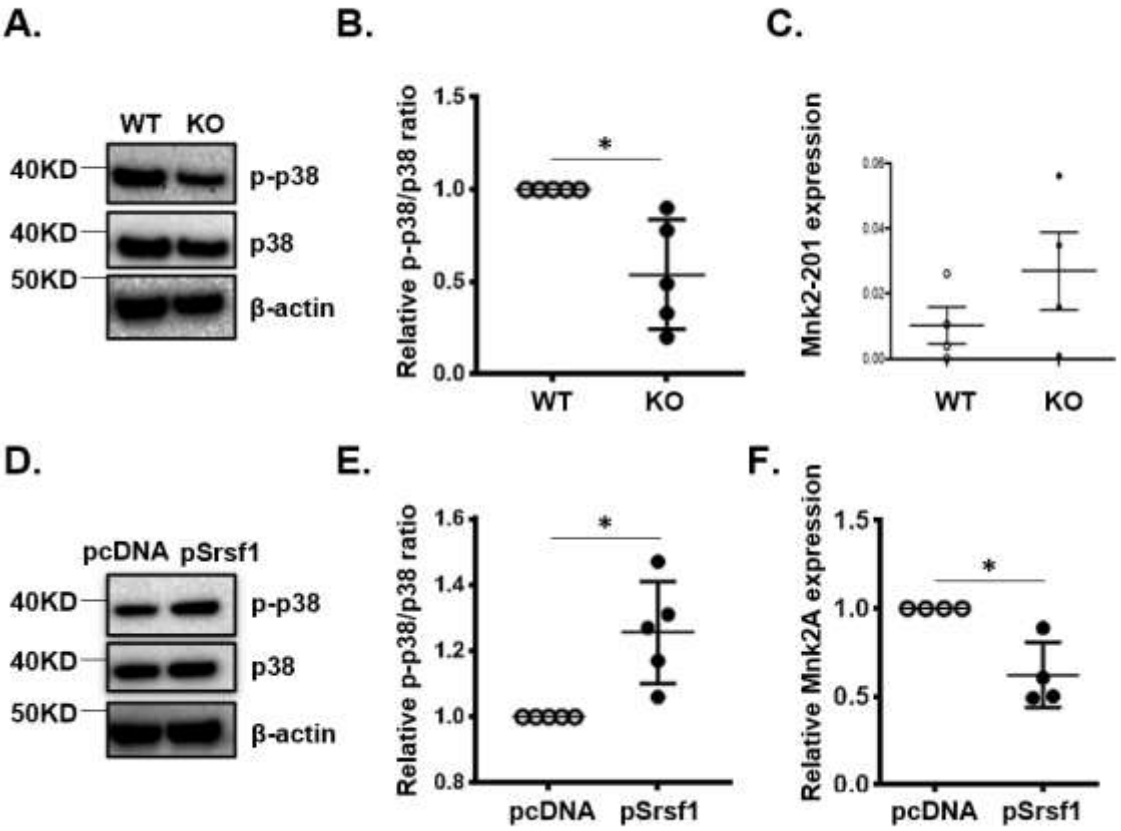

Figure 21. Srsf1 modulates p38 phosphorylation in activated T cells. (**A**) Total mouse T cells were isolated from spleens of WT and *Srsf1*-cKO mice and stimulated with anti-CD3 and anti-CD28. Total protein was immunoblotted for phospho-p38 (p-p38), p38, and β-actin. Image showing one representative blot from 5 independent experiments. (**B**) Graph shows relative quantitation by densitometry. (**C**) mRNA expression of MNK2 201 isoform in mouse spleen cells. (**D**) Peripheral blood T cells were isolated from healthy donors and transfected with empty vector (pcDNA) or *SRSF1* overexpression plasmid (pSrsf1). After transfection, T cells were stimulated with anti-CD3 and anti-CD28. Total protein was immunoblotted for phospho-p38 (p-p38), p38, and β-actin. Image showing one representative blot from 5 independent experiments. (**E**) Graph shows relative quantitation by densitometry. (**F**) Relative mRNA expression of MNK2A isoform in human T cells. (Graphs show mean±SEM *, $p<0.05$ **, $p<0.01$)

3.5. Preliminary alternative splicing analysis involved in IL-17A signaling

One interesting observation we made in T cells deficient in Srsf1, was the upregulation of *Il-17a* and *Il-17f* mRNA expressions in the RNA-seq data of Tregs derived from T cell specific Srsf1 deficient mice. In this subsection, we investigated further how Srsf1 and alternative splicing are associated with signaling pathways that involve IL-17A.

3.5.a. Increased gene expression of IL-17a and IL-17f is not reflected on the protein level in the regulatory T cells of Srsf1$^{fl/fl}$.dLck^{cre} mice in naïve state

Analysis of the RNA-Seq data (GSE173268) showed that Tregs from Srsf1$^{fl/fl}$.dLck^{cre} mice exhibited higher expression of *Il-17a* and *Il-17f*[186]. In order to investigate whether the elevated *Il-17a* and *Il-17f* transcripts also reflect on the protein level in naïve state, we performed flow cytometric analysis on the splenocytes of Srsf1$^{fl/fl}$.dLck^{cre} mice. Our data showed that in naïve state, the Srsf1$^{fl/fl}$.dLck^{cre} mice do not possess significantly altered protein levels of IL-17A or IL-17F in CD4^{+}CD25^{high}CD127^{low} Tregs **(Figure 22)**.

Figure 22

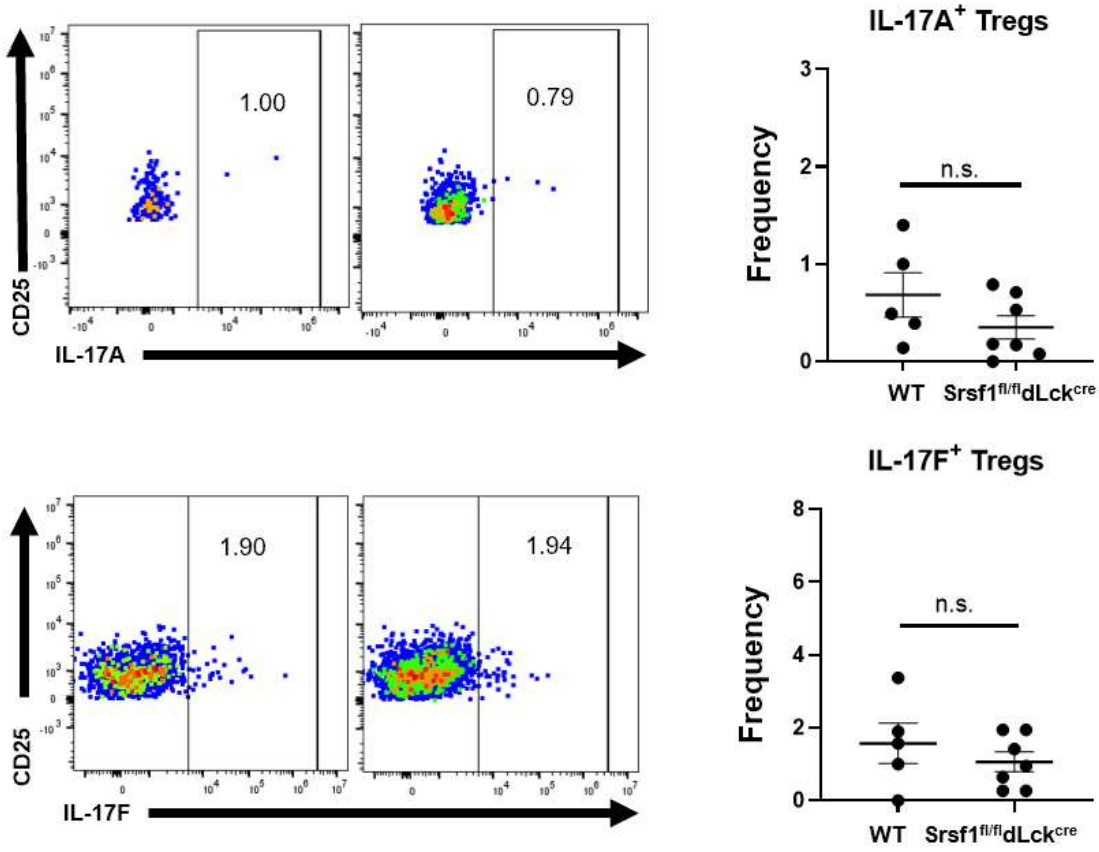

Figure 22. Ablation of Srsf1 in T cells increases the mRNA expression but not the protein levels of IL-17A and IL-17F in regulatory T cells. Representative pseudocolor plots showing IL-17A^{+} CD4^{+}CD25^{high}CD127^{low} natural Tregs, and IL-17F^{+} CD4^{+}CD25^{high}CD127^{low} natural Tregs, from the spleens. (WT: n=5, Srsf1$^{fl/fl}$dLck^{cre}: n=7). The percentage of respective populations of each group are shown on the right. Student t test, unpaired, nonparametric. * $p<0.05$)

3.5.b. Alternative splicing does not regulate the expression of IL-17a and IL-17f in Srsf1$^{fl/fl}$dLck^{cre} mice

The nonsignificant difference observed in the protein levels of IL-17A and IL-17F in Srsf1$^{fl/fl}$dLck^{cre} mice led us to speculate whether the elevated gene expression might be

due to aberrant alternative splicing caused by SRSF1 deficiency. In order to directly capture the effect of SRSF1 deficiency in alternative splicing we compared differentially spliced genes between $Srsf1^{fl/fl}dLck^{cre}$ and control. Differential exon usage analysis identified 578 genes (667 exons) with potential differential usage of exons in $Srsf1^{fl/fl}dLck^{cre}$, under a permissive FDR < 0.1. However, there were only 5 genes falling within the overlap between differentially expressed and differentially spliced genes identified. Further analysis detected that among the 578 genes with potential differential usage of exons, 43% had increased exon usage and 57% had decreased exon usage. Both *Il-17a* and *Il-17f*, although differentially expressed, were not differentially spliced. Following further manual evaluation, 2 out of 3 samples showed RNA processing patterns practically indistinguishable from the control group, while one sample showed some potential differential exon usage. Even under permissive statistical significance thresholds, investigations of differential exon usage did not reveal any statistically significant difference, pointing to differential expression events not directly affected by SRSF1 splicing activity. Subsequently, we analyzed transcription factors RORγt, STAT3, Stat5a, Stat5b, TBX21 and GATA3 that affect *Il-17a* and *Il-17f* expression, but did not detect any significant differential expression or alternatively splicing in these genes [241–243]. Next, we looked at differentially expressed genes (DEGs) that showed differential exon usage that could affect the secretion of IL-17A or IL-17F, such as Rab23, a molecule involved in vesicular trafficking, and Pikfyve, a molecule that affects a number of trafficking pathways. Further visual inspection suggested that the observed effect is limited to a small fraction of the exons. Taken together in these experiments we did not

detect any significant changes that suggest SRSF1 mediated alternative splicing in the expression of *Il-17a* and *Il-17f.*

3.5.c. Srsf1$^{fl/fl}$.dLck^{cre} Treg cells possess distinct gene signatures associated with myeloid cells

In order to explore the potential pathways that the altered gene expression of *Il-17a* and *Il-17f* in Tregs of Srsf1$^{fl/fl}$.dLck^{cre} mice might play a role in, we performed pathway enrichment and over-representation analysis. Our data showed that the deferentially expressed genes are highly enriched in innate immune response pathways, as well as neutrophil and monocyte chemotaxis. Specifically, heatmap of the RNA-seq data showed that, among the differentially expressed genes involved in innate immunity, the Tregs of Srsf1$^{fl/fl}$.dLck^{cre} mice showed elevated chemokine expression related to monocytes and neutrophils, such as *Ccl3, Ccl1, Ccl17, Ccl20,* and *Ccl22*. These data suggested that Srsf1 deficiency might play a role in innate immunity.

3.5.d. Srsf1$^{fl/fl}$·dLck^{cre} mice have reduced innate immune responses upon acute viral infection

In order to demonstrate that Srsf1 deficiency in T cells affects innate immunity, we performed flow cytometry analysis of bone marrow and spleen myeloid cells in WT and Srsf1$^{fl/fl}$dLck^{cre} mice in their naïve state or 24 hours after LCMV infection. We found that Srsf1$^{fl/fl}$dLck^{cre} mice exhibited lower frequency of total CD11B^{+} myeloid cells in bone marrow (**Figure 23A**). In the spleen, however, Srsf1$^{fl/fl}$dLck^{cre} mice exhibited significantly higher CD11B^{+} frequencies at naïve state compared to their WT

counterparts (**Figure 23B**). The difference of $CD11B^+$ cells in the bone marrow between $Srsf1^{fl/fl}dLck^{cre}$ and WT was not altered 24 hours after acute LCMV infection (**Figure 23C**). The difference of splenic $CD11B^+$ myeloid cells between $Srsf1^{fl/fl}dLck^{cre}$ and WT was diminished 24 hours after acute LCMV infection, as the frequency of $CD11B^+$ myeloid cells doubled in WT mice but remained the same in $Srsf1^{fl/fl}dLck^{cre}$ mice (**Figure 23D**).

We then investigated the effect of SRSF1 deficient T cells in MDSCs by measuring the frequencies of $CD11B^+Ly6G^+Ly6C^{lo}$ polymorphonuclear MDSCs (PMN-MDSC) and $CD11B^+Ly6G^-Ly6C^{hi}$ monocytic MDSCs (M-MDSC) in the bone marrow and spleen, using flow cytometric markers as previously described[244]. We observed that $Srsf1^{fl/fl}dLck^{cre}$ mice had higher frequencies of M-MDSC in the bone marrow and higher frequencies of PMN-MDSC in the spleen at naïve state (**Figure 23E, F**). However, 24 hours after acute LCMV infection, unlike the WT mice, the splenic PMN-MDSC frequency of the $Srsf1^{fl/fl}dLck^{cre}$ mice failed to expand (**Figure 23G**). Both WT and $Srsf1^{fl/fl}dLck^{cre}$ mice exhibited decreased PMN-MDSC frequency in the bone marrow 24 hours after acute LCMV infection (**Figure 23H**). Collectively our data suggest that ablation of SRSF1 in mature T cells affects innate immune responses.

Figure 23

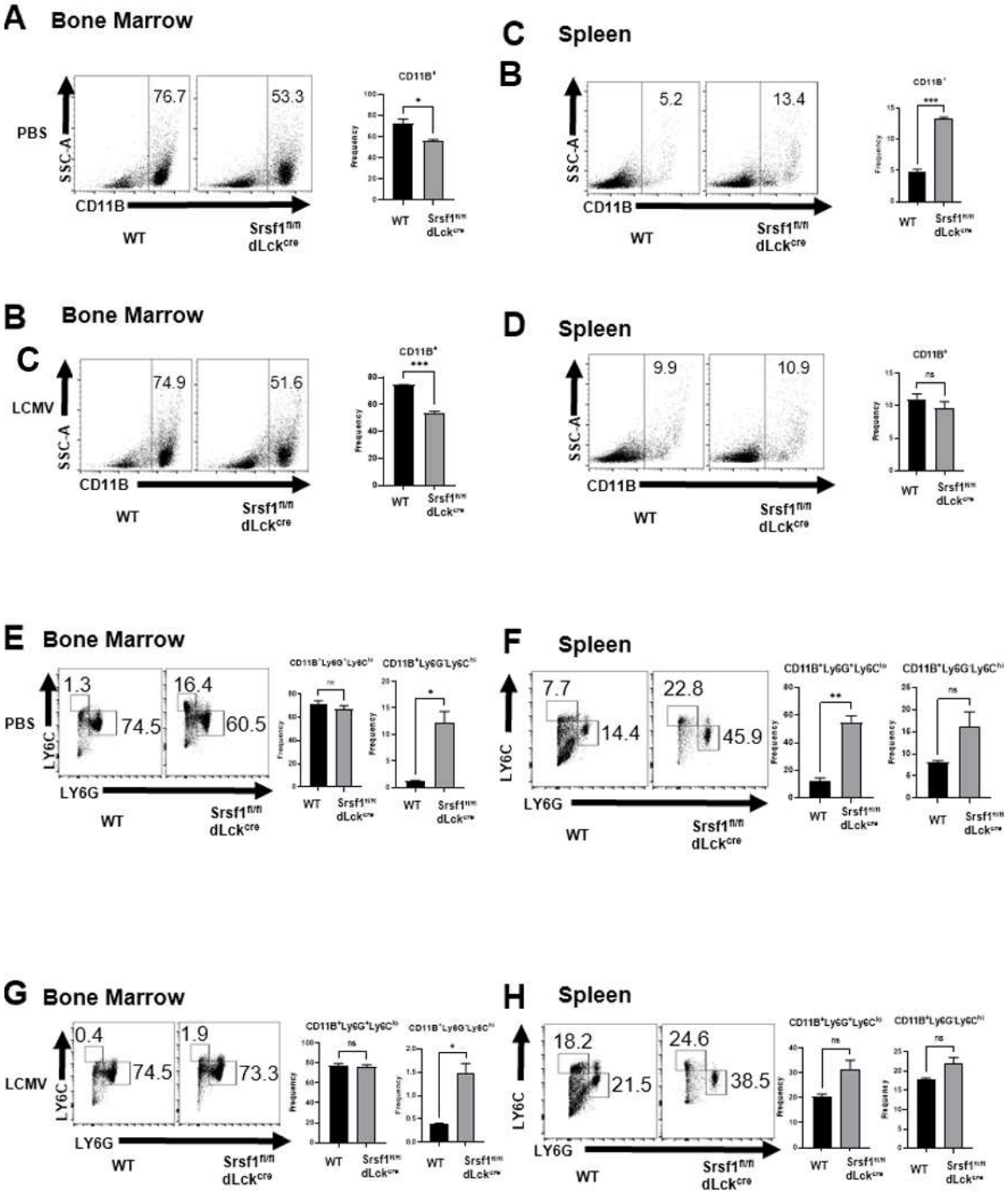
A Bone Marrow
PBS
SSC-A
CD11B
76.7
53.3
WT
Srsf1fl/fl dLckcre
CD11B+
Frequency
C Spleen
B
5.2
13.4
B Bone Marrow
C
LCMV
74.9
51.6
D Spleen
9.9
10.9
E Bone Marrow
LY6C
LY6G
1.3
74.5
16.4
60.5
CD11B+Ly6G+Ly6Clo
CD11B+Ly6G-Ly6Chi
F Spleen
7.7
14.4
22.8
45.9
G Bone Marrow
0.4
74.5
1.9
73.3
H Spleen
18.2
21.5
24.6
38.5

Figure 23. Srsf1 deficiency in T cells affects innate immune cell distribution and migration. Dot plots and graphs showing the populations of CD11B+ myeloid cells in bone marrow and spleen of WT and $Srsf1^{fl/fl}$ $dLck^{cre}$ mice in naïve state (**A, C**) and 24hr after acute LCMV infection (**B, D**). Dot plots and graphs showing the populations of PMN-MDSC (CD11b+Ly6G+Ly6Clo) and M-MDSC (CD11b+Ly6G−Ly6Chi) in the bone marrow and spleen of WT and $Srsf1^{fl/fl}$ $dLck^{cre}$ mice in naïve state (**E, F**) and 24hr after acute LCMV infection (**G, H**). Experiments were performed twice with at least 3 mice per group. Student t test, unpaired, *, $P<0.05$, **, $P<0.01$, ***, $P<0.001$).

CHAPTER FOUR: DISCUSSION

4.1. SR-BIΔCT/LDLR-/-mice develop atherosclerotic cardiovascular disease in a diet dependent manner

In subsection 3.1, I validated an inducible coronary artery disease model using a combination of dietary and genetic intervention with a novel transgenic mouse model. I tested different diet starting time and found that the effect of diet is independent of age or sex regarding the prognosis of the disease. This finding can provide value for future experimental design for cardiovascular studies. Trigatti's group has previously demonstrated that different diets have different atherogenic effects on the pathogenesis of atherosclerosis and myocardial infarction in SR-BI-/-/LDLR-/- mice[235]. My data support the previous studies showing that high fat and high cholesterol Paigen diet can induce coronary artery occlusion in LDLR-/- with dysfunctional SR-BI.

Accumulating animal studies provide us more information about the impact of dietary lipids on the reverse cholesterol transport[245]. The unique feature of Paigen diet is that it contains high fat (15%), high cholesterol (1.25%), and 0.5% cholic acid[246]. The conventional Western diet contains 22% fat and 0.2% cholesterol[246]. It has been shown that cholate-containing diet increases apoB-100-containing particles, such as LDL particle, via posttranscriptional modifications[9,247]. Krieger's group also demonstrated that cholate-containing Paigen diet significantly increased VLDL content in plasma[248]. Our data, in agreement with previous studies, suggest that Paigen diet is a superior diet for rapid readout for murine studies investigating diet-induced CVD.

The PDZK1-/- mice exhibited >95% reduction in the hepatic expression of SR-

BI[32]. PDZK1 deficiency does not affect the SR-BI expression in steroidogenic organs (adrenal, ovary, and testis)[249]. Using x-ray crystallography, it has been shown that PDZK1 binds to the C-terminal of SR-BI ((505)QEAKL(509))[250]. PDZK1-/-/apoE-/- mice did not develop occlusive atherosclerosis[251]. A noteworthy difference is that PDZK1-/- did not affect the hepatic SR-BII, an isoform of SR-BI[251]. It has been shown that SR-BII also mediates HDL updake[164]. PDZK deficiency does not affect the expression of SR-BII. However, in SR-BIΔCT mice, SR-BII expression was increased[62]. The similarity in occlusive atherosclerosis phenotype of SR-BI-/- that eliminate both SR-BI/SR-BII expression, and SR-BIΔCT that eliminated SR-BI but increased SR-BII expression raised questions about the role that SR-BII plays in the development of occlusive atherosclerosis that need to be further determined.

While both the SR-BIΔCT and PDZK1-/- mice have less than 5% of the hepatic SR-BI protein expression compared to the wildtype mice, there is a difference in plasma unesterified cholesterol to total cholesterol ratio between these two transgenic mouse strains. In addition, PDZK1-/-/apoE-/- mice took 3 months on atherogenic diet to present occlusive atherosclerosis whereas both SR-BI-/-/apoE-/- and SR-BIΔCT/apoE-/- could develop spontaneous coronary occlusive atherosclerosis[59,62,252]. The findings of the studies above indicate that the function of SR-BI produced by the SR-BIΔCT and PDZK1-/- mice may be different[62]. Without the stabilization by docking with PDZK1[253], the protein expression of SR-BI dramatically decreases in the liver, which impairs their capacity to handle cholesterol overload and eventually promotes atherogenesis.

This SR-BIΔCT/LDLR-/-model aimed to create a sustainable line that can be used

for therapeutic interventions. It preserves the SR-BI expression in steroidogenic tissues yet exhibits cardiac dysfunction following diet-induced occlusive atherosclerosis in the coronary arteries. The phenotypes observed suggested that the expression of SR-BI in other cell types might contribute to the pathogenesis of cardiovascular disease.

The anemic phenotype observed in the SR-BIΔCT/LDLR-/-model was consistent with previous observations that the RBCs of SR-BI$^{-/-}$ mice failed to mature and elevated HDL cholesterol level caused the membrane abnormalities and shortened the lifespan of RBC[254,255]. Based on pathological evidence of intraplaque hemorrhage and the progression of coronary atheroma in humans[256], it has been suggested that the red blood cells might also play an important role in atherosclerosis.

In addition to phenotypes consistent with previous observations in SR-BI-/-/LDLR-/-, our weekly hematological and cardiac phenotype monitoring provided a temporal progression of lipid induced inflammation and subsequent heart failure. Two weeks of high cholesterol diet feeding significantly induces inflammation with elevated circulating leukocytes. Heart failure phenotype was observed one week after elevation of circulating leukocytes. Our histological studies confirmed that free cholesterol deposit can contribute to the progression of plaque development. In addition, it demonstrated that cardiac fibrosis resulted from the occlusive arteries led to cardiac hypertrophy and left ventricular remodeling. Assessment of cardiac function also confirmed that the structural changes of the ischemic heart that was characterized by cardiac hypertrophy and fibrosis led to impaired cardiac function. All of these factors are interrelated and contribute to the remodeling of left ventricle and eventually lead to heart failure[257].

Lipotoxicity can lead to many diseases related to metabolic inflammation[258]. High dietary cholesterol can lead to elevated tissue ceramide, which is a cardiotoxin in lipotoxic cardiomyopathy[259,260]. There are also other specific lipid species that can cause cardiac dysfunctions[261,262]. It remains to be further investigated the impact of lipotoxicity in this mouse model. Lipidomic studies can be carried out in the future to measure the alterations in different cellular lipids such as ceramides in the heart after the induction of high dietary cholesterol.

In this study, I demonstrated the superiority of SR-BIΔCT/LDLR-/- mice as an atherosclerosis disease model for preclinical studies. The phenotypes we observed in SR-BIΔCT/LDLR-/- mice are similar to the ones observed in SR-BI-/-/LDLR-/- mice on high cholesterol Paigen diet[235]. However, the fertile females of SR-BIΔCT/LDLR-/- overcame the challenges of infertility of mouse models based on SR-BI-/-.

In addition, the SR-BIΔCT/LDLR-/- mouse model can also be a superior model for atherothrombotic disease research as it has been previously demonstrated by the Trigatti group that, after Paigen diet challenge, the occluded coronary arteries of SR-BI-/-/LDLR-/- showed signs of platelet accumulation[235]. In addition, imaging studies have also shown the connection between hypercholesterolemia and atherothrombosis. This connection was made by the detection of ruptures of coronary plaques and thrombi in the SR-BI-/-/hypoE mice (generated by crossing SR-BI-/- mice with hypomorphic apoE (hypoE) mice that express only approximately 5% of normal apoE mRNA levels in all tissues[263]) fed with high fat diet[264].

4.2 Nanomedicine and the amelioration of cardiovascular disease

In subsection 3.2, I tested a new combination of nanoparticle therapy in the newly established coronary artery disease model, SR-BIΔCT/LDLR-/-. This model exhibits occlusive coronary artery atherosclerosis, impaired cardiac function, increased inflammation profiles, in a diet-dependent manner. I found that a targeted antioxidant and antiplatelet dual therapy significantly improved cardiac function and inflammatory profiles of the mice. In addition, the dual therapy with antioxidant and antiplatelet agents was superior to antiplatelet or antioxidant therapy alone.

It has been previously shown that the CREKA (Cys-Arg-Glu-Lys-Ala) can home to the atherosclerotic plaque[233]. To test the feasibility of applying this PVAX-incorporated nanocomplex *in vivo*, we first loaded the nano complex nile red instead of the antiplatelet agent. Because PVAX works in areas with high H_2O_2[110], we used old LDLR-/- mice (>30wks) that are known to have elevated oxidative stress due to age[236]. Twenty-four hours after *i.p.* injection, we assessed the uptake of nano complexes by different tissues. We found accumulation of nano particles in the liver and aorta.

In addition, I also observed that mice receiving antioxidant treatments, with the help of the ROS scavenging nanoparticle, both PVAX and TPM, showed lower fasting glucose levels, indicating some improvement in glucose regulation. It has been shown that increased oxidative stress impairs glucose uptake by the muscle and fat, and ROS has a causal role in insulin resistance[265–268]. Hyperglycemia is closely associated with higher cardiovascular disease burden[269]. Metabolic syndrome, a combination of dyslipidemia and hyperglycemia, is often observed in patients with cardiovascular disease. To further

investigate glucose metabolism in these mice and validate the phenotypical differences observed following different treatments, a post treatment glucose tolerance test and insulin tolerance test need to be performed. In addition, glycolysis of the mouse hepatocytes needs to be measured to determine whether the improved fasting glucose levels were, at least in part, contributed by alleviated mitochondrial oxidative damage in mice that underwent antioxidant treatments.

It has been shown that RBC dysfunctions can be induced by high fat diet[270]. Our data showed that anti-inflammatory therapy, both PVAX and TPM, can rectify anemia in SR-BIΔCT/LDLR-/-are consistent with the previous studies showing that ROS-mediated damage of RBC membranes increases erythrocyte membrane rigidity and fragility, resulting in intravascular hemolysis in an antioxidant enzyme-deficient transgenic mouse[271]. This contributes to the enlarged spleen in these mice on atherogenic diet. However, antioxidant treatment alone could not alleviate spleen enlargement following the switch to an atherogenic diet. This phenotype might be relevant to our observation that PVAX alone did not reduce the circulating total monocyte cell numbers. It has been reported that monocytes exit the spleen in response to myocardial infarction[272]. Specifically, Ly-6C^{hi} monocytes dominate hypercholesterolemia induced monocytosis[273]. Therefore, further identification of the monocyte subsets by flow cytometry is needed to assess the changes of different monocyte populations following the treatments with PBS, tirofiban, PVAX or TPM.

Targeted antiplatelet and antioxidant therapy resulted in attenuated spleen enlargement. This can simply be due to the improved cardiac function as splenic

hematopoiesis has been reported in atherosclerosis and myocardial infarction[274,275]. To rule out the possibility that the reduced spleen size was not caused by the inhibition of Glycoprotein IIb/IIIa (GpIIb/IIIa) by tirofiban that is incorporated into the nanoparticle[85], other antiplatelet drugs that function through different mechanisms, such as thromboxane inhibitors, ADP P2Y receptor antagonists[276], can be also used as cargos in the nanoparticles.

In future studies, in order to further evaluate the ROS scavenging effect of the nano-complex, intracellular ROS staining can be used in cardiac sections of the mice that received different treatments[111]. Further future investigations are also needed to quantify the nanoparticles homing to the diseased area by examining the nanoparticle uptake by other organs using flow cytometry or immunofluorescent staining to visualize the uptake of fluorophore conjugated nanoparticles.

In order to get a better understanding of the mechanistic changes that ameliorate cardiac dysfunctions in SR-BIΔCT/LDLR-/-mice receiving different treatments, temporal changes at the cellular and the molecular level need to be assessed in different tissues. For example, serum amyloid A (SAA), which is a serum marker of myocardial infarction, can be monitored. In addition, functional studies of the HDL can be further investigated in these mice after different treatments.

In this study, I have chosen for drug delivery *i.p.* injection as the means because it has been previously shown that *i.p.* injection results in higher yield of nanoparticle uptake in apoE$^{-/-}$ mice[277]. Using the fluorescent dye Nile Red, which stains for intracellular lipid droplets[278], incorporated into the nanoparticle as a payload, we were able to visualize the

accumulation of oxidative stress sensing nano particles in the liver and aged aorta. This suggested the oxidative stress targeting capacity of the nanocomplex as liver is one of the organs in the Reticuloendothelial System that facilitates the clearance of foreign particles from the circulation[279], and oxidative stress is high in aged aorta[237].

A concern of the nanoparticle design is the degradation time as well as their off-target effects. In this study, we used biodegradable micelles that can be safely degraded in the body. The safety profile of this micelle complex has been previously demonstrated [280]. However, more studies are needed to further validate the safety profile for longer treatment in the context of atherosclerosis and cardiovascular disease. In addition, further studies can be carried out to investigate different concentrations of the nano particles to select the optimal concentrations for this approach required for a specific treatment.

4.3. Treg specific SRSF1 abnormality links autoimmune disease and CVD

In subsection 3.3, I showed that $Srsf1^{fl/fl}$.$Foxp3^{cre}$ mice had impaired cardiac function. This phenotype might contribute, in addition to the hyperinflammatory state of the mice, to the early death of these mice. Katsuyama et al. have previously demonstrated that SRSF1, an essential RNA-binding protein that regulates post-transcriptional modifications, controls T cell hyper-activation and its deficiency promotes pro-inflammatory cytokine production [185]. Recently, they have also found that SRSF1 is crucial for the survival, integrity and function of Tregs [186]. The RNA-sequencing data of Tregs from the T cell specific Srsf1 knockout mice identified several genes that were drastically altered by SRSF1 deficiency, including down-regulation of SCD1 and VLDLR, and up-regulation of ANGPTL2.

Stearoyl-CoA desaturase 1 (SCD1) is the rate-limiting enzyme in the synthesis of monounsaturated fatty acids [281]. Similarly, Fatty Acid Desaturase 2 (FADS2) regulates the biosynthesis of long chain polyunsaturated fatty acids [282].The down-regulation of the expression in Scd1 and Fasd2 could have a detrimental effect on Treg metabolic homeostasis as Tregs rely mainly on fatty acids to promote oxidative phosphorylation through fatty acid oxidation rather than glycolysis for their energy supply [283–285]. It has been found that SCD1 deficiency protects mice from obesity and insulin resistance by reducing plasma triglyceride [286]. Paradoxically, SCD1 deficiency increases inflammation and atherosclerosis, suggesting a link between SCD1 deficiency and impaired resolution of inflammation. In this process, metabolically dysfunctional Tregs could play a role [286–288].

Angiopoietin-like 2 (ANGPTL2) is a secreted glycoprotein member of the angiopoietin-like protein family, which plays a key role in promoting chronic inflammation [289,290]. Its expression can be induced by elevated cell stress [289,290]. Circulating ANGPTL2 levels are elevated in patients with atherosclerosis compared to healthy subjects [291]. It has also been found that in animal models, ANGPTL2 induces pro-inflammatory responses in monocytes and macrophages, contributes to the endothelial dysfunction and the progression of atherosclerosis.

Therefore, ANGPTL2 appears to be a causal player in the observed accelerated heart failure. This effect may be mediated by perturbation of cardiac functions and cardiac energy metabolism via its autocrine/paracrine signaling [292–295]. Since ANGPTL2 exerts its function through an autocrine and paracrine manner, the observed change in the

expression of ANGPTL2 in Treg is expected to affect the expression of other molecules involved in the ANGPTL2 signaling pathways such as FOXO1, NF-kB, p-NF-kB, CCR2, in other neighboring cells [296]. The elevated expression of ANGPTL2 in the Tregs from the T cell specific Srsf1 knockout mice suggests that these Tregs could contribute to the pathogenesis of inflammatory diseases via the ANGPTL2 pathway.

Another one of the most significantly downregulated genes in the Tregs derived from the mice lacking T cell specific Srsf1, is VLDLR. This receptor is found throughout the body, with particularly high expression in fatty acid producing tissues that have high level of triglycerides that are the primary ligand for VLDLR[297]. It has been demonstrated that VLDLR disruption does not affect the plasma lipoprotein profile[298]. It has been previously shown that depletion of $FoxP3^{+}$ Tregs increased plasma triglycerides level and VLDLR mRNA level, and promoted atherosclerosis[154]. Further studies are required to better understand the paradoxical phenotype observed in Tregs deficient in Srsf1.

The heterozygous $Srsf1^{fl/+}$.$Foxp3^{cre}$ mice had impaired anti-inflammatory capacity in response to insults that induce inflammation such as EAE. These data suggested that decreased levels of Srsf1in Tregs renders mice more susceptible to inflammatory stimuli and impairs normal Treg functions. It has been previously shown that Tregs deficient in Srsf1 have elevated chemokine mRNA expression[215]. Chemokines are a family of small, secreted proteins that signal via cell surface G protein-coupled chemokine receptors to stimulate cell migration[299]. Depending on the structure of the chemokines, they can be classified into CC chemokines, in which the N-terminal two cysteine residues are adjacent to each other, as well as CXC chemokines, in which the N-terminal two

cysteines are separated by one different amino acid, presented as X^{300301}. Chemokines are responsible for leukocyte recruitment to inflamed tissues[301]. This can partially explain the worse disease progression of EAE in that the heterozygous $Srsf1^{fl/+}.Foxp3^{cre}$ mice. In addition, the Tregs of $Srsf1^{fl/+}.Foxp3^{cre}$ mice may also have decreased LDL receptor expression as observed in Srsf1 deficient T cells. Cholesterol is required for myelin sheath formation[302]. While blood cholesterol level does not affect EAE progression[303], local cholesterol metabolism orchestrates remylination[304]. However, global LDL receptor deficiency attenuates EAE progression in females but not males[305]. These studies suggest that cell specific cholesterol metabolism may affect the EAE progression.

Based on the elevated leukocyte infiltration in the heterozygous $Srsf1^{fl/+}.Foxp3^{cre}$ mice, this model could be potentially useful for atherosclerosis research when crossed with apoE-/- or LDLR-/- mice.

4.4. SRSF1 regulation of CD8 functions and its implications in CVD

In subsection 3.4, we demonstrated that the absence of Srsf1 caused a marked decrease in the CD8 T cell population in mice, as evidenced by the low frequency of these cells in the spleen. The low numbers of CD8 T cells were a result of both defective proliferation and increased apoptosis. The CD8 T cells from $Srsf1^{fl/fl}.dLck^{cre}$ mice also have defective cytotoxic capacity. When the $Srsf1^{fl/fl}.dLck^{cre}$ mice were challenged with acute LCMV infection, their CD8 T cells exhibited reduced IFN-γ production capacity in response to re-stimulation with LCMV-specific peptides as well as decreased differentiation of naïve CD8 T cells into effector memory T cells. Our transcriptomics data provides information of the altered gene expressions and their associated pathways

including cytokine production, T cell activation and IFN signaling in Srsf1$^{fl/fl}$.dLck^{cre} mice post LCMV infection. Our data indicated that SRSF1 controls the expressions and activity of several signaling pathways, including the Mnk2-p38-MAPK signaling axis. In addition, our data showed that SRSF1 plays a crucial role in CD8 homeostasis and function and in the regulation of host antiviral immunity.

Furthermore, we identified previously unrecognized roles for Srsf1 as one of the main molecules involved in the development of an effective CD8 T cell response. The absence of Srsf1 in CD8 T cells leads to defects in its homeostasis, both under basal conditions and in the context of a viral infection. Srsf1 has already been identified as a key post-transcriptional regulator in the late stages of thymocyte development. Our study showed that CD8 T cells lacking SRSF1 are unable to generate an effective response to LCMV infection, thus limiting their maturation and differentiation into memory cells (Ignacio Martin, personal communications), resulting in impaired response to LCMV-specific peptides. The impairment of CD8 response may be mediated by a direct effect of the absence of SRSF1 in the CD8 T cells. It could also be the consequence of the absence of SRSF1 in all T cell populations in this mouse model that impaired their coordinated anti-viral responses. The present study sheds light to the potential cause of increased susceptibility to viral infections of patients with immune-mediated diseases who have low SRSF1 expression in their T lymphocytes.

RNAseq data also showed an important alteration of pathways that mediate the response to viral infection. These pathways included IFN (type I and II) response, T cell activation and proliferation and cytokine production, which renders SRSF1 as an

important mediator of the response to viral infections.

In this work, we also explored one mechanistic pathway that involves Mnk2, which implicates SRSF1 in viral infections. The kinase Mnk2 controls the phosphorylation of p38, one of the main proteins involved in the MAPK pathway. In humans, the Mnk2a splicing isoform has the MAPK binding domain and activates p38. Non-canonical p38 activation occurs in T-lymphocytes upon antigen presentation. The pro-survival mechanisms of p38 involve the modulation of alternative splicing through MNK1/2. Here we have shown that SRSF1 controls the expression of Mnk2a isoform. This is the first time that the Srsf1-MNK2-p38 pathway was linked to a T cell response. Work by others indicates that the pharmacological blockade of p38 leads to an exacerbated proliferation in CD8 T cells.

A limitation of this study is that the $Srsf1^{fl/fl}$.$dLck^{cre}$ mice are a total T cell-specific knockout, which involves all the T cell subsets (Th1, Th2, Treg, etc) that may affect CD8 T cell function and differentiation. An E8i-cre Srsf1-flox (mature CD8 T cell conditional $Srsf1^{fl/fl}$.$dLck^{cre}$ mice) is required to assess more precisely the role of SRSF1 in CD8 T cell population. In addition, our transcriptomics data provided an array of pathways that were altered in $Srsf1^{fl/fl}$.$dLck^{cre}$ mice in the context of LCMV infection. There may be other pathways that act in concert with the MAPK pathway, such as IFNα response and IL2/STAT5 signaling pathways. Future studies on these pathways would provide more insights on the role of SRSF1 in host immunity.

In conclusion, we have demonstrated an essential role of splicing factor SRSF1 in CD8 T cell functions. These findings will facilitate a better understanding of host

immunity against viral infections. The results from the LCMV studies might serve as a link between viral infection and cardiovascular disease.

4.5. Alternative splicing analysis involved in IL-17A expression

SRSF1 is regulating adaptive and innate immune functions pertinent to the pathogenesis of autoimmune and autoinflammatory diseases. Since SRSF1 is a splicing factor it would be expected to contribute to autoimmunity by gene expression regulation through alternatively spicing of mRNAs [204,306–310]. However, in our case, although we observed elevated *Il-17a* and *Il-17f* expression levels in our transcriptomic analysis, we did not detect any difference in the splicing patterns between WT and the Srsf1$^{fl/fl}$dLck^{cre} mice in *Il-17a* or *Il-17f*, or any of the transcription factors that regulate their expression. A recent study that looked at alternatively splicing events in the Srsf1$^{fl/fl}$dLck^{cre} mice detected changes in IRF7 and IL-27RA but no indication on IL-17A or IL-17F[311]. These data suggest that the elevated *Il-17a* and *Il-17f* mRNA levels are regulated by other mechanisms independent of alternative splicing.

An increase of IL-17A and IL-17F could also be achieved indirectly by inhibition of immune tolerance. Immune tolerance is achieved by multiple cell types including Tregs and myeloid suppressor cells. Indeed, deficiency of SRSF1 in Tregs is associated with autoimmunity [186]. An effect on Tregs is highly plausible as the distal Lck promoter-driven Cre, also affects other cell types including innate-like T cells, including invariant natural killer T cells and γδT cells[312]. In this study, however, we observed no difference in Treg frequency or IL-17A^{+}Tregs in Srsf1$^{fl/fl}$dLck^{cre} mice. The discrepancy of IL-17Aand IL-17F expression on the protein and mRNA level observed in this study

supports the previous findings that SRSF1 associates with translating ribosomes and stimulates translation[313,314]. Without SRSF1, the elevation in the expression of *Il-17a* and *Il-17f* mRNA level is diminished on the protein level. Since the changes in transcripts and proteins are not synchronized in the absence of SRSF1, proteomic studies are needed to comprehensively investigate the effect of SRSF1.

An additional way that SRSF1 may break tolerance is via the inhibition of myeloid-derived suppressor cells (MDSCs), which are major negative regulators of immune responses. MDSCs are categorized into two groups of cells, termed polymorphonuclear (PMN-MDSCs) and monocytic (M-MDSCs), which are phenotypically and morphologically similar to neutrophils and monocytes, respectively [315] and suppress the immune responses of $CD8^+$ T cells [212]. Our gene ontology pathway analysis showed many differentially expressed genes in the $Srsf1^{fl/fl}dLck^{cre}$ mice that are involved in many innate immunity pathways including cytokine receptors, neutrophil, and monocyte chemotaxis pathways that are pertinent to the function of MDSCs [316]. Moreover, our experiments with LCMV infection highlighted the impaired immune response to viral challenge and clearly demonstrated that the SRSF1 splicing factor regulates autoimmune processes through indirect effects on other cell types to prolong CD8 responses leading to autoimmunity. Therefore, we have uncovered an additional mechanism by which SRSF1 contributes to chronic inflammation leading to autoimmunity.

Those mechanisms could be critical in autoimmune diseases such as arthritis and/or psoriasis where IL-17A expression is paramount to pathogenesis. The frequency

of IL-17A producing $CD8^+$ T cells, namely Tc17 cells, is elevated in psoriatic skin and even after disease resolution, the tissue-resident memory Tc17 cells are still capable of contributing to the site-specific recurrence of psoriatic lesions[317,318]. The Tc17 cells and their cytokines also form a positive feedback loop as IL-17A can induce CCL20 expression in keratinocytes, which in turn recruits more Tc17 cells into the skin [319,320]. In our mouse model, the RNA-seq data showed that the Tregs of the $Srsf1^{fl/fl}dLck^{cre}$ mice also expressed elevated CCL20 level, suggesting that Srsf1 deficiency in T cells might lead to a higher predisposition to psoriasis given certain stimuli.

A more global effect on inflammatory signaling may be perturbated in SRSF1 aberrant signaling. Eukaryotic cells produce mRNA in the nucleus through a series of events including 5' capping, 3'-end processing and splicing, which are coupled with transcription and exported from the nucleus to the cytoplasm where it can be translated to generate proteins. SRSF1 is implicated in this nuclear export, by reducing the nuclear export of inflammatory mRNAs [321]. It is therefore possible that the elevated *Il-17a* and *Il-17f* expression we observed in the RNA-seq data was the result of increased nuclear export in the absence of Srsf1 rather than altered AS events [322].

CHAPTER FIVE: CONCLUSION AND FUTURE DIRECTIONS

The findings presented in this dissertation showed that C terminal deletion of SR-BI impaired cardiac function of the mice on LDLR-/- background. Such impairment can be rectified when receiving dual targeted antioxidant and antiplatelet therapy. These studies demonstrated the superiority of SR-BIΔCT/LDLR-/- mice as a new diet-inducible mouse model for research in coronary artery disease.

It has been previously demonstrated that deletion of the SR-BI carboxyl terminus increased the expression of its alternatively spliced isoform, SR-BII, and this alternative splicing is, at least in part, controlled by the splicing factor SRSF1[183,323]. We observed alterations in gene signatures involved in lipid metabolism in Tregs deficient in *Srsf1*. Further studies can be pursued to investigate how SRSF1 plays a role in lipid metabolism and its effects in the development of cardiovascular disease.

We also observed elevated *Il-17a* and *Il-17f* mRNA expression level and reduced innate immune response in T cell-specific Srsf1 knockout mice. However, we did not detect significant alternative splicing events in these mice, suggesting that SRSF1 may regulate inflammation via its role as a shuttling protein over splicing factor. In addition, SRSF1 also plays a role in motility, cell division, and the activation of mTOR pathway, which may be a result of the alternative splicing of certain genes[324–326]. The results of this dissertation opened up new research opportunities to connect alternative splicing, immune regulation and cardiovascular disease.

There are also some translational aspects of the projects presented as we learned about different functional consequences of alternative splicing. One possible therapeutic

approach is to modulate the splicing direction to enhance beneficial splicing yet repress pathological splicing. Different approaches of RNA splicing modulation have been implemented to improve the therapeutic efficacy. For example, several pharmacologic drugs have been tested in animal models and showed that they were able to enhance the checkpoint blockade in anti-tumor immunity by modulating their RNA splicing[327]. Another approach is the use of splice-switching oligonucleotides (SSOs) as potential therapeutic drugs[328]. While these approaches could have great clinical implications, careful considerations are required to ensure efficient and safe delivery methods, as the splicing factors are ubiquitously expressed in different cells, the same alternative splicing might be pathological in some tissues yet necessary in others, tissue- or cell-specific targeted intervention is therefore desired[166,329].

Efforts have been made to use nanotechnology to improve the outcome of certain diseases. In this dissertation we used nanoparticles that carry antioxidants and antiplatelet drugs for targeted therapy. In recent years, nanoparticle assisted mRNA delivery has also emerged to be an important area of research. For example, a lipid-based nanoparticle carrying a specially designed antisense oligonucleotide has been developed to redirect the mRNA splicing of IL-1 Receptor Accessory Protein in order to inhibit IL-1-driven inflammation signaling [330]. With the help of nanomedicine, we can potentially apply SSOs to increase the expression of cardioprotective genes.

BIBLIOGRAPHY

1. Ross R, Harker L. Hyperlipidemia and Atherosclerosis. *Science*. 1976;193(4258):1094–1100.

2. Grundy SM, Benjamin IJ, Burke GL, Chait A, Eckel RH, Howard B V., Mitch W, Smith SC, Sowers JR. Diabetes and Cardiovascular Disease. *Circulation*. 1999;100(10):1134–1146.

3. Libby P, Ridker PM, Maseri A. Inflammation and Atherosclerosis. *Circulation*. 2002;105(9):1135–1143.

4. Soehnlein O, Libby P. Targeting inflammation in atherosclerosis — from experimental insights to the clinic. *Nature Reviews Drug Discovery* 2021;20(8):589–610.

5. Libby P, Ridker PM, Maseri A. Inflammation and Atherosclerosis. *Circulation*. 2002;105(9):1135–1143.

6. Brown MS, Goldstein JL. Familial Hypercholesterolemia: A Genetic Defect in the Low-Density Lipoprotein Receptor. *New England Journal of Medicine*. 1976;294(25):1386–1390.

7. Goldstein JL, Kita T, Brown MS. Defective Lipoprotein Receptors and Atherosclerosis. *New England Journal of Medicine*. 1983;309(5):288–296.

8. Khalil MF, Wagner WD, Goldberg IJ. Molecular interactions leading to lipoprotein retention and the initiation of atherosclerosis. *Arteriosclerosis, Thrombosis, and Vascular Biology*. 2004;24(12):2211–2218.

9. Linton MF, Yancey PG, Davies SS, Jerome WG, Linton EF, Song WL, Doran AC, Vickers KC. The Role of Lipids and Lipoproteins in Atherosclerosis. *Science*. 2019;111(2877):166–186.

10. Ference BA, Ginsberg HN, Graham I, Ray KK, Packard CJ, Bruckert E, Hegele RA, Krauss RM, Raal FJ, Schunkert H, Watt GF, Borén J, Fazio S, Horton JD, Masana L, et al. Low-density lipoproteins cause atherosclerotic cardiovascular disease. 1. Evidence from genetic, epidemiologic, and clinical studies. A consensus statement from the European Atherosclerosis Society Consensus Panel. *European Heart Journal*. 2017;38(32):2459.

11. Gordon DJ, Probstfield JL, Garrison RJ, Neaton JD, Castelli WP, Knoke JD, Jacobs DR, Bangdiwala S, Tyroler HA. High-density lipoprotein cholesterol and

cardiovascular disease. Four prospective American studies. *Circulation*. 1989;79(1):8–15.

12. Voight BF, Peloso GM, Orho-Melander M, Frikke-Schmidt R, Barbalic M, Jensen MK, Hindy G, Hólm H, Ding EL, Johnson T, Schunkert H, Samani NJ, Clarke R, Hopewell JC, Thompson JF, et al. Plasma HDL cholesterol and risk of myocardial infarction: a mendelian randomisation study. *Lancet*. 2012;380(9841):572.

13. Hesler CB, Tall AR, Swenson TL, Weech PK, Marcel YL, Milne RW. Monoclonal antibodies to the Mr 74,000 cholesteryl ester transfer protein neutralize all of the cholesteryl ester and triglyceride transfer activities in human plasma. *Journal of Biological Chemistry*. 1988;263(11):5020–5023.

14. Tall A. Plasma lipid transfer proteins. *Annual Review of Biochemistry*. 1995;64:235–257.

15. Inazu A, Brown ML, Hesler CB, Agellon LB, Koizumi J, Takata K, Maruhama Y, Mabuchi H, Tall AR. Increased High-Density Lipoprotein Levels Caused by a Common Cholesteryl-Ester Transfer Protein Gene Mutation. *New England Journal of Medicine*. 1990;323(18):1234–1238.

16. Marotti KR, Castle CK, Boyle TP, Lin AH, Murray RW, Melchior GW. Severe atherosclerosis in transgenic mice expressing simian cholesteryl ester transfer protein. *Nature 1993 364:6432*. 1993;364(6432):73–75.

17. Plump AS, Masucci-Magoulas L, Bruce C, Bisgaier CL, Breslow JL, Tall AR. Increased Atherosclerosis in ApoE and LDL Receptor Gene Knock-Out Mice as a Result of Human Cholesteryl Ester Transfer Protein Transgene Expression. *Arteriosclerosis, Thrombosis, and Vascular Biology*. 1999;19(4):1105–1110.

18. Tall AR, Rader DJ. Trials and Tribulations of CETP Inhibitors. *Circulation Research*. 2018;122(1):106–112.

19. Rye K-A, Barter PJ. Cardioprotective functions of HDLs. *Journal of Lipid Research*, 55(2), 168–179.

20. Barter PJ, Rye KA. HDL cholesterol concentration or HDL function: which matters? *European Heart Journal*. 2017;38(32):2487–2489.

21. Smith JD. Dysfunctional HDL as a diagnostic and therapeutic target. *Arteriosclerosis, Thrombosis, and Vascular Biology*. 2010;30(2):151–155.

22. Zannis VI, Chroni A, Krieger M. Role of apoA-I, ABCA1, LCAT, and SR-BI in the biogenesis of HDL. *Journal of Molecular Medicine* 2006;84(4):276–294.

23. Fisher EA, Feig JE, Hewing B, Hazen SL, Smith JD. HDL Function, Dysfunction, and Reverse Cholesterol Transport. *Arteriosclerosis, Thrombosis, and Vascular Biology*. 2012;32(12):2813.

24. Wang HH, Garruti G, Liu M, Portincasa P, Wang DQ-H. Cholesterol and Lipoprotein Metabolism and Atherosclerosis: Recent Advances in Reverse Cholesterol Transport. *Annals of Hepatology*. 2017;16(Suppl. 1): s3-105.):S27–S42.

25. Shen WJ, Azhar S, Kraemer FB. SR-B1: A Unique Multifunctional Receptor for Cholesterol Influx and Efflux. *Annual Review of Physiology*. 2018;80:95.

26. Krieger M. Charting the fate of the "good cholesterol": Identification and characterization of the high-density lipoprotein receptor SR-BI. *Annual Review of Biochemistry*. 1999;68:523–558.

22. Acton S, Rigotti A, Landschulz KT, Xu S, Hobbs HH, Kriegert M. Identification of scavenger receptor SR-BI as a high density lipoprotein receptor. *Science*. 1996; 271(5248):518–520.

28. Vishnyakova TG, Bocharov A V., Baranova IN, Kurlander R, Drake SK, Chen Z, Amar M, Sviridov D, Vaisman B, Poliakov E, Remaley AT, Eggerman TL, Patterson AP. SR-BI mediates neutral lipid sorting from LDL to lipid droplets andfacilitates their formation. *PLoS ONE*. 2020;15(10).

29. Ghaffari S, Jang E, Naderinabi F, Sanwal R, Khosraviani N, Wang C, Steinberg BE, Goldenberg NM, Ikeda J, Lee WL. Endothelial HMGB1 Is a Critical Regulator of LDL Transcytosis via an SREBP2-SR-BI Axis. *Arteriosclerosis, Thrombosis, and Vascular Biology*. 2021;41(1):200–216.

30. Adorni MP, Zimetti F, Billheimer JT, Wang N, Rader DJ, Phillips MC, Rothblat GH. The roles of different pathways in the release of cholesterol from macrophages. *Journal of Lipid Research*. 2007;48(11):2453–2462.

31. Silver DL. A Carboxyl-terminal PDZ-interacting Domain of Scavenger Receptor B, Type I Is Essential for Cell Surface Expression in Liver. *Journal of Biological Chemistry*. 2002;277(37):34042–34047.

32. Kocher O, Yesilaltay A, Cirovic C, Pal R, Rigotti A, Krieger M. Targeted Disruption of the PDZK1 Gene in Mice Causes Tissue-specific Depletion of the High Density Lipoprotein Receptor Scavenger Receptor Class B Type I and Altered Lipoprotein Metabolism. *Journal of Biological Chemistry*. 2003;278(52):52820–52825.

33. Hoekstra M. SR-BI as target in atherosclerosis and cardiovascular disease - A comprehensive appraisal of the cellular functions of SR-BI in physiology and disease. *Atherosclerosis*. 2017;258:153–161.

34. Trigatti BL. SR-B1 and PDZK1: Partners in HDL regulation. *Current Opinion in Lipidology*. 2017;28(2):201–208.

35. Zanoni P, Khetarpal SA, Larach DB, Hancock-Cerutti WF, Millar JS, Cuchel M, DerOhannessian S, Kontush A, Surendran P, Saleheen D, Trompet S, Wouter Jukema J, De Craen A, Deloukas P, Sattar N, et al. Rare variant in scavenger receptor BI raises HDL cholesterol and increases risk of coronary heart disease. *Science*. 2016;351(6278):1166–1171.

36. Liao J, Huang W, Liu G. Animal models of coronary heart disease. *Journal of Biomedical Research*. 2017;31(1):3–10.

37. Trigatti B, Rayburn H, Viñals M, Braun A, Miettinen H, Penman M, Hertz M, Schrenzel M, Amigo L, Rigotti A, Krieger M. Influence of the high density lipoprotein receptor SR-BI on reproductive and cardiovascular pathophysiology. *Proceedings of the National Academy of Sciences of the United States of America*. 1999;96(16):9322–9327.

38. Cutler RG, Kelly J, Storie K, Pedersen WA, Tammara A, Hatanpaa K, Troncoso JC, Mattson MP. Involvement of oxidative stress-induced abnormalities in ceramide and cholesterol metabolism in brain aging and Alzheimer's disease. *Proceedings of the National Academy of Sciences of the United States of America*.. 2004;101(7):2070–2075.

39. Cutler RG, Pedersen WA, Camandola S, Rothstein JD, Mattson MP. Evidence that accumulation of ceramides and cholesterol esters mediates oxidative stress–induced death of motor neurons in amyotrophic lateral sclerosis. *Annals of Neurology*. 2002;52(4):448–457.

40. Lee J, Homma T, Kurahashi T, Kang ES, Fujii J. Oxidative stress triggers lipid droplet accumulation in primary cultured hepatocytes by activating fatty acid synthesis. *Biochemical and Biophysical Research Communications*. 2015;464(1):229–235.

41. Soppert J, Lehrke M, Marx N, Jankowski J, Noels H. Lipoproteins and lipids in cardiovascular disease: from mechanistic insights to therapeutic targeting. *Advanced Drug Delivery Reviews*. 2020;159:4–33.

42. Poznyak A V., Nikiforov NG, Markin AM, Kashirskikh DA, Myasoedova VA, Gerasimova E V., Orekhov AN. Overview of OxLDL and Its Impact on Cardiovascular Health: Focus on Atherosclerosis. *Frontiers in Pharmacology*.

2020;11.

43. McMurray HF, Parthasarathy S, Steinberg D. Oxidatively modified low density lipoprotein is a chemoattractant for human T lymphocytes. *The Journal of Clinical Investigation*. 1993;92(2):1004–1008.

44. Quinn MT, Parthasarathy S, Fong LG, Steinberg D. Oxidatively modified low density lipoproteins: a potential role in recruitment and retention of monocyte/macrophages during atherogenesis. *Proceedings of the National Academy of Sciences of the United States of America*. 1987;84(9):2995–2998.

45. Stocker R, Keaney JF. Role of oxidative modifications in atherosclerosis. *Physiological Reviews*. 2004;84(4):1381–1478.

46. Harrison D, Griendling KK, Landmesser U, Hornig B, Drexler H. Role of oxidative stress in atherosclerosis. *The American Journal of Cardiology*. 2003;91(3A):7–11.

47. Hulsmans M, Holvoet P. The vicious circle between oxidative stress and inflammation in atherosclerosis. *Journal of Cellular and Molecular Medicine*. 2010;14(1–2):70–78.

48. Tabas I, Williams KJ, Borén J. Subendothelial lipoprotein retention as the initiating process in atherosclerosis: Update and therapeutic implications. *Circulation*. 2007;116(16):1832–1844.

49. Vasile E, Simionescu M, Simionescu N. Visualization of the binding, endocytosis, and transcytosis of low- density lipoprotein in the arterial endothelium in situ. *The Journal of Cell Biology*. 1983;96(6):1677.

50. Getz GS, Reardon CA. Apoprotein E as a lipid transport and signaling protein in the blood, liver, and artery wall. *Journal of Lipid Research*. 2009;50(Suppl):S156.

51. Goldstein JL, Brown MS. The LDL receptor. *Arteriosclerosis, Thrombosis, and Vascular Biology*. 2009;29(4):431–438.

52. Nakashima Y, Plump AS, Raines EW, Breslow JL, Ross R. ApoE-deficient mice develop lesions of all phases of atherosclerosis throughout the arterial tree. *Arteriosclerosis and Thrombosis : A Journal of Vascular Biology*. 1994;14(1):133–140.

53. Ishibashi S, Brown MS, Goldstein JL, Gerard RD, Hammer RE, Herz J. Hypercholesterolemia in low density lipoprotein receptor knockout mice and its reversal by adenovirus-mediated gene delivery. *The Journal of clinical investigation*. 1993;92(2):883–893.

54. Liu J, Gillard BK, Yelamanchili D, Gotto AM, Rosales C, Pownall HJ. High Free Cholesterol Bioavailability Drives the Tissue Pathologies in Scarb1-/-Mice. *Arteriosclerosis, Thrombosis, and Vascular Biology*. 2021:E453–E467.

55. Rigotti A, Trigatti BL, Penman M, Rayburn H, Herz J, Krieger M. A targeted mutation in the murine gene encoding the high density lipoprotein (HDL) receptor scavenger receptor class B type I reveals its key role in HDL metabolism. *Proceedings of the National Academy of Sciences of the United States of America*. 1997;94(23):12610–12615.

56. Rosenson RS, Brewer HB, Ansell BJ, Barter P, Chapman MJ, Heinecke JW, Kontush A, Tall AR, Webb NR. Dysfunctional HDL and atherosclerotic cardiovascular disease. *Nature Reviews Cardiology 2015 13:1*. 2015;13(1):48–60.

57. Cao J, Xu Y, Li F, Shang L, Fan D, Yu H. Protein markers of dysfunctional HDL in scavenger receptor class B type I deficient mice. *Journal of Translational Medicine*. 2018;16(1):1–13.

58. Trigatti B, Rayburn H, Viñals M, Braun A, Miettinen H, Penman M, Hertz M, Schrenzel M, Amigo L, Rigotti A, Krieger M. Influence of the high density lipoprotein receptor SR-BI on reproductive and cardiovascular pathophysiology. *Proceedings of the National Academy of Sciences of the United States of America*. 1999;96(16):9322.

59. Braun A, Trigatti BL, Post MJ, Sato K, Simons M, Edelberg JM, Rosenberg RD, Schrenzel M, Krieger M. Loss of SR-BI expression leads to the early onset of occlusive atherosclerotic coronary artery disease, spontaneous myocardial infarctions, severe cardiac dysfunction, and premature death in apolipoprotein E-deficient mice. *Circulation Research*. 2002;90(3):270–276.

60. Covey SD, Krieger M, Wang W, Penman M, Trigatti BL. Scavenger receptor class B type I-mediated protection against atherosclerosis in LDL receptor-negative mice involves its expression in bone marrow-derived cells. *Arteriosclerosis, Thrombosis, and Vascular Biology*. 2003;23(9):1589–1594.

61. Kozarsky KF, Donahee MH, Glick JM, Krieger M, Rader DJ. Gene Transfer and Hepatic Overexpression of the HDL Receptor SR-BI Reduces Atherosclerosis in the Cholesterol-Fed LDL Receptor–Deficient Mouse. *Arteriosclerosis, Thrombosis, and Vascular Biology*. 2000;20(3):721–727.

62. Pal R, Ke Q, Pihan GA, Yesilaltay A, Penman ML, Wang L, Chitraju C, Kang PM, Krieger M, Kocher O. Carboxy-terminal deletion of the HDL receptor reduces receptor levels in liver and steroidogenic tissues, induces hypercholesterolemia, and causes fatal heart disease. *American Journal of Physiology. Heart and Circulatory Physiology*. 2016;311(6):H1392–H1408.

63. Tsutsui H, Kinugawa S, Matsushima S. Oxidative stress and heart failure. *American journal of physiology. Heart and Circulatory Physiology*. 2011;301(6):2181–2190.

64. Kattoor AJ, Pothineni NVK, Palagiri D, Mehta JL. Oxidative Stress in Atherosclerosis. *Current Atherosclerosis Reports*. 2017;19(11).

65. Madamanchi NR, Vendrov A, Runge MS. Oxidative stress and vascular disease. *Arteriosclerosis, Thrombosis, and Vascular Biology*. 2005;25(1):29–38.

66. Pizzino G, Irrera N, Cucinotta M, Pallio G, Mannino F, Arcoraci V, Squadrito F, Altavilla D, Bitto A. Oxidative Stress: Harms and Benefits for Human Health. *Oxidative Medicine and Cellular Longevity*. 2017; 8416763.

67. Folcik VA, Nivar-Aristy RA, Krajewski LP, Cathcart MK. Lipoxygenase contributes to the oxidation of lipids in human atherosclerotic plaques. *Journal of Clinical Investigation*. 1995;96(1):504.

68. Navab M, Hama SY, Anantharamaiah GM, Hassan K, Hough GP, Watson AD, Reddy ST, Sevanian A, Fonarow GC, Fogelman AM. Normal high density lipoprotein inhibits three steps in the formation of mildly oxidized low density lipoprotein: steps 2 and 3. *Journal of Lipid Research*. 2000;41(9):1495–1508.

69. Watson AD, Berliner JA, Hama SY, La Du BN, Faull KF, Fogelman AM, Navab M. Protective effect of high density lipoprotein associated paraoxonase. Inhibition of the biological activity of minimally oxidized low density lipoprotein. *Journal of Clinical Investigation*. 1995;96(6):2882–2891.

70. Liu Z, Ren Z, Zhang J, Chuang CC, Kandaswamy E, Zhou T, Zuo L. Role of ROS and nutritional antioxidants in human diseases. *Frontiers in Physiology*. 2018;9(May):477.

71. Fitó M, Guxens M, Corella D, Sáez G, Estruch R, De La Torre R, Francés F, Cabezas C, López-Sabater MDC, Marrugat J, García-Arellano A, Arós F, Ruiz-Gutierrez V, Ros E, Salas-Salvadó J, et al. Effect of a traditional Mediterranean diet on lipoprotein oxidation: A randomized controlled trial. *Archives of Internal Medicine*. 2007;167(11):1195–1203.

72. Goszcz K, Deakin SJ, Duthie GG, Stewart D, Leslie SJ, Megson IL. Antioxidants in Cardiovascular Therapy: Panacea or False Hope? *Frontiers in Cardiovascular Medicine*. 2015;2:29.

73. Leopold JA. Antioxidants and Coronary Artery Disease: From Pathophysiology to Preventive Therapy. *Coronary Artery Disease*. 2015;26(2):176.

74. Levonen AL, Vähäkangas E, Koponen JK, Ylä-Herttuala S. Antioxidant gene therapy for cardiovascular disease: Current status and future perspectives. *Circulation*. 2008;117(16):2142–2150.

75. Münzel T, Gori T, Bruno RM, Taddei S. Is oxidative stress a therapeutic target in cardiovascular disease? *European Heart Journal*. 2010;31(22):2741–2748.

76. Galkina E, Ley K. Vascular adhesion molecules in atherosclerosis. *Arteriosclerosis, Thrombosis, and Vascular Biology*. 2007;27(11):2292–2301.

77. Kunjathoor V V, Febbraio M, Podrez EA, Moore KJ, Andersson L, Koehn S, Rhee JS, Silverstein R, Hoff HF, Freeman MW. Scavenger Receptors Class A-I/II and CD36 Are the Principal Receptors Responsible for the Uptake of Modified Low Density Lipoprotein Leading to Lipid Loading in Macrophages. *The Journal of Biological Chemistry*. 2002;277(51):49982–49988.

78. Moore KJ, Sheedy FJ, Fisher EA. Macrophages in atherosclerosis: a dynamic balance. *Nature Reviews. Immunology*. 2013;13(10):709.

79. Libby P, Ridker PM, Hansson GK. Progress and challenges in translating the biology of atherosclerosis. *Nature.* 2011;473(7347):317–325.

80. Bennett MR, Sinha S, Owens GK. Vascular smooth muscle cells in atherosclerosis. *Circulation Research*. 2016;118(4):692.

81. Newby AC. Metalloproteinases and Vulnerable Atherosclerotic Plaques. *Trends in Cardiovascular Medicine*. 2007;17(8):253.

82. Bhatt DL, Hulot JS, Moliterno DJ, Harrington RA. Antiplatelet and anticoagulation therapy for acute coronary syndromes. *Circulation Research*. 2014;114(12):1929–1943.

83. Chiarito M, Stefanini GG. Antiplatelet therapy for secondary prevention of cardiovascular disease: challenging the certainties. *The Lancet*. 2021;397(10293):2443–2444.

84. Anderson JL. 2013 ACCF/AHA guideline for the management of ST-elevation myocardial infarction: Executive summary: A report of the American College of Cardiology Foundation/American Heart Association Task Force on practice guidelines. *Circulation*. 2013;127(4):529–555.

85. King SB. Effects of platelet glycoprotein IIb/IIIa blockade with tirofiban on adverse cardiac events in patients with unstable angina or acute myocardial infarction undergoing coronary angioplasty. *Circulation*. 1997;96(5):1445–1453.

86. Gremmel T, Michelson AD, Frelinger AL, Bhatt DL. Novel aspects of antiplatelet therapy in cardiovascular disease. *Research and Practice in Thrombosis and Haemostasis*. 2018;2(3):439.

87. He T, Rial PT, Nvestigators I. Inhibition of Platelet Glycoprotein IIb/IIIa with Eptifibatide in Patients with Acute Coronary Syndromes. *New England Journal of Medicine*. 2009;339(7):436–443.

88. Tcheng JE. Clinical challenges of platelet glycoprotein IIb/IIIa receptor inhibitor therapy: Bleeding, reversal, thrombocytopenia, and retreatment. *American Heart Journal*. 2000;139(2):s38–s45.

89. Ross JS, Stagliano NE, Donovan MJ, Breitbart RE, Ginsburg GS. Atherosclerosis and Cancer. *Annals of the New York Academy of Sciences*. 2001;947(1):271–293.

90. Tapia-Vieyra JV, Delgado-Coello B, Mas-Oliva J. Atherosclerosis and Cancer; A Resemblance with Far-reaching Implications. *Archives of Medical Research*. 2017;48(1):12–26.

91. Lobatto ME, Fuster V, Fayad ZA, Mulder WJM. Perspectives and opportunities for nanomedicine in the management of atherosclerosis. *Nature Reviews Drug Discovery*. 2011;10(11):835–852.

92. Kim Y, Lobatto ME, Kawahara T, Chung BL, Mieszawska AJ, Sanchez-Gaytan BL, Fay F, Senders ML, Calcagno C, Becraft J, Saung MT, Gordon RE, Stroes ESG, Ma M, Farokhzad OC, et al. Probing nanoparticle translocation across the permeable endothelium in experimental atherosclerosis. *Proceedings of the National Academy of Sciences of the United States of America*. 2014;111(3):1078–1083.

93. Lee WL, Slutsky AS. Sepsis and Endothelial Permeability. *New England Journal of Medicine*. 2010;363(7):689–691.

94. Blanco E, Shen H, Ferrari M. Principles of nanoparticle design for overcoming biological barriers to drug delivery. *Nature Biotechnology*. 2015;33(9):941–951.

95. Rees P, Wills JW, Brown MR, Barnes CM, Summers HD. The origin of heterogeneous nanoparticle uptake by cells. *Nature Communications*. 2019;10(1):1–8.

96. Pelaz B, Alexiou C, Alvarez-Puebla RA, Alves F, Andrews AM, Ashraf S, Balogh LP, Ballerini L, Bestetti A, Brendel C, Bosi S, Carril M, Chan WCW, Chen C, Chen X, et al. Diverse Applications of Nanomedicine. *ACS Nano*. 2017;11(3):2313–2381.

97. Blanco E, Shen H, Ferrari M. Principles of nanoparticle design for overcoming biological barriers to drug delivery. *Nature Biotechnology*. 2015;33(9):941.

98. Simberg D, Duza T, Park JH, Essler M, Pilch J, Zhang L, Derfus AM, Yang M, Hoffman RM, Bhatia S, Sailor MJ, Ruoslahti E. Biomimetic amplification of nanoparticle homing to tumors. *Proceedings of the National Academy of Sciences of the United States of America*. 2007;104(3):932–936.

99. Hamzah J, Kotamraju VR, Seo JW, Agemy L, Fogal V, Mahakian LM, Peters D, Roth L, Gagnon MKJ, Ferrara KW, Ruoslahti E. Specific penetration and accumulation of a homing peptide within atherosclerotic plaques of apolipoprotein E-deficient mice. *Proceedings of the National Academy of Sciences of the United States of America*. 2011;108(17):7154–7159.

100. Zhang Y, Wei J, Liu S, Wang J, Han X, Qin H, Lang J, Cheng K, Li Y, Qi Y, Anderson GJ, Sukumar S, Li S, Nie G. Inhibition of platelet function using liposomal nanoparticles blocks tumor metastasis. *Theranostics*. 2017;7(5):1062–1071.

101. Ferreira TH, de Oliveira Freitas LB, Fernandes RS, dos Santos VM, Resende JM, Cardoso VN, de Barros ALB, de Sousa EMB. Boron nitride nanotube-CREKA peptide as an effective target system to metastatic breast cancer. *Journal of Pharmaceutical Investigation*. 2020;50(5):469–480.

102. Petros RA, Desimone JM. Strategies in the design of nanoparticles for therapeutic applications. *Nature Reviews. Drug Discovery.* 2010;9(8):615–627.

103. Banik BL, Fattahi P, Brown JL. Polymeric nanoparticles: the future of nanomedicine. *Wiley Interdisciplinary Reviews. Nanomedicine and Nanobiotechnology*. 2016;8(2):271–299.

104. Husseini GA, Pitt WG. Micelles and nanoparticles for ultrasonic drug and gene delivery. *Advanced Drug Delivery Reviews*. 2008;60(10):1137–1152.

105. Trivedi R, Kompella UB. Nanomicellar formulations for sustained drug delivery: Strategies and underlying principles. *Nanomedicine*. 2010;5(3):485–505.

106. Hong D, Song B, Kim H, Kwon J, Khang G, Lee D. Biodegradable polyoxalate and copolyoxalate particles for drug-delivery applications. *Therapeutic Delivery*. 2011;2(11):1407–1417.

107. Bezerra-Filho CSM, Barboza JN, Souza MTS, Sabry P, Ismail NSM, de Sousa DP. Therapeutic Potential of Vanillin and its Main Metabolites to Regulate the Inflammatory Response and Oxidative Stress. *Mini Reviews in Medicinal Chemistry*. 2019;19(20):1681–1693.

108. Lee D, Bae S, Hong D, Lim H, Yoon JH, Hwang O, Park S, Ke Q, Khang G, Kang PM. H2O2 -responsive molecularly engineered polymer nanoparticles as ischemia/reperfusion-targeted nanotherapeutic agents. *Scientific Reports*. 2013;3.

109. Tao W, He Z. ROS-responsive drug delivery systems for biomedical applications. *Asian Journal of Pharmaceutical Sciences*. 2018;13(2):101–112.

110. Lee D, Bae S, Ke Q, Lee J, Song B, Karumanchi SA, Khang G, Choi HS, Kang PM. Hydrogen peroxide-responsive copolyoxalate nanoparticles for detection and therapy of ischemia-reperfusion injury. *Journal of Controlled Release*. 2013;172(3):1102–1110.

111. Bae S, Park M, Kang C, Dilmen S, Kang TH, Kang DG, Ke Q, Lee SU, Lee D, Kang PM. Hydrogen Peroxide-Responsive Nanoparticle Reduces Myocardial Ischemia/Reperfusion Injury. *Journal of the American Heart Association*. 2016;5(11).

112. Minami K, Bae S, Uehara H, Zhao C, Lee D, Iske J, Fanger MW, Reder J, Morrison I, Azuma H, Wiens A, Van Keuren E, Houser B, ElKhal A, Kang PM, et al. Targeting of intragraft reactive oxygen species by APP-103, a novel polymer product, mitigates ischemia/reperfusion injury and promotes the survival of renal transplants. *American Journal of Transplantation*. 2020;20(6):1527–1537.

113. Li R, Rhee SJ, Bae S, Su S, Kang CS, Ke Q, Koo YE, Ryu C, Song CG, Lee D, Kang PM. H2O2-Responsive Antioxidant Nanoparticle Attenuates Whole Body Ischemia/Reperfusion-Induced Multi-Organ Damages. *Journal of Cardiovascular Pharmacology and Therapeutics*. 2021;26(3):279–288.

114. Grundy SM, Benjamin IJ, Burke GL, Chait A, Eckel RH, Howard B V., Mitch W, Smith SC, Sowers JR. Diabetes and Cardiovascular Disease. *Circulation*. 1999;100(10):1134–1146.

115. Xie Y, Xu E, Bowe B, Al-Aly Z. Long-term cardiovascular outcomes of COVID-19. *Nature Medicine.* 2022;28(3):583–590.

116. Jankowski J, Floege J, Fliser D, Böhm M, Marx N. Cardiovascular Disease in Chronic Kidney Disease. *Circulation*. 2021;143:1157–1172.

117. Rabe KF, Hurst JR, Suissa S. Cardiovascular disease and COPD: dangerous liaisons? *European Respiratory Review*. 2018;27(149).

118. Wolf D, Ley K. Immunity and Inflammation in Atherosclerosis. *Circulation Research*. 2019;124(2):315–327.

119. Rurik JG, Aghajanian H, Epstein JA. Immune Cells and Immunotherapy for Cardiac Injury and Repair. *Circulation Research*. 2021;128:1766–1779.

120. Skaggs BJ, Hahn BH, McMahon M. Accelerated atherosclerosis in patients with SLE—mechanisms and management. *Nature Reviews. Rheumatology*. 2012;8(4):214–223.

121. Skeoch S, Bruce IN. Atherosclerosis in rheumatoid arthritis: is it all about inflammation? *Nature Reviews. Rheumatology*. 2015;11(7):390–400.

122. Späh F. Inflammation in atherosclerosis and psoriasis: common pathogenic mechanisms and the potential for an integrated treatment approach. *The British Journal of Dermatology*. 2008;159 Suppl 2(Suppl.2):10–17.

123. Schoenfeld SR, Kasturi S, Costenbader KH. The epidemiology of atherosclerotic cardiovascular disease among patients with SLE: a systematic review. *Seminars in Arthritis and Rheumatism*. 2013;43(1):77–95.

124. Manzi S, Meilahn EN, Rairie JE, Conte CG, Medsger TA, Jansen-McWilliams L, D'Agostino RB, Kuller LH. Age-specific incidence rates of myocardial infarction and angina in women with systemic lupus erythematosus: comparison with the Framingham Study. *American Journal of Epidemiology*. 1997;145(5):408–415.

125. Esdaile JM, Abrahamowicz M, Grodzicky T, Li Y, Panaritis C, Du Berger R, Côté R, Grover SA, Fortin PR, Clarke AE, Senécal J-L. Traditional Framingham Risk Factors Fail to Fully Account for Accelerated Atherosclerosis in Systemic Lupus Erythematosus. *Arthritis and Rheumatism*. 2001;44(10):2331–2337.

126. Park JK, Kim JY, Moon JY, Ahn EY, Lee EY, Lee EB, Cho KH, Song YW. Altered lipoproteins in patients with systemic lupus erythematosus are associated with augmented oxidative stress: A potential role in atherosclerosis. *Arthritis Research and Therapy*. 2016;18(1):1–9.

127. Schanberg LE, Sandborg C, Barnhart HX, Ardoin SP, Yow E, Evans GW, Mieszkalski KL, Ilowite NT, Eberhard A, Imundo LF, Kimura Y, Von Scheven E, Silverman E, Bowyer SL, Punaro M, et al. Use of Atorvastatin in Systemic Lupus Erythematosus in Children and Adolescents. *Arthritis and Rheumatism*. 2012;64(1):285.

128. Elkon K, Casali P. Nature and functions of autoantibodies. *Nature Clinical Practice. Rheumatology*. 2008;4(9):491–498.

129. Salonen JT, Korpela H, Salonen R, Nyyssonen K, Yla-Herttuala S, Yamamoto R, Butler S, Palinski W, Witztum JL. Autoantibody against oxidised LDL and progression of carotid atherosclerosis. *Lancet*. 1992;339(8798):883–887.

130. Barros MRAC, Bertolami MC, Abdalla DSP, Ferreira WP. Identification of mildly oxidized low-density lipoprotein (electronegative LDL) and its auto-antibodies IgG in children and adolescents hypercholesterolemic offsprings. *Atherosclerosis*. 2006;184(1):103–107.

131. Tsimikas S, Palinski W, Witztum JL. Circulating Autoantibodies to Oxidized LDL Correlate With Arterial Accumulation and Depletion of Oxidized LDL in LDL Receptor–Deficient Mice. *Arteriosclerosis, Thrombosis, and Vascular Biology*. 2001;21(1):95–100.

132. Tall AR, Yvan-Charvet L. Cholesterol, inflammation and innate immunity. *Nature Reviews. Immunology*. 2015;15(2):104.

133. Lahoute C, Herbin O, Mallat Z, Tedgui A. Adaptive immunity in atherosclerosis: mechanisms and future therapeutic targets. *Nature Reviews. Cardiology*. 2011;8(6):348–358.

134. Hansson GK, Libby P, Schönbeck U, Yan ZQ. Innate and adaptive immunity in the pathogenesis of atherosclerosis. *Circulation Research*. 2002;91(4):281–291.

135. Wolf D, Ley K. Immunity and Inflammation in Atherosclerosis. *Circulation Research*. 2019;124(2):315–327.

136. Winkels H, Ehinger E, Vassallo M, Buscher K, Dinh HQ, Kobiyama K, Hamers AAJ, Cochain C, Vafadarnejad E, Saliba AE, Zernecke A, Pramod AB, Ghosh AK, Michel NA, Hoppe N, et al. Atlas of the Immune Cell Repertoire in Mouse Atherosclerosis Defined by Single-Cell RNA-Sequencing and Mass Cytometry. *Circulation Research*. 2018;122(12):1675–1688.

137. Cochain C, Vafadarnejad E, Arampatzi P, Pelisek J, Winkels H, Ley K, Wolf D, Saliba AE, Zernecke A. Single-Cell RNA-Seq Reveals the Transcriptional Landscape and Heterogeneity of Aortic Macrophages in Murine Atherosclerosis. *Circulation Research*. 2018;122(12):1661–1674.

138. Duque GA, Descoteaux A. Macrophage Cytokines: Involvement in Immunity and Infectious Diseases. *Frontiers in Immunology*. 2014;5(Oct).

139. Edsfeldt A, Swart M, Singh P, Dib L, Sun J, Cole JE, Park I, Al-Sharify D, Persson A, Nitulescu M, Das Neves Borges P, Kassiteridi C, Goddard ME, Lee R, Volkov P, et al. Interferon regulatory factor-5-dependent CD11c+ macrophages contribute to the formation of rupture–prone atherosclerotic plaques. *European Heart Journal*. 2022;00:1–14.

140. Ketelhuth DFJ, Hansson GK, Libby P, Bornfeldt KE, Tall AR. Adaptive Response of T and B Cells in Atherosclerosis. *Circulation Research*. 2016;118(4):668–678.

141. Wolf D, Ley K. Immunity and Inflammation in Atherosclerosis. *Circulation Research*. 2019;124(2):315–327.

142. Zhou X, Stemme S, Hansson GK. Evidence for a local immune response in atherosclerosis. CD4+ T cells infiltrate lesions of apolipoprotein-E-deficient mice. *The American Journal of Pathology*. 1996;149(2):359.

143. Saigusa R, Winkels H, Ley K. T cell subsets and functions in atherosclerosis. *Nature Reviews. Cardiology*. 2020;17(7):387.

144. Zhou X, Nicoletti A, Elhage R, Hansson GK. Transfer of CD4+ T Cells Aggravates Atherosclerosis in Immunodeficient Apolipoprotein E Knockout Mice. *Circulation*. 2000;102(24):2919–2922.

145. Ait-Oufella H, Salomon BL, Potteaux S, Robertson A-KL, Gourdy P, Zoll J, Merval R, Esposito B, Cohen JL, Fisson S, Flavell RA, Hansson GK, Klatzmann D, Tedgui A, Mallat Z. Natural regulatory T cells control the development of atherosclerosis in mice. *Nature Medicine*. 2006;12(2):178–180.

146. Vignali DAA, Collison LW, Workman CJ. How regulatory T cells work. *Nature Reviews Immunology*. 2008;8(7):523–532.

147. Curotto de Lafaille MA, Lafaille JJ. Natural and Adaptive Foxp3+ Regulatory T Cells: More of the Same or a Division of Labor? *Immunity*. 2009;30(5):626–635.

148. Shevyrev D, Tereshchenko V. Treg Heterogeneity, Function, and Homeostasis. *Frontiers in Immunology*. 2020;10:3100.

149. Van Der Vliet HJJ, Nieuwenhuis EE. IPEX as a Result of Mutations in FOXP3. *Clinical and Developmental Immunology*. 2007;2007:89017

150. de Boer OJ, van der Meer JJ, Teeling P, van der Loos CM, van der Wal AC. Low Numbers of FOXP3 Positive Regulatory T Cells Are Present in all Developmental Stages of Human Atherosclerotic Lesions. *PLoS ONE*. 2007;2(8):e779.

151. Maganto-García E, Tarrio ML, Grabie N, Bu DX, Lichtman AH. Dynamic changes in regulatory T cells are linked to levels of diet-induced hypercholesterolemia. *Circulation*. 2011;124(2):185.

152. Butcher MJ, Filipowicz AR, Waseem TC, McGary CM, Crow KJ, Magilnick N, Boldin M, Lundberg PS, Galkina E V. Atherosclerosis-Driven Treg Plasticity Results in Formation of a Dysfunctional Subset of Plastic IFNγ+ Th1/Tregs. *Circulation Research*. 2016;119(11):1190–1203.

153. Berger A. Th1 and Th2 responses: what are they? *BMJ: British Medical Journal*.. 2000;321(7258):424.

154. Klingenberg R, Gerdes N, Badeau RM, Gisterå A, Strodthoff D, Ketelhuth DFJ, Lundberg AM, Rudling M, Nilsson SK, Olivecrona G, Zoller S, Lohmann C, Lüscher TF, Jauhiainen M, Sparwasser T, et al. Depletion of FOXP3+ regulatory T cells promotes hypercholesterolemia and atherosclerosis. *Journal of Clinical Investigation*. 2013;123(3):1323–1334.

155. Bansal SS, Ismahil MA, Goel M, Zhou G, Rokosh G, Hamid T, Prabhu SD. Dysfunctional and Proinflammatory Regulatory T-Lymphocytes Are Essential for Adverse Cardiac Remodeling in Ischemic Cardiomyopathy. *Circulation*. 2019;139(2):206–221.

156. Feng G, Bajpai G, Ma P, Koenig A, Bredemeyer A, Lokshina I, Lai L, Förster I, Leuschner F, Kreisel D, Lavine KJ. CCL17 Aggravates Myocardial Injury by Suppressing Recruitment of Regulatory T-cells. *Circulation*. 2022;145:765–782

157. Sharma M, Schlegel MP, Afonso MS, Brown EJ, Rahman K, Weinstock A, Sansbury BE, Corr EM, Van Solingen C, Koelwyn GJ, Shanley LC, Beckett L, Peled D, Lafaille JJ, Spite M, et al. Regulatory T Cells License Macrophage Pro-Resolving Functions During Atherosclerosis Regression. *Circulation Research*. 2020;127(3):335–353.

158. Wolf D, Gerhardt T, Winkels H, Michel NA, Pramod AB, Ghosheh Y, Brunel S, Buscher K, Miller J, McArdle S, Baas L, Kobiyama K, Vassallo M, Ehinger E, Dileepan T, et al. Pathogenic Autoimmunity in Atherosclerosis Evolves from Initially Protective Apolipoprotein B100-Reactive CD4+T-Regulatory Cells. *Circulation*. 2020:1279–1293.

159. Ono M. Control of regulatory T-cell differentiation and function by T-cell receptor signalling and Foxp3 transcription factor complexes. *Immunology*. 2020;160(1):24.

160. Mailer RKW. Alternative splicing of FOXP3-virtue and vice. *Frontiers in Immunology*. 2018;9(Mar).

161. Joly AL, Seitz C, Liu S, Kuznetsov N V., Gertow K, Westerberg LS, Paulsson-Berne G, Hansson GK, Andersson J. Alternative splicing of FoxP3 controls regulatory T cell effector functions and is associated with human atherosclerotic plaque stability. *Circulation Research*. 2018;122(10):1385–1394.

162. Mailer RKW, Joly A-L, Liu S, Elias S, Tegner J, Andersson J. IL-1β promotes Th17 differentiation by inducing alternative splicing of FOXP3. *Scientific Reports*. 2015;5.

163. Webb NR, Connell PM, Graf GA, Smart EJ, De Villiers WJS, De Beer FC, Van Der Westhuyzen DR. SR-BII, an Isoform of the Scavenger Receptor BI Containing an Alternate Cytoplasmic Tail, Mediates Lipid Transfer between High Density Lipoprotein and Cells. *Journal of Biological Chemistry*. 1998;273(24):15241–15248.

164. Eckhardt ERM, Cai L, Sun B, Webb NR, Van Der Westhuyzen DR. High Density Lipoprotein Uptake by Scavenger Receptor SR-BII. *Journal of Biological Chemistry*. 2004;279(14):14372–14381.

165. Webb NR, Connell PM, Graf GA, Smart EJ, De Villiers WJS, De Beer FC, Van Der Westhuyzen DR. SR-BII, an Isoform of the Scavenger Receptor BI Containing an Alternate Cytoplasmic Tail, Mediates Lipid Transfer between High Density Lipoprotein and Cells. *Journal of Biological Chemistry*. 1998;273(24):15241–15248.

166. Kelemen O, Convertini P, Zhang Z, Wen Y, Shen M, Falaleeva M, Stamm S. Function of alternative splicing. *Gene*. 2013;514(1):1.

167. Scotti MM, Swanson MS. RNA mis-splicing in disease. *Nature Reviews Genetics*. 2016;17(1):19–32.

168. Medina MW, Gao F, Ruan W, Rotter JI, Krauss RM. Alternative splicing of 3-hydroxy-3-methylglutaryl coenzyme a reductase is associated with plasma low-density lipoprotein cholesterol response to simvastatin. *Circulation*. 2008;118(4):355–362.

169. Medina MW, Gao F, Naidoo D, Rudel LL, Temel RE, McDaniel AL, Marshall SM, Krauss RM. Coordinately Regulated Alternative Splicing of Genes Involved in Cholesterol Biosynthesis and Uptake. *PLoS ONE*. 2011;6(4):e19420.

170. Yu CY, Theusch E, Lo K, Mangravite LM, Naidoo D, Kutilova M, Medina MW. HNRNPA1 regulates HMGCR alternative splicing and modulates cellular cholesterol metabolism. *Human Molecular Genetics*. 2014;23(2):319–332.

171. Fu XD. The superfamily of arginine/serine-rich splicing factors. *RNA*. 1995;1(7):663–680.

172. Cáceres JF, Stamm S, Helfman DM, Krainer AR. Regulation of alternative splicing in vivo by overexpression of antagonistic splicing factors. *Science*. 1994;265(5179):1706–1709.

173. Nilsen TW, Graveley BR. Expansion of the eukaryotic proteome by alternative splicing. *Nature*. 2010;463(7280):457.

174. Lee SC-W, Abdel-Wahab O. Therapeutic Targeting of Splicing in Cancer. *Nature Medicine*. 2016;22(9):976.

175. Xu X, Yang D, Ding JH, Wang W, Chu PH, Dalton ND, Wang HY, Bermingham JR, Ye Z, Liu F, Rosenfeld MG, Manley JL, Ross J, Chen J, Xiao RP, et al. ASF/SF2-regulated CaMKIIdelta alternative splicing temporally reprograms excitation-contraction coupling in cardiac muscle. *Cell*. 2005;120(1):59–72.

176. Blanco FJ, Bernabéu C. The splicing factor SRSF1 as a marker for endothelial senescence. *Frontiers in Physiology*. 2012;3 Mar:54.

177. Xie N, Chen M, Dai R, Zhang Y, Zhao H, Song Z, Zhang L, Li Z, Feng Y, Gao H, Wang L, Zhang T, Xiao R-P, Wu J, Cao C-M. SRSF1 promotes vascular smooth muscle cell proliferation through a Δ133p53/EGR1/KLF5 pathway. *Nature Communications.* 2017;8(1):1–19.

178. Liu Y, Luo Y, Shen L, Guo R, Zhan Z, Yuan N, Sha R, Qian W, Wang Z, Xie Z, Wu W, Feng Y. Splicing Factor SRSF1 Is Essential for Satellite Cell Proliferation and Postnatal Maturation of Neuromuscular Junctions in Mice. *Stem Cell Reports*. 2020;15(4):941–954.

179. Raihan O, Brishti A, Li Q, Li J, Zhang J, Liu Correspondence Q. SRSF11 Loss Leads to Aging-Associated Cognitive Decline by Modulating LRP8 and ApoE. *Cell Reports*. 2019;28:78-90.e6.

180. Mulcahy J V., Riddell DR, Owen JS. Human scavenger receptor class B type II (SR-BII) and cellular cholesterol efflux. *Biochemical Journal*. 2004;377(3):741–747.

181. Svensson PA, Englund MCO, Snäckestrand MSC, Hägg DA, Ohlsson BG, Stemme V, Mattsson-Hulten L, Thelle DS, Fagerberg B, Wiklund O, Carlsson LMS, Carlsson B. Regulation and splicing of scavenger receptor class B type I in human macrophages and atherosclerotic plaques. *BMC Cardiovascular Disorders*. 2005;5.

182. Baranova IN, Souza ACP, Bocharov A V., Vishnyakova TG, Hu X, Vaisman BL, Amar MJ, Chen Z, Kost Y, Remaley AT, Patterson AP, Yuen PST, Star RA, Eggerman TL. Human SR-BI and SR-BII Potentiate Lipopolysaccharide-Induced Inflammation and Acute Liver and Kidney Injury in Mice. *The Journal of Immunology*. 2016;196(7):3135–3147.

183. Zhang X, Moor AN, Merkler KA, Liu Q, McLean MP. Regulation of Alternative Splicing of Liver Scavenger Receptor Class B Gene by Estrogen and the Involved Regulatory Splicing Factors. *Endocrinology*. 2007;148(11):5295–5304.

184. Zheng Z, Ai J, Guo L, Ye X, Bondada S, Howatt D, Daugherty A, Li XA. Scavenger receptor BI is critical in maintaining normal T cell development and enhancing thymic regeneration. *Arteriosclerosis, Thrombosis, and Vascular Biology*. 2018;38(11):2706.

185. Katsuyama T, Li H, Comte D, Tsokos GC, Moulton VR. Splicing factor SRSF1 controls T cell hyperactivity and systemic autoimmunity. *Journal of Clinical Investigation*. 2019;129(12):5411–5423.

186. Katsuyama T, Moulton VR. Splicing factor SRSF1 is indispensable for regulatory T cell homeostasis and function. *Cell Reports*. 2021;36(1):109339.

187. Feingold KR, Grunfeld C. The Effect of Inflammation and Infection on Lipids and Lipoproteins. *Endotext*. 2022.

188. Bachmann MF, Wolint P, Walton S, Schwarz K, Oxenius A. Differential role of IL-2R signaling for CD8+ T cell responses in acute and chronic viral infections. *European Journal of Immunology*. 2007;37(6):1502–1512.

189. Kwong JC, Schwartz KL, Campitelli MA, Chung H, Crowcroft NS, Karnauchow T, Katz K, Ko DT, McGeer AJ, McNally D, Richardson DC, Rosella LC, Simor A, Smieja M, Zahariadis G, et al. Acute Myocardial Infarction after Laboratory-Confirmed Influenza Infection. *New England Journal of Medicine*. 2018;378(4):345–353.

190. Saad M, Kennedy KF, Imran H, Louis DW, Shippey E, Poppas A, Wood KE, Abbott JD, Aronow HD. Association Between COVID-19 Diagnosis and In-Hospital Mortality in Patients Hospitalized With ST-Segment Elevation Myocardial Infarction. *JAMA: The Journal of the American Medical Association*. 2021;326(19):1940–1952.

191. Netea MG, Quintin J, Van Der Meer JWM. Trained Immunity: A Memory for Innate Host Defense. *Cell Host & Microbe*. 2011;9(5):355–361.

192. Tercan H, Riksen NP, Joosten LAB, Netea MG, Bekkering S. Trained Immunity ; Long-term adaptation in innate immune responses. *Arteriosclerosis, Thrombosis, and Vascular Biology*. 2021;41(1):55–61.

193. Netea MG, Domínguez-Andrés J, Barreiro LB, Chavakis T, Divangahi M, Fuchs E, Joosten LAB, van der Meer JWM, Mhlanga MM, Mulder WJM, Riksen NP, Schlitzer A, Schultze JL, Stabell Benn C, Sun JC, et al. Defining trained immunity and its role in health and disease. *Nature Reviews. Immunology*. 2020;20(6):375–388.

194. Leentjens J, Bekkering S, Joosten LAB, Netea MG, Burgner DP, Riksen NP. Trained innate immunity as a novel mechanism linking infection and the development of atherosclerosis. *Circulation Research*. 2018;122(5):664–669.

195. Bekkering S, Quintin J, Joosten LAB, Van Der Meer JWM, Netea MG, Riksen NP. Oxidized low-density lipoprotein induces long-term proinflammatory cytokine production and foam cell formation via epigenetic reprogramming of monocytes. *Arteriosclerosis, Thrombosis, and Vascular Biology*. 2014;34(8):1731–1738.

196. Santos-Zas I, Lemarié J, Zlatanova I, Cachanado M, Seghezzi JC, Benamer H, Goube P, Vandestienne M, Cohen R, Ezzo M, Duval V, Zhang Y, Su JB, Bizé A, Sambin L, et al. Cytotoxic CD8+ T cells promote granzyme B-dependent adverse post-ischemic cardiac remodeling. *Nature Communications.* 2021;12(1):1–13.

197. Kolbus D, Ramos OH, Berg KE, Persson J, Wigren M, Björkbacka H, Fredrikson GN, Nilsson J. CD8+T cell activation predominate early immune responses to hypercholesterolemia in Apoe-/-mice. *BMC Immunology*. 2010;11(1):1–14.

198. Van Lenten BJ, Wagner AC, Nayak DP, Hama S, Navab M, Fogelman AM. High-density lipoprotein loses its anti-inflammatory properties during acute influenza a infection. *Circulation*. 2001;103(18):2283–2288.

199. Huber SR, van Beek J, de Jonge J, Luytjes W, van Baarle D. T Cell Responses to Viral Infections – Opportunities for Peptide Vaccination. *Frontiers in Immunology*. 2014;5(Apr).

200. Khan D, Ahmed SA. Regulation of IL-17 in autoimmune diseases by transcriptional factors and microRNAs. *Frontiers in Genetics*. 2015;6:236.

201. Bonnal SC, López-Oreja I, Valcárcel J. Roles and mechanisms of alternative splicing in cancer — implications for care. *Nature Reviews Clinical Oncology*. 2020;17(8):457–474.

202. Mailer RKW, Joly A-L, Liu S, Elias S, Tegner J, Andersson J. IL-1β promotes Th17 differentiation by inducing alternative splicing of FOXP3. *Scientific Reports*. 2015;5(1):1–9.

203. Graveley BR, Maniatis T. Arginine/serine-rich domains of SR proteins can function as activators of pre-mRNA splicing. *Molecular Cell*. 1998;1(5):765–771.

204. Sun Q, Mayeda A, Hampson RK, Krainer AR, Rottman FM. General splicing factor SF2/ASF promotes alternative splicing by binding to an exonic splicing enhancer. *Genes & Development*. 1993;7(12b):2598–2608.

205. Das S, Krainer AR. Emerging functions of SRSF1, splicing factor and oncoprotein, in RNA metabolism and cancer. *Molecular Cancer Research*. 2014;12(9):1195–1204.

206. Fregoso OI, Das S, Akerman M, Krainer AR. Splicing-Factor Oncoprotein SRSF1 Stabilizes p53 via RPL5 and Induces Cellular Senescence. *Molecular Cell*. 2013;50(1):56–66.

207. Lemaire R, Prasad J, Kashima T, Gustafson J, Manley JL, Lafyatis R. Stability of a PKCI-1-related mRNA is controlled by the splicing factor ASF/SF2: A novel function for SR proteins. *Genes and Development*. 2002;16(5):594–607.

208. Katsuyama T, Martin-Delgado IJ, Krishfield SM, Kyttaris VC, Moulton VR. Splicing factor SRSF1 controls T cell homeostasis and its decreased levels are linked to lymphopenia in systemic lupus erythematosus. *Rheumatology*. 2020;59(8):2146–2155.

209. Sun D, Novotny M, Bulek K, Liu C, Li X, Hamilton T. Treatment with IL-17 prolongs the half-life of chemokine CXCL1 mRNA via the adaptor TRAF5 and the splicing-regulatory factor SF2 (ASF). *Nature Immunology*. 2011;12(9):853–860.

210. Swaidani S, Liu C, Zhao J, Bulek K, Li X. TRAF regulation of IL-17 cytokine signaling. *Frontiers in Immunology*. 2019;10:1293.

211. Gabrilovich DI, Nagaraj S. Myeloid-derived suppressor cells as regulators of the immune system. *Nature Reviews Immunology*. 2009;9(3):162–174.

212. Norris BA, Uebelhoer LS, Nakaya HI, Price AA, Grakoui A, Pulendran B. Chronic but Not Acute Virus Infection Induces Sustained Expansion of Myeloid Suppressor Cell Numbers that Inhibit Viral-Specific T Cell Immunity. *Immunity*. 2013;38(2):309–321.

213. Zeng Y, Li Y, Xu Z, Gan W, Lu L, Huang X, Lin C. Myeloid-derived suppressor cells expansion is closely associated with disease severity and progression in HBV-related acute-on-chronic liver failure. *Journal of Medical Virology*. 2019;91(8):1510–1518.

214. Moulton VR, Gillooly AR, Perl MA, Markopoulou A. Serine arginine-rich splicing factor 1 (SRSF1) contributes to the transcriptional activation of CD3ζ in human T cells. *PLoS ONE*. 2015;10(7):e0131073.

215. Katsuyama T, Moulton VR. Splicing factor SRSF1 is indispensable for regulatory T cell homeostasis and function. *Cell Reports.* 2021;36(1):109339.

216. Vinhas M, Araújo AC, Ribeiro S, Rosário LB, Belo JA. Transthoracic echocardiography reference values in juvenile and adult 129/Sv mice. *Cardiovascular Ultrasound*. 2013;11(1):1–10.

217. Sackett DL, Wolff J. Nile red as a polarity-sensitive fluorescent probe of hydrophobic protein surfaces. *Analytical Biochemistry*. 1987;167(2):228–234.

218. Yoshida N, Comte D, Mizui M, Otomo K, Rosetti F, Mayadas TN, Crispín JC, Bradley SJ, Koga T, Kono M, Karampetsou MP, Kyttaris VC, Tenbrock K, Tsokos GC. ICER is requisite for Th17 differentiation. *Nature Communications*. 2016;7.

219. Andrews S, Krueger F, Seconds-Pichon A, Biggins F, Wingett S. FastQC. A quality control tool for high throughput sequence data. Babraham Bioinformatics. *Babraham Institute*. https://www.bioinformatics.babraham.ac.uk/projects/fastqc/

220. Martin M. Cutadapt removes adapter sequences from high-throughput sequencing reads. *EMBnet.journal*. 2011;17(1):10.

221. Conesa A, Madrigal P, Tarazona S, Gomez-Cabrero D, Cervera A, McPherson A, Szcześniak MW, Gaffney DJ, Elo LL, Zhang X, Mortazavi A. A survey of best practices for RNA-seq data analysis. *Genome Biology*. 2016;17(1):1–19.

222. Dobin A, Davis CA, Schlesinger F, Drenkow J, Zaleski C, Jha S, Batut P, Chaisson M, Gingeras TR. STAR: ultrafast universal RNA-seq aligner. *Bioinformatics*. 2013;29(1):15–21.

223. Liao Y, Smyth GK, Shi W. featureCounts: an efficient general purpose program for assigning sequence reads to genomic features. *Bioinformatics*. 2014;30(7):923–930.

224. Love MI, Huber W, Anders S. Moderated estimation of fold change and dispersion for RNA-seq data with DESeq2. *Genome Biology*. 2014;15(12):1–21.

225. Yu G, Wang LG, Han Y, He QY. clusterProfiler: an R package for comparing biological themes among gene clusters. *Omics*. 2012;16(5):284–287.

226. Storey JD, Tibshirani R. Statistical significance for genomewide studies. *Proceedings of the National Academy of Sciences of the United States of America*. 2003;100(16):9440–9445.

227. Anders S, Reyes A, Huber W. Detecting differential usage of exons from RNA-seq data. *Genome Research*. 2012;22(10):2008–2017.

228. Reyes A, Anders S, Weatheritt RJ, Gibson TJ, Steinmetz LM, Huber W. Drift and conservation of differential exon usage across tissues in primate species.

Proceedings of the National Academy of Sciences of the United States of America. 2013;110(38):15377–15382.

229. Wickham H. ggplot2: create elegant data visualisations using the grammar of graphics. *Wiley Interdisciplinary Reviews: Computational Statistics*. 2011;3(2):180–185.

230. Gu Z, Eils R, Schlesner M. Complex heatmaps reveal patterns and correlations in multidimensional genomic data. *Bioinformatics*. 2016;32(18):2847–2849.

231. Garrido-Martín D, Palumbo E, Guigó R, Breschi A. ggsashimi: Sashimi plot revised for browser- and annotation-independent splicing visualization. *PLoS Computational Biology*. 2018;14(8):e1006360.

232. Chen Y, Guo H, Xu D, Xu X, Wang H, Hu X, Lu Z, Kwak D, Xu Y, Gunther R, Huo Y, Weir EK. Left ventricular failure produces profound lung remodeling and pulmonary hypertension in mice: heart failure causes severe lung disease. *Hypertension*. 2012;59(6):1170.

233. Peters D, Kastantin M, Kotamraju VR, Karmali PP, Gujraty K, Tirrell M, Ruoslahti E. Targeting atherosclerosis by using modular, multifunctional micelles. *Proceedings of the National Academy of Sciences of the United States of America*. 2009;106(24):9815–9819.

234. Braun A, Trigatti BL, Post MJ, Sato K, Simons M, Edelberg JM, Rosenberg RD, Schrenzel M, Krieger M. Loss of SR-BI Expression Leads to the Early Onset of Occlusive Atherosclerotic Coronary Artery Disease, Spontaneous Myocardial Infarctions, Severe Cardiac Dysfunction, and Premature Death in Apolipoprotein E–Deficient Mice. *Circulation Research*. 2002;90(3):270–276.

235. Fuller M, Dadoo O, Serkis V, Abutouk D, MacDonald M, Dhingani N, Macri J, Igdoura SA, Trigatti BL. The effects of diet on occlusive coronary artery atherosclerosis and myocardial infarction in scavenger receptor class B, type 1/low-density lipoprotein receptor double knockout mice. *Arteriosclerosis, Thrombosis, and Vascular Biology*. 2014;34(11):2394–2403.

236. Wang Y, Wang W, Wang N, Tall AR, Tabas I. Mitochondrial Oxidative Stress Promotes Atherosclerosis and Neutrophil Extracellular Traps in Aged Mice. *Arteriosclerosis, Thrombosis, and Vascular Biology*. 2017;37(8):e99–e107.

237. Merat S, Fruebis J, Sutphin M, Silvestre M, Reaven PD. Effect of aging on aortic expression of the vascular cell adhesion molecule-1 and atherosclerosis in murine models of atherosclerosis. *The Journals of Gerontology. Series A, Biological Sciences and Medical Sciences*. 2000;55(2).

238. Koutrolos M, Berer K, Kawakami N, Wekerle H, Krishnamoorthy G. Treg cells mediate recovery from EAE by controlling effector T cell proliferation and motility in the CNS. *Acta Neuropathologica Communications*. 2014;2(1).

239. Othy S, Jairaman A, Dynes JL, Dong TX, Tune C, Yeromin A V., Zavala A, Akunwafo C, Chen F, Parker I, Cahalan MD. Regulatory T cells suppress Th17 cell Ca2+ signaling in the spinal cord during murine autoimmune neuroinflammation. *Proceedings of the National Academy of Sciences of the United States of America*. 2020;117(33):20088–20099.

240. Surova O, Zhivotovsky B. Various modes of cell death induced by DNA damage. *Oncogene.* 2012;32(33):3789–3797.

241. Laurence A, Tato CM, Davidson TS, Kanno Y, Chen Z, Yao Z, Blank RBB, Meylan F, Siegel R, Hennighausen L, Shevach EM, O'Shea JJJ. Interleukin-2 signaling via STAT5 constrains T helper 17 cell generation. *Immunity*. 2007;26(3):371–381.

242. Lazarevic V, Chen X, Shim JH, Hwang ES, Jang E, Bolm AN, Oukka M, Kuchroo VK, Glimcher LH. T-bet represses TH 17 differentiation by preventing Runx1-mediated activation of the gene encoding RORγt. *Nature Immunology*. 2011;12(1):96–104.

243. van Hamburg JP, de Bruijn MJW, Ribeiro de Almeida C, van Zwam M, van Meurs M, de Haas E, Boon L, Samsom JN, Hendriks RW. Enforced expression of GATA3 allows differentiation of IL-17-producing cells, but constrains Th17-mediated pathology. *European Journal of Immunology*. 2008;38(9):2573–2586.

244. Bronte V, Brandau S, Chen SH, Colombo MP, Frey AB, Greten TF, Mandruzzato S, Murray PJ, Ochoa A, Ostrand-Rosenberg S, Rodriguez PC, Sica A, Umansky V, Vonderheide RH, Gabrilovich DI. Recommendations for myeloid-derived suppressor cell nomenclature and characterization standards. *Nature Communications.* 2016;7(1):1–10.

245. Papotti B, Escolà-Gil JC, Julve J, Potì F, Zanotti I. Impact of Dietary Lipids on the Reverse Cholesterol Transport: What We Learned from Animal Studies. *Nutrients*. 2021;13(8).

246. Getz GS, Reardon CA. Diet and Murine Atherosclerosis. *Arteriosclerosis, Thrombosis and Vascular Biology*. 2006;26(2):242–249.

247. Srivastava RAK, Averna M, Srivastava N, Pape ME. Dietary cholate increases plasma levels of apolipoprotein B in mice by posttranscriptional mechanisms. *The International Journal of Biochemistry & Cell Biology*. 2001;33(12):1215–1226.

248. Nakagawa-Toyama Y, Zhang S, Krieger M. Dietary Manipulation and Social Isolation Alter Disease Progression in a Murine Model of Coronary Heart Disease. *PLoS ONE*. 2012;7(10).

249. Kocher O, Yesilaltay A, Cirovic C, Pal R, Rigotti A, Krieger M. Targeted Disruption of the PDZK1 Gene in Mice Causes Tissue-specific Depletion of the High Density Lipoprotein Receptor Scavenger Receptor Class B Type I and Altered Lipoprotein Metabolism. *Journal of Biological Chemistry*. 2003;278(52):52820–52825.

250. Kocher O, Birrane G, Tsukamoto K, Fenske S, Yesilaltay A, Pal R, Daniels K, Ladias JAA, Krieger M. In vitro and in vivo analysis of the binding of the C terminus of the HDL receptor scavenger receptor class B, type I (SR-BI), to the PDZ1 domain of its adaptor protein PDZK1. *The Journal of Biological Chemistry*. 2010;285(45):34999–35010.

251. Kocher O, Yesilaltay A, Shen CH, Zhang S, Daniels K, Pal R, Chen J, Krieger M. Influence of PDZK1 on lipoprotein metabolism and atherosclerosis. *Biochimica et Biophysica Acta*. 2008;1782(5):310–316.

252. Yesilaltay A, Daniels K, Pal R, Krieger M, Kocher O. Loss of PDZK1 Causes Coronary Artery Occlusion and Myocardial Infarction in Paigen Diet-Fed Apolipoprotein E Deficient Mice. *PLoS ONE*. 2009;4(12).

253. Yesilaltay A, Kocher O, Pal R, Leiva A, Quiñones V, Rigotti A, Krieger M. PDZK1 Is Required for Maintaining Hepatic Scavenger Receptor, Class B, Type I (SR-BI) Steady State Levels but Not Its Surface Localization or Function. *Journal of Biological Chemistry*. 2006;281(39):28975–28980.

254. Holm TM, Braun A, Trigatti BL, Brugnara C, Sakamoto M, Krieger M, Andrews NC. Failure of red blood cell maturation in mice with defects in the high-density lipoprotein receptor SR-BI. *Blood*. 2002;99(5):1817–1824.

255. Meurs I, Hoekstra M, Van Wanrooij EJA, Hildebrand RB, Kuiper J, Kuipers F, Hardeman MR, Van Berkel TJC, Van Eck M. HDL cholesterol levels are an important factor for determining the lifespan of erythrocytes. *Experimental Hematology*. 2005;33(11):1309–1319.

256. Kolodgie FD, Gold HK, Burke AP, Fowler DR, Kruth HS, Weber DK, Farb A, Guerrero LJ, Hayase M, Kutys R, Narula J, Finn A V., Virmani R. Intraplaque hemorrhage and progression of coronary atheroma. *The New England Journal of Medicine*. 2003;349(24):2316–2325.

257. Burchfield JS, Xie M, Hill JA. Pathological ventricular remodeling: Mechanisms: Part 1 of 2. *Circulation*. 2013;128(4):388–400.

258. Ertunc ME, Hotamisligil GS. Lipid signaling and lipotoxicity in metaflammation: indications for metabolic disease pathogenesis and treatment. *Journal of Lipid Research*. 2016;57(12):2099–2114.

259. Ichi I, Nakahara K, Kiso K, Kojo S. Effect of dietary cholesterol and high fat on ceramide concentration in rat tissues. *Nutrition*. 2007;23(7–8):570–574.

260. Park TS, Hu Y, Noh HL, Drosatos K, Okajima K, Buchanan J, Tuinei J, Homma S, Jiang XC, Abel ED, Goldberg IJ. Ceramide is a cardiotoxin in lipotoxic cardiomyopathy. *Journal of Lipid Research*. 2008;49(10):2101.

261. Schulze PC, Drosatos K, Goldberg IJ. Lipid Use and Misuse by the Heart. *Circulation Research*. 2016;118(11):1736–1751.

262. Drosatos K, Schulze PC. Cardiac Lipotoxicity: Molecular Pathways and Therapeutic Implications. *Current Heart Failure Reports*. 2013;10(2):109.

263. Raffa RL, Weisgraber KH. Hypomorphic apolipoprotein E mice: a new model of conditional gene repair to examine apolipoprotein E-mediated metabolism. *The Journal of Biological Chemistry*. 2002;277(13):11064–11068.

264. Hermann S, Kuhlmann MT, Starsichova A, Eligehausen S, Schäfers K, Stypmann J, Tiemann K, Levkau B, Schäfers M. Imaging reveals the connection between spontaneous coronary plaque ruptures, atherothrombosis, and myocardial infarctions in HypoE/SRBI2/2 Mice. *Journal of Nuclear Medicine*. 2016;57(9):1420–1427.

265. Maddux BA, See W, Lawrence JC, Goldfine AL, Goldfine ID, Evans JL. Protection against oxidative stress-induced insulin resistance in rat L6 muscle cells by mircomolar concentrations of alpha-lipoic acid. *Diabetes*. 2001;50(2):404–410.

266. Rudich A, Tlrosh A, Potashnik R, Hemi R, Kanety H, Bashan N. Prolonged oxidative stress impairs insulin-induced GLUT4 translocation in 3T3-L1 adipocytes. *Diabetes*. 1998;47(10):1562–1569.

267. Furukawa S, Fujita T, Shimabukuro M, Iwaki M, Yamada Y, Nakajima Y, Nakayama O, Makishima M, Matsuda M, Shimomura I. Increased oxidative stress in obesity and its impact on metabolic syndrome. *The Journal of Clinical Investigation*. 2017;114(12):1752–1761.

268. Houstis N, Rosen ED, Lander ES. Reactive oxygen species have a causal role in multiple forms of insulin resistance. *Nature*. 2006;440(7086):944–948.

269. Fox CS, Coady S, Sorlie PD, D'Agostino RB, Pencina MJ, Vasan RS, Meigs JB, Levy D, Savage PJ. Increasing cardiovascular disease burden due to diabetes mellitus: the Framingham Heart Study. *Circulation*. 2007;115(12):1544–1550.

270. Unruh D, Srinivasan R, Benson T, Haigh S, Coyle D, Batra N, Keil R, Sturm R, Blanco V, Palascak M, Franco RS, Tong W, Chatterjee T, Hui DY, Davidson WS, et al. Red Blood Cell Dysfunction Induced by High-Fat Diet: Potential Implications for Obesity-Related Atherosclerosis. *Circulation*. 2015;132(20):1898–1908.

271. Diederich L, Suvorava T, Sansone R, Keller TCS, Barbarino F, Sutton TR, Kramer CM, Lückstädt W, Isakson BE, Gohlke H, Feelisch M, Kelm M, Cortese-Krott MM. On the effects of reactive oxygen species and nitric oxide on red blood cell deformability. *Frontiers in Physiology*. 2018;9(May):332.

272. Swirski FK, Nahrendorf M, Etzrodt M, Wildgruber M, Cortez-Retamozo V, Panizzi P, Figueiredo JL, Kohler RH, Chudnovskiy A, Waterman P, Aikawa E, Mempel TR, Libby P, Weissleder R, Pittet MJ. Identification of Splenic Reservoir Monocytes and Their Deployment to Inflammatory Sites. *Science*. 2009;325(5940):612.

273. Swirski FK, Libby P, Aikawa E, Alcaide P, Luscinskas FW, Weissleder R, Pittet MJ. Ly-6Chi monocytes dominate hypercholesterolemia-associated monocytosis and give rise to macrophages in atheromata. *The Journal of Clinical Investigation*. 2007;117(1):195–205.

274. Dutta P, Courties G, Wei Y, Leuschner F, Gorbatov R, Robbins CS, Iwamoto Y, Thompson B, Carlson AL, Heidt T, Majmudar MD, Lasitschka F, Etzrodt M, Waterman P, Waring MT, et al. Myocardial infarction accelerates atherosclerosis. *Nature*. 2012;487(7407):325–329.

275. Leuschner F, Rauch PJ, Ueno T, Gorbatov R, Marinelli B, Lee WW, Dutta P, Wei Y, Robbins C, Iwamoto Y, Sena B, Chudnovskiy A, Panizzi P, Keliher E, Higgins JM, et al. Rapid monocyte kinetics in acute myocardial infarction are sustained by extramedullary monocytopoiesis. *Journal of Experimental Medicine*. 2012;209(1):123–137.

276. Badimon L, Padró T, Vilahur G. Atherosclerosis, platelets and thrombosis in acute ischaemic heart disease. *European Heart Journal. Acute Cardiovascular Care*. 2012;1(1):60.

277. Jung C, Kaul MG, Bruns OT, Ducic T, Freund B, Heine M, Reimer R, Meents A, Salmen SC, Weller H, Nielsen P, Adam G, Heeren J, Ittrich H. Intraperitoneal injection improves the uptake of nanoparticle-labeled high-density lipoprotein to atherosclerotic plaques compared with intravenous injection: a multimodal

imaging study in ApoE knockout mice. *Circulation. Cardiovascular Imaging*. 2014;7(2):303–311.

278. Greenspan P, Mayer EP, Fowler SD. Nile Red" A Selective Fluorescent Stain for Intracellular Lipid Droplets. *Journal of Cell Biology*. 1985;100(3):965-973

279. Tang Y, Wang X, Li J, Nie Y, Liao G, Yu Y, Li C. Overcoming the Reticuloendothelial System Barrier to Drug Delivery with a “don’t-Eat-Us” Strategy. *ACS Nano*. 2019;13(11): 13015–13026.

280. Kang C, Gwon S, Song C, Kang PM, Park SC, Jeon J, Hwang DW, Lee D. Fibrin-Targeted and H2O2-Responsive Nanoparticles as a Theranostics for Thrombosed Vessels. *ACS Nano*. 2017;11(6):6194–6203.

281. Miyazaki M, Ntambi JM. Role of stearoyl-coenzyme A desaturase in lipid metabolism. *Prostaglandins Leukotrienes and Essential Fatty Acids*. 2003;68(2):113–121.

282. Sibbons CM, Irvine NA, Eduardo Pérez-Mojica J, Calder PC, Lillycrop KA, Fielding BA, Burdge GC. Polyunsaturated fatty acid biosynthesis involving Δ8 desaturation and differential DNA methylation of FADS2 regulates proliferation of human peripheral blood mononuclear cells. *Frontiers in Immunology*. 2018;9(Mar).

283. Geltink RIK, Kyle RL, Pearce EL. Unraveling the Complex Interplay between T Cell Metabolism and Function. *Annual Review of Immunology*. 2018;36:461–488.

284. Newton R, Priyadharshini B, Turka LA. Immunometabolism of regulatory T cells. *Nature Immunology*. 2016;17(6):618–625.

285. Michalek RD, Gerriets VA, Jacobs SR, Macintyre AN, MacIver NJ, Mason EF, Sullivan SA, Nichols AG, Rathmell JC. Cutting Edge: Distinct Glycolytic and Lipid Oxidative Metabolic Programs Are Essential for Effector and Regulatory CD4 + T Cell Subsets . *The Journal of Immunology*. 2011;186(6):3299–3303.

286. Brown JM, Chung S, Sawyer JK, Degirolamo C, Alger HM, Nguyen T, Zhu X, Duong MN, Wibley AL, Shah R, Davis MA, Kelley K, Wilson MD, Kent C, Parks JS, et al. Inhibition of Stearoyl-Coenzyme A Desaturase 1 Dissociates Insulin Resistance and Obesity from Atherosclerosis. *Circulation*. 2008;118(14):1467–1475.

287. MacDonald MLE, Van Eck M, Hildebrand RB, Wong BWC, Bissada N, Ruddle P, Kontush A, Hussein H, Pouladi MA, Chapman MJ, Fievet C, Van Berkel TJC, Staels B, McManus BM, Hayden MR. Despite antiatherogenic metabolic characteristics, SCD1-deficient mice have increased inflammation and

atherosclerosis. *Arteriosclerosis, Thrombosis, and Vascular Biology*. 2009;29(3):341–347.

288. Liu X, Strable MS, Ntambi JM. Stearoyl CoA desaturase 1: Role in cellular inflammation and stress. *Advances in Nutrition*. 2011;2(1):15–22.

289. Takano M, Hirose N, Sumi C, Yanoshita M, Nishiyama S, Onishi A, Asakawa Y, Tanimoto K. ANGPTL2 Promotes Inflammation via Integrin α5β1 in Chondrocytes. *Cartilage*. 2019. 13(2_suppl), 885S–897S.

290. Kadomatsu T, Endo M, Miyata K, Oike Y. Diverse roles of ANGPTL2 in physiology and pathophysiology. *Trends in Endocrinology and Metabolism*. 2014;25(5):245–254.

291. Oike Y, Tabata M. Angiopoietin-like proteins - Potential therapeutic targets for metabolic syndrome and cardiovascular disease. *Circulation Journal*. 2009;73(12):2192–2197.

292. Horio E, Kadomatsu T, Miyata K, Arai Y, Hosokawa K, Doi Y, Ninomiya T, Horiguchi H, Endo M, Tabata M, Tazume H, Tian Z, Takahashi O, Terada K, Takeya M, et al. Role of endothelial cell-derived angptl2 in vascular inflammation leading to endothelial dysfunction and atherosclerosis progression. *Arteriosclerosis, Thrombosis, and Vascular Biology*. 2014;34(4):790–800.

293. Tian Z, Miyata K, Kadomatsu T, Horiguchi H, Fukushima H, Tohyama S, Ujihara Y, Okumura T, Yamaguchi S, Zhao J, Endo M, Morinaga J, Sato M, Sugizaki T, Zhu S, et al. ANGPTL2 activity in cardiac pathologies accelerates heart failure by perturbing cardiac function and energy metabolism. *Nature Communications*. 2016;7(13016).

294. Oike Y, Tian Z, Miyata K, Morinaga J, Endo M, Kadomatsu T. ANGPTL2: A new causal player in accelerating heart disease development in the aging. *Circulation Journal*. 2017;81(10):1379–1385.

295. Umikawa M, Umikawa A, Asato T, Takei K, Matsuzaki G, Kariya KI, Zhang CC. Angiopoietin-like protein 2 induces proinflammatory responses in peritoneal cells. *Biochemical and Biophysical Research Communications*. 2015;467(2):235–241.

296. Zacchigna S, Martinelli V, Moimas S, Colliva A, Anzini M, Nordio A, Costa A, Rehman M, Vodret S, Pierro C, Colussi G, Zentilin L, Gutierrez MI, DIrkx E, Long C, et al. Paracrine effect of regulatory T cells promotes cardiomyocyte proliferation during pregnancy and after myocardial infarction. *Nature Communications*. 2018;9(1).

297. Goudriaan JR, Santo SMSE, Voshol PJ, Teusink B, Willems Van Dijk K, Van Vlijmen BJM, Romijn JA, Havekes LM, Rensen PCN, Santo MSE, Voshol PJ, Teu-Sink B, Van Dijk KW, Van Vlijmen BJM, Romijn JA, et al. The VLDL receptor plays a major role in chylomicron metabolism by enhancing LPL-mediated triglyceride hydrolysis. *Journal of Lipid Research*. 2004;45(8):1475–1481.

298. Frykman PK, Brown MS, Yamamoto T, Goldstein JL, Herz J. Normal plasma lipoproteins and fertility in gene-targeted mice homozygous for a disruption in the gene encoding very low density lipoprotein receptor. *Proceedings of the National Academy of Sciences of the United States of America*. 1995;92(18):8453.

299. Hughes CE, Nibbs RJB. A guide to chemokines and their receptors. *The FEBS Journal*. 2018;285(16):2944–2971.

300. Korbecki J, Grochans S, Gutowska I, Barczak K, Baranowska-Bosiacka I. CC Chemokines in a Tumor: A Review of Pro-Cancer and Anti-Cancer Properties of Receptors CCR5, CCR6, CCR7, CCR8, CCR9, and CCR10 Ligands. *International Journal of Molecular Sciences*. 2020;21(20):1–34.

301. Romagnani P, Lasagni L, Annunziato F, Serio M, Romagnani S. CXC chemokines: the regulatory link between inflammation and angiogenesis. *Trends in Immunology*. 2004;25(4):201–209.

302. Saher G, Brügger B, Lappe-Siefke C, Möbius W, Tozawa RI, Wehr MC, Wieland F, Ishibashi S, Nave KA. High cholesterol level is essential for myelin membrane growth. *Nature Neuroscience*. 2005;8(4):468–475.

303. Vigne S, Duc D, Peter B, Rebeaud J, Yersin Y, Ruiz F, Bressoud V, Collet TH, Pot C. Lowering blood cholesterol does not affect neuroinflammation in experimental autoimmune encephalomyelitis. *Journal of Neuroinflammation*. 2022;19(1).

304. Berghoff SA, Spieth L, Saher G. Local cholesterol metabolism orchestrates remyelination. *Trends in Neurosciences*. 2022;45(4):272–283.

305. Mailleux J, Timmermans S, Nelissen K, Vanmol J, Vanmierlo T, van Horssen J, Bogie JFJ, Hendriks JJA. Low-density lipoprotein receptor deficiency attenuates neuroinflammation through the induction of apolipoprotein E. *Frontiers in Immunology*. 2017;8(Nov).

306. Caceres JF, Krainer AR. Functional analysis of pre-mRNA splicing factor SF2/ASF structural domains. *The EMBO Journal*. 1993;12(12):4715–4726.

307. Das S, Anczuków O, Akerman M, Krainer AR. Oncogenic Splicing Factor SRSF1

Is a Critical Transcriptional Target of MYC. *Cell Reports*. 2012;1(2):110–117.

308. Anczuków O, Akerman M, Cléry A, Wu J, Shen C, Shirole NH, Raimer A, Sun S, Jensen MA, Hua Y, Allain FHT, Krainer AR. SRSF1-Regulated Alternative Splicing in Breast Cancer. *Molecular Cell*. 2015;60(1):105–117.

309. Zhou X, Wang R, Li X, Yu L, Hua D, Sun C, Shi C, Luo W, Rao C, Jiang Z, Feng Y, Wang Q, Yu S. Splicing factor SRSF1 promotes gliomagenesis via oncogenic splice-switching of MYO1B. *The Journal of Clinical Investigation*. 2019;129(2):676–693.

310. Qi Z, Wang F, Yu G, Wang D, Yao Y, You M, Liu J, Liu J, Sun Z, Ji C, Xue Y, Yu S. SRSF1 serves as a critical posttranscriptional regulator at the late stage of thymocyte development. *Science Advances*. 2021;7(16):eabf0753.

311. Sharma R, Sung SSJ, Fu SM, Ju S Te. Regulation of multi-organ inflammation in the regulatory T cell-deficient scurfy mice. *Journal of Biomedical Science*. 2009;16(1):20.

312. Figueroa MG, Parker LM, Krol K, Zhao M. Distal Lck Promoter–Driven Cre Shows Cell Type–Specific Function in Innate-like T Cells. *ImmunoHorizons*. 2021;5(9):772–781.

313. Sanford JR, Gray NK, Beckmann K, Cáceres JF. A novel role for shuttling SR proteins in mRNA translation. *Genes & Development*. 2004;18(7):755–768.

314. Michlewski G, Sanford JR, Cáceres JF. The splicing factor SF2/ASF regulates translation initiation by enhancing phosphorylation of 4E-BP1. *Molecular cell*. 2008;30(2):179–189.

315. Gabrilovich DI. Myeloid-derived suppressor cells. *Cancer immunology research*. 2017;5(1):3–8.

316. Veglia F, Sanseviero E, Gabrilovich DI. Myeloid-derived suppressor cells in the era of increasing myeloid cell diversity. *Nature Reviews Immunology* 2021;21(8):485–498.

317. Ortega C, Fernández-A S, Carrillo JM, Romero P, Molina IJ, Moreno JC, Santamaría M. IL-17-producing CD8+ T lymphocytes from psoriasis skin plaques are cytotoxic effector cells that secrete Th17-related cytokines. *Journal of Leukocyte Biology*. 2009;86(2):435–443.

318. Cheuk S, Wikén M, Blomqvist L, Nylén S, Talme T, Ståhle M, Eidsmo L. Epidermal Th22 and Tc17 Cells Form a Localized Disease Memory in Clinically Healed Psoriasis. *The Journal of Immunology*. 2014;192(7):3111–3120.

319. Harper EG, Guo C, Rizzo H, Lillis J V., Kurtz SE, Skorcheva I, Purdy D, Fitch E, Iordanov M, Blauvelt A. Th17 Cytokines Stimulate CCL20 Expression in Keratinocytes In Vitro and In Vivo: Implications for Psoriasis Pathogenesis. *Journal of Investigative Dermatology*. 2009;129(9):2175–2183.

320. Blauvelt A, Chiricozzi A. The Immunologic Role of IL-17 in Psoriasis and Psoriatic Arthritis Pathogenesis. *Clinical Reviews in Allergy & Immunology 2018 55:3*. 2018;55(3):379–390.

321. Zhou H, Bulek K, Li X, Herjan T, Yu M, Qian W, Wang H, Zhou G, Chen X, Yang H, Hong L, Zhao J, Qin L, Fukuda K, Flotho A, et al. IRAK2 directs stimulus-dependent nuclear export of inflammatory mRNAs. *eLife*. 2017;6:e29630.

322. Huang Y, Gattoni R, Stévenin J, Steitz JA. SR splicing factors serve as adapter proteins for TAP-dependent mRNA export. *Molecular cell*. 2003;11(3):837–843.

323. Zhang X, Merkler KA, McLean MP. Characterization of regulatory intronic and exonic sequences involved in alternative splicing of scavenger receptor class B gene. *Biochemical and Biophysical Research Communications*. 2008;372(1):173–178.

324. Ghigna C, Giordano S, Shen H, Benvenuto F, Castiglioni F, Comoglio PM, Green MR, Riva S, Biamonti G. Cell motility is controlled by SF2/ASF through alternative splicing of the Ron protooncogene. *Molecular Cell*. 2005;20(6):881–890.

325. Maslon MM, Heras SR, Bellora N, Eyras E, Cáceres JF. The translational landscape of the splicing factor SRSF1 and its role in mitosis. *eLife*. 2014;3(3):e02028.

326. Cibrian D, de la Fuente H, Sánchez-Madrid F. Metabolic Pathways That Control Skin Homeostasis and Inflammation. *Trends in Molecular Medicine*. 2020;26(11):975–986.

327. Lu SX, De Neef E, Thomas JD, Sabio E, Rousseau B, Gigoux M, Knorr DA, Greenbaum B, Elhanati Y, Hogg SJ, Chow A, Ghosh A, Xie A, Zamarin D, Cui D, et al. Pharmacologic modulation of RNA splicing enhances anti-tumor immunity. *Cell*. 2021;184(15):4032-4047.e31.

328. Havens MA, Hastings ML. Splice-switching antisense oligonucleotides as therapeutic drugs. *Nucleic Acids Research*. 2016;44(14):6549.

329. Ward AJ, Cooper TA. The Pathobiology of Splicing. *The Journal of Pathology*. 2010;220(2):152.

330. Yılmaz-Eliş AS, Aartsma-Rus A, Hoen PA ‘t, Safdar H, Breukel C, Vlijmen BJ van, Deutekom J van, Kimpe S de, Ommen G-J van, Verbeek JS. Inhibition of IL-1 Signaling by Antisense Oligonucleotide-mediated Exon Skipping of IL-1 Receptor Accessory Protein (IL-1RAcP). *Molecular Therapy. Nucleic Acids*. 2013;2(1):e66.

CURRICULUM VITAE